A Detailed Study of Water Content Variation During Pumping and Recovery in an Unconfined Aquifer

by

Michael J. Bevan

A thesis

presented to the University of Waterloo

in fulfillment of the

thesis requirement for the degree of

Master of Science

in

Earth Sciences

Waterloo, Ontario, Canada, 2002

I hereby declare that I am the sole author of this thesis.

I authorize the University of Waterloo to lend this thesis to other institutions or individuals for the purpose of scholarly research.

Michael J. Bevan

I further authorize the University of Waterloo to reproduce this thesis by photocopying or by other means, in total or in part, at the request of other institutions or individuals for the purpose of scholarly research.

Michael J. Bevan

Borrower's Page

The University of Waterloo requires the signatures of all persons using or photocopying this thesis. Please sign below, and give address and date.

Acknowledgements

Many thanks go to Dr. Tony Endres who presented the potential research topic to me, and provided guidance and assistance through all stages of the project. His suggestions and advice throughout the preparation and editing of this manuscript have been invaluable. Thesis committee members, Drs. David Rudolph and Gary Parkin provided insight and helpful comments on the preparation of this document. Thanks also to Paul Johnson for assistance with equipment and field installations, and Drs. Cherry and Parker for the loan of time- and effort-saving pressure transducers and data loggers. Funding for this project was provided through NSREC research grants to Dr. Endres and Dr. Rudolph.

This work could not have been performed without the help of many generous field assistants – Michelle Bester, Francois Bouyssiere, Derek Brunner, Tessa DiIorio, Elizabeth Dowsett, Heather Fenton, Sharla Howard, Jen Hurley, Tina Jung, Jon Keizer, Jennifer Levenick, Charlie Magnusson, Christine March, Tracy McMunn, Russ Pagulayan, Chris Phillips, Scott Piggott, and Leslie Veale – I owe you more than I gave you!

Finally, I would like to thank Agnieszka and my family who helped me retain (regain?) motivation and focus, and for their continued support. Agnieszka agreed to spend not one, but two long summer Civic Holiday weekends at CFB Borden to help with my field work; she had understanding and patience with me through the ups and downs of this research – I appreciate everything you have done for me and will not forget it.

Abstract

Several pumping and recovery tests were performed in the unconfined aquifer at CFB Borden. Neutron moisture content logging showed that the moisture content profile essentially translates downward with pumping and upwards with aquifer recovery. It was shown that analyses of temporal GPR profiles can provide a measure of the translation movement of the transition zone. It can also provide a detailed spatial image of drainage and subsequent imbibition occurring as a result of pumping. A drainage cone was inferred from the GPR data and the volume of water released from this cone was calculated based on previously published values of specific yield. Calculated volumes including a measure of GPR-identified heterogeneity provided better estimates than those assuming a single distance-drawdown relationship; however they were still insufficient to account for all of the water pumped from the aquifer.

The drawdown of the moisture content profile is slower than that of the water table. This results in an extension of the tension-saturated capillary fringe zone and the formation of excess storage. Extension of the capillary fringe was observed to 20 m radial distance from the pumping well and is expected to exist to a distance of up to 25 m. This extension and excess storage grew throughout most of the pumping portion of the experiment and approached a quasi-steady state at later times. Extension grew to 0.25 m at radial distances of 1 and 3 m from the pumping well, and 0.06 m at 15 m. Contrary to the previously published hypothesis of Nwankwor et al. (1992), the capillary fringe extension and excess storage did not diminish at late-times of the pumping test. This suggests that the use of the volume-balance method may give inaccurate values of specific yield.

Recovery of the moisture content profile translates upward with minor variations in thickness and shape. As during drawdown, the hydraulic head levels respond more quickly than the transition zone. This results in a compression of the capillary fringe. This compression results in the lack of full recovery of the unsaturated zone profile. After 5 days of recovery, the transition zone remains almost 0.20 m below its pre-pumping level while the hydraulic heads have nearly fully recovered. Only very small vertical hydraulic gradients exist at this time; it is suspected that horizontal flow both below and above the water table will ultimately lead to the full recovery of both the moisture content profile and the hydraulic head levels.

Table of Contents

List of Figures

Chapter 1
Introduction

Knowledge of aquifer hydraulic parameters is very important in several areas of the natural sciences. These parameters include hydraulic conductivity, transmissivity, storativity and specific yield - the parameters most importantly used to determine the quality of an aquifer for use as a water resource and the quantity of water that can be extracted without detrimental effects. This data is also essential in planning and evaluating aquifer remediation techniques. Other important information that can be derived from knowledge of the aquifer hydraulic parameters includes estimation of flow paths and transport times of groundwater contaminants and estimating the recharge area of, and interference between, water supply wells.

Several techniques are used for determining the hydraulic properties of an aquifer, including both point measurements and bulk measurements. Point measurements can be performed both in the field and in the laboratory. The primary field method is the slug test; laboratory techniques include grain size analyses and permeameter tests. The results of these tests can be used to calculate pertinent hydraulic parameters at small spatial scales.

The most widely used technique to evaluate the bulk properties of an aquifer is a pumping test. This method is useful in that it provides averaged values of the hydraulic properties over a significant area; point measurement techniques provide information limited to very near the point of observation (i.e., immediately surrounding an observation well screen or the location of a sediment sample). The principle of a pumping test is explained by Kruseman and de Ridder (2000): "…if we pump water from a well and measure the discharge of the well and the drawdown in the well and in piezometers at known distances from the well, we can substitute these measurements into an appropriate well-flow equation and can calculate the hydraulic characteristics of the aquifer." These authors did not, however, indicate that other methods might be used to monitor the drawdown or drainage due to pumping an unconfined aquifer, a relatively new and little explored area of research.

1.1 Pumping Tests in an Unconfined Aquifer

There are several different techniques that can be used to determine water level drawdowns due to pumping water from an aquifer. These include the conventional method of measuring water levels in nearby observation wells and recently investigated surface imaging techniques that can provide images of pumping-induced water level drawdown. Ground penetrating radar (GPR), seismic reflection and electrical resistivity techniques have been attempted in this capacity. Background

information on these geophysical techniques may be found in a number of textbooks (e.g., Sharma, 1997).

1.1.1 Traditional Pumping Tests in an Unconfined Aquifer

The traditional method of performing an aquifer pumping test is to pump water from one well and measure hydraulic head variations in several small diameter observation wells in the immediate vicinity (Driscoll, 1986). One observation well is enough to obtain an estimate of the aquifer characteristics but will provide limited spatial information. Kruseman and de Ridder (2000) recommend at least three observation wells as they will provide more accurate analyses which will be representative of a larger aquifer volume.

While the methodology of performing a pumping test in a confined and unconfined aquifer are very similar, some very important differences exist between the two types of test. Kruseman and de Ridder (2000) summarize these differences:

i) a confined aquifer is not dewatered during pumping, whereas in an unconfined aquifer, drainage accompanies drawdown of the potentiometric surface;

ii) water produced from a well in a confined aquifer comes from an expansion of the water due to a reduction of water pressure and from compaction of the aquifer due to increased effective stress;

iii) in a confined aquifer, flow to the well is horizontal, while vertical flow components exist in an unconfined aquifer pumping test.

Immediately prior to the initiation of a pumping test, static water levels must be measured in all observation wells. Upon the onset of pumping, all observed hydraulic head drawdown is interpreted to be a direct result of pumping. Water levels must be measured at short intervals during the first one or two hours of the test, as the hydraulic heads change quickly during this time. As the duration of pumping increases, the interval between water level measurements also increases because changes in hydraulic head slows. The rate of discharge should also be measured during a test. It is convenient to maintain a constant discharge rate, although some methods of analyses use a variable rate. If a recovery test is performed, hydraulic head measurements should be made following the same time scheme as for the pumping portion of the test.

Several assumptions must be made in the analysis of unconfined aquifer pumping test data:

i) the aquifer has an infinite areal extent;

ii) the aquifer is homogeneous and of uniform thickness over the area influenced by the test;

iii) prior to pumping, the watertable is horizontal over the area that will be influenced by the test;

iv) the aquifer is pumped at a constant discharge rate;

v) the well penetrates the entire aquifer and receives water from the entire saturated thickness of the aquifer. However, there are analytical solutions available that account for partially penetrating pumping wells.

Plotting time versus drawdown from an unconfined aquifer pumping test on a bi-logarithmic scale shows three characteristic segments. The first is a steep "early-time" segment seen only in the first few minutes of pumping and is similar in form to that of the Theis confined aquifer type-curve. This segment is explained as the instantaneous release of water from elastic storage by the expansion of water and compaction of the aquifer material. The second "intermediate-time" segment is nearly flat and is thought to be a result of either vertical gradients (Neuman, 1973) or dewatering as the transition zone/capillary fringe declines (Boulton, 1963). The final "late-time" segment is relatively steep and reflects predominantly horizontal flow to the pumping well (again conforming to the Theis type-curve) after dewatering has equilibrated with the pumping rate. If recovery data is obtained, it is often analyzed using the solutions based on the drawdown of a confined aquifer.

The most common method of analyzing pumping test data is through matching "type-curves" (sets of ideal aquifer responses) to the field data. Hydraulic parameters are determined based on curve matching criterion. Several modifications have been made to the original Theis (1935) type-curve method to more accurately represent conditions that occur during the pumping of an unconfined aquifer. Boulton (1963) presented an analytical solution accounting for 'delayed yield' from above the water table. This concept is based on the hypothesis that as the water table declines, the material through which it falls does not immediately release its water. Neuman (1973) disagreed with the idea of delayed yield and created a solution assuming that drainage from above the water table is instantaneous and complete. Kruseman and de Ridder (2000) recommend the use of the Neuman curve-fitting methods for analyzing unsteady-state flow.

Several authors have raised questions regarding the accuracy of traditional type-curve methods for determining aquifer parameters. In particular, the methods used to determine specific yield have come under much criticism in the literature. Type-curve analyses methods often results in values of specific yield that are unrealistically low (Nwankwor et al., 1984, 1992) and do not adequately represent drainage from above the water table. Nwankwor et al. (1984) proposed the volume-balance method of determining specific yield. This method uses late-time shallow observation well data to calculate the volume of the drawdown cone. The specific yield is then calculated as volume of water

discharged divided by the volume of the drawdown cone. Using this method, the authors observed a time-increasing specific yield that approached laboratory-determined values. Neuman (1987) disagreed with the claims of Nwankwor et al. (1984) and suggested that at late times, significant volumes of water come from outside the observable cone of depression and thus, the volume-balance method is not valid. He went on to say that if the water budget is properly accounted for in the volume-balance method, similar values to those determined from the type-curve methods will be obtained. In response, Nwankwor et al. (1992) performed detailed field studies and Akindunni et al. (1992) performed numerical modeling experiments, both concluding that the volume-balance method does correctly account for all of the pumped water and is valid for calculating specific yield.

These studies have identified problems with the usual type-curve methods, specifically with the way that they account for drainage from the unsaturated zone and calculate specific yield. Moench (1995) and Moench et al. (2001) have presented updated analytical models that provide for the gradual release of water from above the water table. However, these models incorporate empirical constants that are not based on observed physical processes. A more appropriate solution would be based on physical processes observed to occur during pumping-induced drainage.

1.1.2 Ground Penetrating Radar Imaging of Pumping Tests

GPR can be used to image drawdown of the variably saturated transition zone during a pumping test, although this method is still in a research stage. Ideally, all that would be required is the pumping well and GPR equipment. However, hydraulic head measurements of drawdown and recovery from observation wells would be of use to calibrate the GPR-derived drawdown.

During the pumping of an aquifer, the water table declines and is accompanied by a decline in the overlying water content profile that should be detectable through GPR. GPR techniques image the subsurface through contrasts in electrical properties; water has a very high dielectric permittivity and provides an excellent target for GPR. However, the water table is not the boundary of 100% water saturation (see Figure 2-1). Above the water table, 100% water saturation is present under tension-saturated conditions. This region is known as the capillary fringe and has an upper boundary that coincides with the 100% saturation boundary; the lower boundary coincides with the water table (point of zero gauge pressure). Above this is a transition zone where the water content gradually decreases to the level of residual saturation. GPR responds to the varying water content in the transition zone, not the water table. This may cause differences when comparing GPR-derived drawdown to hydraulic head drawdown from observation wells, since the two values are of different phenomena; GPR monitors drainage, water level drawdown measures variations in hydraulic head.

Several researchers have attempted to use GPR imaging to analyze pumping tests in unconfined aquifers. Endres et al. (1997, 2000) performed a 48-hour pumping test in a clean, well-sorted, medium- to fine-grained sand aquifer. Two near-perpendicular GPR profile lines were acquired prior to, several times during, and again after pumping ceased. A strong reflection originating from the transition zone was identified on all profiles. During pumping, this reflection was seen to arrive at later times, which is related to an increase in its depth from the ground surface. Depths to the transition zone reflector were calculated and distance-drawdown relationships were determined for several times during pumping. It was observed that during the pumping test, the depth to the transition zone reflection increased and the radial distance over which drainage occurred became larger.

Upon comparison of GPR-derived transition zone drawdown with hydraulic head drawdown, Endres et al. (2000) found that the transition zone reflection drawdown was both less and the response was delayed. Discrepancies in the shapes of the distance-drawdown curves were also evident. The authors determined that the response of the water content profile in the transition zone, including the top of the capillary fringe, was delayed in time with respect to the response of the hydraulic head data. They suggested that this was a result of downward drainage in the transition zone being considerably slower than the movement of pressure transients in the saturated zone. Another observed manifestation of this property was an increased thickness of the capillary fringe and transition zones during pumping. The thickness of the capillary fringe appeared to increase by a threshold level of 0.20 m, which then remained constant throughout the duration of the test. It was suggested that this threshold thickness relates to the nature of the soil moisture release characteristics and is required for the initiation and maintenance of drainage under dynamic conditions.

Finally, Endres et al. (2000) estimated the drained aquifer volume to calculate specific yield. To do this, the transient response of the capillary fringe and the transition zone was determined; ideally, the drawdown of the transition zone as seen on the GPR profiles would directly correspond to the drawdown of the capillary fringe and water table and define a drainage cone. This drainage cone would then give a measure of the volume of water released by gravitational drainage. The volume of the drained aquifer was calculated and the volume of water drained was determined by multiplying this volume by a previously determined specific yield. Less than half of the actual volume of pumped water was accounted for. Several sources of the large discrepancy were presented, including invalid corrections for changing surface conditions or that drainage in the transition zone was not completely described by the drawdown of the GPR reflection. Endres et al. (2000) suggested that increased knowledge of the mechanisms controlling the response of unconfined aquifers to pumping and the

physics underlying GPR imaging of aquifer behaviour are required to more fully understand GPR imaging and monitoring of pumping tests in unconfined aquifers.

A second group of researchers used GPR and electrical resistivity methods to analyze pumping and recovery tests (Dolynchuk et al., 1998). This group performed both distance-drawdown and time-drawdown analyses on two pumping tests performed in an unconfined aquifer in Massachusetts, USA. The researchers concluded that the data provided by the GPR profiles and resistivity soundings were inconclusive in the unique identification of the water table and as a result, a cone of depression could not be adequately identified to calculate estimates of the aquifer properties. They determined that the data sets were dominated by stratigraphic information. While only limited processing was performed, it was suggested that increased processing and inversion of the GPR profiles and resistivity pseudosections, along with a detailed stratigraphic analysis, might enhance the data to levels where the water table and cone of depression may be identified.

However, Dolynchuk et al. (1998) determined that the results of the GPR time-drawdown experiment proved more useful than the distance-drawdown data and an estimate of the aquifer hydraulic conductivity was presented. The data used for this analysis were from the recovery portion of the test, as they proposed that this portion of the test provided a more accurate image of the water table than during pumping. It was suggested that during recovery, the water table will rise at a rate exceeding that of the capillary fringe, thus the imaged GPR boundary will be that of the coinciding water table/top of capillary fringe. Data processing showed a strongly dipping reflector interpreted to be the recovering water table. When compared to observation well measurements of hydraulic head recovery, a constant discrepancy was present which was explained to be a result of differences in elevation of the two monitoring points and the uncertainty in the radar wave velocity used to calculate the apparent depth to the water table reflector. They concluded that the time-drawdown data could be used to help constrain the water table position in distance-drawdown experiments.

The above experiments demonstrate that there is potential for GPR to be used in monitoring unconfined aquifer pumping and recovery tests. However, there are many questions that must be answered before it may be practically deployed in such a capacity, both in regard to GPR response and the relationship between drainage and imbibiton to pumping.

1.1.3 Seismic Reflection Imaging of Pumping Tests

Seismic reflection imaging operates on a similar principle to that of GPR – a pulse of energy propagates downwards from the surface and is reflected back from an interface. The reflection of seismic waves is based on the acoustical properties of a material, which also dictate the velocity with

which the waves travel. Interfaces of highly contrasting acoustical properties will produce strong reflections detected by surface receivers. The surface of 100% saturation should be an excellent reflector, since both the density and seismic P-wave velocity are greater in saturated material than in the unsaturated zone (Sharma, 1997). Whereas the GPR method images a reflector of ambiguous origin (somewhere within the transition zone), seismic reflections should theoretically provide an image of the interface of 100% saturation (top of capillary fringe).

The above properties lead Birkelo et al. (1987) to use seismic reflection methods to study the response of an unconfined aquifer to pumping. Careful and proper selection of equipment and recording parameters was necessary to successfully image very shallow reflectors, such as the water table. An eight day pumping test was conducted, during which four seismic lines were acquired – one line prior to, two lines during, and one after pumping the aquifer. Water level drawdowns were measured using traditional observation well techniques and variations in water content were measured using neutron probe techniques. After filtering and processing, the researchers observed an increase in the arrival time of reflections interpreted to originate at the top of the capillary fringe. This time increase was directly attributed to the pumping of the aquifer. The time differences amounted to increases in depth of up to 3.2 metres.

Through comparison with neutron probe data, the researchers determined that the interface depth of the saturated zone compared well with the seismic reflections. However, it was observed that water levels obtained through hydraulic head measurements decreased much more than the top of the fully saturated zone. The authors proposed this difference was the result of a thin near surface clay layer that acted as a semi-confining layer, causing a perched water table. They suggested that the water in the upper portion of the aquifer slowly drained through or around this clay layer causing the reflecting surface to drop much more slowly than the water levels in observation wells. They recommended that to detect the true water table drawdown using seismic reflection methods, pumping should be of a long enough duration to allow equilibrium between the top of the fully saturated zone and the water table.

The method of seismic reflection is time consuming. This fact makes it difficult to acquire significant spatial information, especially at early times of pumping. Also, post-acquisition data processing of reflection seismic data is complex, making this option less attractive.

1.1.4 Electrical Resistivity Imaging Analysis of Pumping Tests

Attempts have been made by several groups of researchers to use electrical resistivity methods to image the drawdown of the moisture content profile during a pumping test. Resistivity surveys are performed by placing electrodes into the ground at specific spacings. An electrical current is applied to the ground through two electrodes and the resulting electrical potential is measured between the remaining electrodes. Variations in electrical potential can be due to variations in subsurface resistivities resulting from variations in water content; decreases in water content result in an increase in electrical resistivity. It is theorized that the variations in water content due to water table drawdown from aquifer pumping will result in corresponding increases in measured resistivity (Barker and Moore, 1998). These time dependent resistivity variations are expected to be visible in resistivity pseudosections. Researchers in this field have attempted to correlate time-dependant variations in resistivity to water table drawdowns with the expectation of obtaining quantitative estimates of aquifer properties.

One pumping test experiment monitored with electrical resistivity was performed along with GPR analyses (Dolynchuk et al., 1998) and was discussed above. These resistivity experiments found limited success and advanced processing and inversion of the data sets was suggested to improve results. The researchers noted one significant downfall to the resistivity method: the measurements are not point measurements – they are representative of an "averaged" resistivity of a subsurface volume. GPR was determined to be superior in this respect (Dolynchuk et al., 1998).

Barker and Moore (1998) also performed a study applying electrical resistivity methods to monitor a pumping test. An unconfined gravel aquifer was pumped for four hours and both pumping and recovery images were obtained at several time intervals. Resisitivity images were presented as the percent change in resistivity from background levels. The technique successfully showed the expected increase in resistivity believed to reflect a decrease in the level of the moisture content profile as a result of pumping. The resistivity images showed an asymmetry inferred to be a result of differential drainage from textural variations within the aquifer (Barker and Moore, 1998). This asymmetry implied that the aquifer was heterogeneous, violating an important assumption in the analysis of pumping test data. The researchers incorporated ground water models into their experiment in hopes of describing the asymmetry and gaining some interpretation of the aquifer properties. The ground water and resistivity models corresponded with the observed data at close distances from the pumping well, but deviated significantly at greater distances. The conclusions of this experiment were that more accurate values of resistivity would be required (i.e., from in-situ

measurements) and that time related variations in resistivity must be related directly to the aquifers hydraulic parameters. If these conditions can be met, then resistivity techniques might be able to provide quantitative interpretations of subsurface hydraulic conditions.

1.2 Drainage and Imbibition in the Unsaturated Zone

A region above the water table, the capillary fringe, remains fully saturated for some thickness due to capillary forces. Overlying this zone, there exists a region of variable saturation, the transition zone, which is fully saturated at the bottom and residually saturated at the top. Above this, the aquifer material is residually saturated to the surface. Monitoring drainage and imbibition in the transition zone is not possible through traditional hydraulic head measurement techniques. However, there are methods that can be used to obtain data in this region of an aquifer. Nuclear logging and gravimetric measurement methods can provide a direct measure of the drainage and imbibition occurring in the variably saturated zone, while the use of tensiometers can provide indirect measures based on the movement of the hydraulic pressure profile.

1.2.1 Nuclear Monitoring of Pumping Tests

Nuclear methods may be used to monitor the movement of the moisture content profile due to pumping. One tool that is used for this purpose is a neutron moisture probe, which is common in measuring agricultural soil moisture. The tool operates by emitting high-energy neutrons from a radioactive source and counting the number of low-energy neutrons that return to a built-in detector. The high-energy neutrons have a similar mass to that of a hydrogen atom and as they collide, they lose energy and become low-energy thermal neutrons. Therefore, the number of low-energy neutrons that return to the detector is proportional to the water content of the formation.

Meyer (1962) used a neutron moisture probe to determine the storage coefficient and specific yield of an unconfined aquifer. In this pumping test, temporal moisture content readings were performed at the same depth in several access holes. As the test proceeded, the author monitored the moisture content as the aquifer drained past the predetermined measurement points. The specific yield was calculated as the difference between the fully saturated water content and that of residual water content. The results were similar to those determined through the analyses of water levels using the Theis method.

Jones and Schneider (1969) also used a neutron moisture probe to determine the specific yield of an aquifer. A borehole was logged with a neutron moisture probe both before and after a pumping

test. The number of returning neutrons was converted to a water content both during fully saturated conditions and again after the water table fell through the portion of the aquifer that was being studied. As in Meyer (1962), the specific yield was calculated as the difference between the fully and residually saturated moisture contents. The results were comparable to those obtained through laboratory studies, but were higher than those obtained through traditional hydraulic head drawdown-based type-curve analyses. The neutron results were reasonable and were considered to be representative of the section of the aquifer that was studied.

More recently, Birkelo et al. (1987) used a neutron moisture probe during a pumping test. They monitored movement of the moisture content profile and used it for comparison with results of seismic reflection imaging (discussed in Section 1.1.3).

Another nuclear method sometimes used to quantify the water content of subsurface materials is gamma attenuation. Nwankwor (1985) summarized the theory of gamma attenuation; the method operates on the principle that gamma rays are attenuated based on the density and mass attenuation coefficient of the material through which they pass. Assuming density is constant, any change in attenuation is a result of variations in water content. In the field, two sealed access tubes are installed to the depth of interest. The tubes must be kept at a known constant distance from each other. A radioactive gamma source is lowered into one hole while a detector is lowered in the second. In a manner similar to the neutron probe, gamma rays are emitted from the source and counted by the detector. As the gamma rays travel through the aquifer material, they become attenuated. While the method is effective, the accuracy is highly dependent on the calibration of the measuring system. This can be difficult to achieve when the interval of interest is at considerable depth below the ground surface.

While the application of neutron moisture probe and gamma attenuation techniques are useful in determining specific yield, the utilization of such a device can be inconvenient. Radioactive sources are often regulated by governmental agencies and properly trained operators must operate the tools.

1.2.2 Tensiometer Measurements

A tensiometer is a device that is used to measure hydraulic pressures above the water table. Because water in this region is held in tension, this tool can be used to indirectly monitor drainage and imbibition by comparing background pre-pumping hydraulic pressures with those acquired during pumping or recovery. As water drains due to a lowering water table, a corresponding decline of the hydraulic pressure profile will occur. A tensiometer can be used to monitor the changes in hydraulic tension during drainage or imbibition, which can be correlated to a decline or rise of the tension- and

variably-saturated zones. Stannard (1990) discusses the theory, construction and application of tensiometers in detail; Nwankwor et al. (1984, 1992) used tensiometers during a pumping test to evaluate hydraulic gradients in the unsaturated zone during drawdown.

1.2.3 Gravimetric Measurements

Gravimetric measurement is a process of measuring moisture content based on the wet and dry masses of a sample of aquifer material. One must obtain a sample of aquifer material (often through coring), remove the sample from the ground and weigh it without losing any water. The sample is then dried and weighed again. The difference in mass is a result of evaporated water. The gravimetric water content is then calculated using the dry bulk density of the sample. In performing this procedure during a drainage or imbibition experiment, samples must be taken rapidly and frequently. Several potential sources of error exist, most importantly the possibility of losing water as the core is extracted. Nwankwor (1985) outlines a method for performing this type of analysis during a pumping test.

1.3 Purpose, Scope, Goals

Presently, the typical method of large-scale local aquifer characterization is through pumping and recovery tests conducted and analyzed using traditional hydraulic head measurements. While this provides acceptable averaged estimates of important aquifer parameters, spatial information is restricted to the discrete sampling points corresponding to observation well screens. Small-scale local variations between these points are hidden within the response at these discrete points and are unrecognizable.

To obtain a more complete understanding of aquifer response during pumping and recovery, it would be desirable to have a method of acquiring increased spatial information on drawdown/drainage and recovery/imbibition. During an unconfined aquifer pumping test, the main source of pumped water is drainage from the unsaturated zone, so knowledge of the drainage process and progress is important. Several geophysical methods have the potential to provide an image of subsurface variations due to the extraction of water. However, several methods require significant time and effort to acquire. Post-acquisition processing can be complex while yielding only “average” measures of subsurface properties. GPR is expected to provide a detailed image of the unsaturated – saturated zone, while being non-invasive, efficient and inexpensive. Often, limited processing is required to obtain “interpretable” sections.

The present experiments were performed to further study the applicability of GPR to monitoring pumping-induced drawdown and recovery within an unconfined aquifer. From this grew the need for an increased understanding of the drainage and imbibition processes occurring in the transition zone and capillary fringe. To obtain information on drainage and imbibition in the variably saturated zone, a neutron moisture probe was employed. From the increased data on pumping-induced drainage and imbibition, it may be possible to prepare solutions for unconfined aquifer pumping test analyses including observed physical processes rather than empirical parameters.

This thesis is organized as a general introduction (Chapter 1) followed by two independent papers (Chapter 2 and 3) which have or will be submitted for publication in refereed journals. Chapter 2 discusses the application of GPR to the monitoring of an unconfined aquifer pumping test. Observations and results of a pumping test conducted in August 2000 are presented. Chapter 3 covers a second pumping test conducted in August 2001, during which intensive observations on temporal and spatial aquifer drainage were made using various techniques. A final chapter (Chapter 4) summarizes the observations and conclusions of the two experiments.

Chapter 2
The Non-Invasive Characterization of Pumping Induced Dewatering Using Ground Penetrating Radar

Abstract

Ground penetrating radar (GPR) profiling is a non-invasive geophysical technique that has been used by Endres et al. (2000) to successfully image pumping-induced drainage in an unconfined aquifer. However, the drained water volume calculated from the GPR data was significantly less than the actual pumped volume. To investigate the reasons for this discrepancy, a seven-day pumping test and five-day recovery test was performed at Canadian Forces Base Borden in Ontario, Canada. A dense spatial coverage of GPR profiles was used to better quantify variations in drainage due to small-scale aquifer heterogeneity. In addition, a neutron moisture content probe was used to directly observe drainage and the soil moisture profile at a sealed well near the pumping well.

Neutron logging indicated that the transition zone translated downward during pumping without undergoing significant extension or compression. Comparison of the GPR- and neutron-derived transition zone drawdowns shows nearly equal responses. Both of these observations support the hypothesis that the behaviour of the GPR reflection is an accurate measure of the transition zone drawdown. In contrast, transition zone drawdown obtained from both GPR and neutron logging are significantly delayed relative to potentiometric drawdown, resulting in an extended capillary fringe.

The drained water volume was determined from the GPR-derived transition zone drawdown data using a number of different approaches. Methods that incorporated information about spatial variations in drainage gave larger estimates of drained water volume; however, those estimates were still lower than the actual pumped volume.

The unaccountable volume of water could be a result of several factors - aquifer heterogeneity may still not be adequately represented by the increased GPR coverage, and/or leakage from the underlying aquitard may be providing a significant volume of water.

2.1 Introduction

Traditionally, the local-scale hydraulic characteristics of an unconfined aquifer are obtained through the analysis of pumping test data. During such a test, an aquifer is pumped at a controlled rate while water level variations due to this stress are monitored spatially and temporally within nearby

observation wells. Several techniques can be applied to analyze the data, dependant on the particular conditions at a specific site (e.g., Neuman, 1974; Moench, 1995).

To perform such an analysis, at least one observation well must used (Driscoll, 1986); however, Kruseman and de Ridder (2000) recommend a minimum of three observation wells to obtain a more accurate representation of a larger aquifer volume. This "ideal" situation would provide hydraulic head drawdown information at three discrete points within often heterogeneous aquifers. However, the installation of multiple observation wells is often undesirable from the standpoints of increased time and expense, as well as possible liability associated with potentially contaminated sites.

Surface geophysics provides a number of potential non-invasive methods for monitoring the response of an unconfined aquifer to pumping. In general, geophysical methods are very sensitive to variations in physical properties resulting from changing water content. Hence, these techniques can supply information about dewatering caused by pumping whereas water-level measurements give hydraulic head information. Both seismic reflection (Birkelo et al., 1987) and electrical resistivity profiling (Barker and Moore, 1998) have been used with limited success to monitor pumping-induced dewatering. It has been demonstrated that ground penetrating radar (GPR) profiling can provide high resolution images of pumping-induced drainage (Endres et al., 2000; Tsoflias et al., 2001) and subsequent recovery (Dolynchuk et al., 1998). A further benefit of using GPR is its ability to efficiently provide extensive spatial data that cannot be easily or economically obtained from observation wells.

A GPR unit emits high frequency electromagnetic (EM) pulses that propagate into the Earth from a transmitting antenna. When the EM wave encounters an interface between materials with differing electrical properties, a portion of the energy is reflected back to the surface receiver. The traveltime of the reflected energy is a measure of the depth to the interface; its amplitude is a function of the contrast in electrical properties across the interface. Dielectric permittivity is the principal electrical property governing EM wave propagation. Given the high permittivity of water (ε=80) relative to other commonly occurring earth materials (ε~10), the propagation of radar signals is sensitive to changes in water content.

In an unconfined aquifer, the transition zone between the residually and fully saturated zones is a region where significant variation in water content occurs. A strong reflection event is usually expected from this region due to the large contrast in dielectric permittivity between residually and fully saturated sands ($\varepsilon \cong 6$ and $\varepsilon \cong 30$, respectively (Reynolds, 1997)). While GPR cannot be used to directly measure the water table depth, it can be used to estimate the depth to the transition zone.

Endres et al. (2000) used a transition zone drawdown-distance relationship derived from GPR profiles to determine the drained water volume for various times during a pumping test; the values were significantly less than the actual pumping well production (ranging between 25% and 40% of the actual pumped water). Several potential causes were suggested for this discrepancy. A limited spatial coverage of GPR profile lines may not have adequately characterized small-scale variations in dewatering related to aquifer heterogeneity. Further, the nature of the water content profile within the transition zone could have evolved during the pumping test. This change would affect the nature of GPR reflection from the transition zone and the relationship between the actual transition zone drawdown and its estimate derived from GPR profiling.

To further investigate the use of GPR to monitor pumping-induced dewatering, a seven-day constant rate pumping test and five-day recovery test was performed in August, 2000 at Canadian Forces Base Borden, in Ontario, Canada. A series of GPR profile lines with significantly increased spatial coverage in comparison to the previous experiment by Endres et al. (2000) was used to detect small-scale variations in dewatering related to aquifer heterogeneity. In addition, a neutron moisture probe was used to directly observe the behaviour of the soil moisture profile, in particular the transition zone, throughout the pumping and recovery test. These in-situ measurements allow a direct comparison between actual transition zone drawdown and the estimate derived from the GPR profiles.

2.2 Site Description

A test site at Canadian Forces Base Borden, near Barrie, Ontario, Canada was selected for this pumping test experiment. The unconfined aquifer in the vicinity of the test site is of glaciofluvial or glaciodeltaic origin and is a clean, well-sorted, medium-grained sand. The sand grades from fine near the surface to medium at depth. The aquifer is locally heterogeneous due to beds and lenses of fine-, medium- and coarse-grained sand (MacFarlane et al., 1983). Sudicky (1986) also identified horizontally discontinuous beds of one to a few metres in length that had contrasting hydraulic conductivities.

The aquifer is approximately 9 m thick at the test site and is underlain by a clayey silt aquitard. The water table is 2 to 3 m below ground surface, although seasonal variations occur; a water table gradient of about 1×10^{-3} exists in a southward to northward direction (Nwankwor et al., 1992). At the time of the test, the water table was at a depth of approximately 1.95 m below ground surface. Laboratory work by Nwankwor et al. (1984) determined a residual water content in the unsaturated zone of 0.07 and a fully saturated water content of 0.37. The thickness of the transition zone is

approximately 0.40 m with a capillary fringe thickness of 0.30 m. This places the bottom of the residually saturated zone at a height of approximately 0.70 m above the static water table. Figure 2-1 summarizes the features of the static soil moisture profile at the site.

The test site is instrumented with a pumping well and 42 observation wells. The pumping well is steel and has a 0.13 m inner diameter with a #14 slot telescopic stainless steel screen spanning the bottom 3.65 m of the aquifer and 0.35 m of the aquitard. Observation wells are PVC and range in diameter from 0.015 to 0.05 m. Most wells have 0.35 m screens and are completed at various depths within the aquifer. For the present study, one observation well located 1 m from the pumping well was modified with a sealed insert to allow for moisture content logging using a neutron probe. The sealed well was constructed of a 0.05 m diameter stainless steel tube sealed at one end and inserted into a pre-existing PVC observation well.

A series of eight radial GPR profile lines were set up, varying in orientation and length (from 35 m to 60 m) dictated by the location of surrounding roads and bush. The origin of these lines was offset from the pumping well by 1 m. This displacement was necessary to minimize interference with the GPR signal by the steel pumping well. Subsequent analyses referenced all data to a common origin centred at the pumping well. Figure 2-2 shows the layout of the existing instrumentation and GPR profile lines.

2.3 Field Methods

A seven-day, constant-rate pumping test was performed, followed by a five-day recovery test. The pumping rate was maintained at 44 ± 1 l/min and the extracted water was discharged several hundred metres down-gradient of the test site.

The aquifer response during the experiment was monitored in a network of 42 observation wells and through GPR profiling, GPR common midpoint (CMP) surveys and neutron moisture content logging. Water levels in the observation wells were measured using acoustic sounders accurate to 0.005 m. Detailed temporal monitoring was performed in two wells screened at shallow depths at distances of 3 and 5 m from the pumping well (WD1B and WD2A, respectively). Water levels in the remaining forty wells were measured a minimum of twice daily to obtain spatial drawdown information.

GPR data was acquired using a Sensors and Software Inc. PulseEKKO IV system equipped with a 400 V transmitter and 200 MHz antennae. GPR profiles were acquired twice daily on all eight radial lines to provide extensive spatial coverage over the anticipated zone of influence. These

profiles were collected with an antennae separation (i.e. offset) of 0.50 m and a step-size (i.e., station spacing) of 0.20 m. In addition, detailed profiling was performed three times daily on lines 3 and 5 with a step-size of 0.10 m. This reduced step-size was used to improve the image of the transition zone reflector. CMP surveys were performed on lines 3, 5 and 8 to determine the subsurface electromagnetic velocity structure. In the CMP procedure, the antennae are moved in opposite directions from a centre point and the resulting data are analyzed using the NMO technique (Sheriff and Geldart, 1995) to determine the EM wave velocity of the aquifer material. The same CMP positions were reoccupied daily to observe temporal changes in the EM velocity structure.

To directly observe aquifer drainage due to pumping, the soil moisture profile was measured throughout the experiment using a neutron moisture probe. The CPN Corporation 503DR thermal neutron probe has a 50mCi Americium-241/Berylium source. It emits high-energy neutrons that are moderated enroute to a detector; the number of returning thermal neutrons is related to volumetric water content. Neutron logging was performed between depths of 0.75 and 4.0 m below ground surface with a sampling interval of 0.10 m; this depth range was sufficient to characterize the moisture profile from the residually to fully saturated zones as the profile changed throughout the experiment. Moisture distribution profiles were obtained a minimum of twice daily, either immediately before or after potentiometric water levels and GPR profiles were collected. A full suite of measurements (GPR profiles on eight lines, water levels in all wells and a neutron moisture content log) took approximately 2.5 hours to collect.

2.4 Results

2.4.1 Potentiometric Data

Detailed temporal potentiometric water levels were collected in two observation wells located at distances of 3 (WD1B) and 5 m (WD2A) from the pumping well. Both wells are screened at a depth of 3.2 m below ground surface. The potentiometric data for these two wells are shown in Figure 2-3. Both data sets show the typical three-phase curve for an unconfined aquifer described by Neuman (1972). The response observed between both wells is similar during the pumping and recovery portions of the test, although there are minor variations due to the different distances from the pumping well (i.e., closer well has a greater drawdown/recovery). Potentiometric data from all wells may be found in Appendix A and on the accompanying CD-ROM.

Analysis of the two potentiometric data sets using the Neuman (1974) method yields very similar results with an average transmissivity of approximately 5×10^{-4} m^2/sec and storativity of 1×10^{-4}.

The calculated hydraulic conductivity is 7.7 x 10^{-5} m/sec; this value is close to average hydraulic conductivities between 3.0 x 10^{-5} and 1.8 x 10^{-4} m/sec determined by previous research at the site (Nwankwor et al., 1984; Nwankwor, 1985) (See Appendix E). All of these values are consistent with literature values for well-sorted medium sand (Fetter, 2001). Specific yield values of about 0.01 were also calculated through the above analyses. Yields of this magnitude are significantly lower than would be expected for the material comprising the Borden aquifer. Nwankwor et al. (1984) proposed that drainage is not adequately represented through traditional drawdown measurements. Nwankwor et al. (1992) stated that specific yields derived through type-curve methods often result in unrealistically low values. The laboratory determined specific yield of 0.30 of Nwankwor et al. (1984) is used in all calculations in this document.

The hydraulic head levels in the observation wells did not return to their pre-pumping positions after five days of recovery; levels stabilized at 0.15 to 0.20 m below the pre-pumping level. This behaviour is likely due to a lowering of the regional water table in response to extremely warm and dry weather. In this area, a decline in the water table of 0.75 to 1 m during the summer and early fall was identified by MacFarlane et al. (1983), so the measured decline during this test is reasonable.

2.4.2 Moisture Content Data

Temporal moisture content data were obtained in the sealed well located 1 m from the pumping well. Volumetric water content was calculated based on a linear field calibration between the neutron count-rate and the known residual and fully saturated water contents. Selected water content profiles obtained during both drawdown and recovery portions of the test are presented in Figure 2-4. Raw moisture content data, the technique to calculate water content and an estimate of potential error is included in Appendix C and on the accompanying CD-ROM.

The pre-pumping thickness of the transition zone, as measured from the base of the residually saturated zone to the top of the fully saturated capillary fringe, is approximately 0.40 m; this value is consistent with that of Nwankwor et al. (1992). It is seen in Figure 2-4 that the thickness of the transition zone does not become significantly altered during the test (i.e., little or no extension during drawdown, little, if any, compression during recovery.) Instead, the transition zone has translated downward as a result of pumping and translated back upward during recovery, maintaining approximately the same shape as seen in the different temporal moisture content profiles.

The water content profiles clearly show that the drained portion of the aquifer is at residual water content. The profiles also show that drainage continues throughout the experiment. This continuous

decline of the transition zone and drainage to residual saturation is contrary to Grimestad (2002) who suggested that unsaturated drainage in the Borden aquifer stops within the first day of pumping and that excess moisture becomes trapped in the unsaturated zone.

The upward translation of the water content profiles during recovery begins within two hours of the pump being turned off. As the profile translates upward, the previously dewatered portions of the aquifer are completely refilled to full saturation. As with the hydraulic head data, the soil moisture profile does not fully recover; it remains approximately 0.25 m lower than its pre-pumping position.

2.4.3 Ground Penetrating Radar Data

GPR profiles were processed using a spherical exponential compensation (SEC) gain and first break corrections. In addition, a three-point vertical and horizontal averaging filter was applied to enhance reflection signals. A summary of the acquired GPR profiles is provided in Appendix F and raw data is provided on the accompanying CD-ROM. Figure 2-5 presents GPR profiles acquired along the southward trending Line 5. Figure 2-5a shows the background pre-pumping profile; Figure 2-5b shows the same line acquired at maximum drawdown, immediately prior to turning the pump off after seven days of drawdown.

The event labeled X-X' was identified as the transition zone reflection on the basis of the following two criteria. First, the high amplitude of this reflection is consistent with the large permittivity contrast between the residually and fully saturated zones. Second, using an average EM wave velocity of 0.114 m/ns obtained from the CMP data analyses, the average pre-pumping reflector depth was estimated to be approximately 1.60 m. This depth is consistent with the measured depth to the water table of about 1.95 m and a capillary fringe thickness of 0.30 m.

It should be noted that the relationship between the reflection traveltime and the transition zone depth is complex in nature. The transition zone is not a discrete interface, but a zone of continuously varying dielectric permittivity from $\varepsilon \cong 6$ at the top to $\varepsilon \cong 30$ at the base. This structure implies that the source of the reflected energy for the transition zone event is distributed over this region, making it difficult to assign an effective reflection point within the transition zone that corresponds to the measured traveltime. However, the moisture content profiles shown in Figure 2-4 clearly show that the transition zone has simply translated downward and back upward without being significantly altered in thickness or shape. The invariant shape and thickness implies that we can assume the relationship between traveltime and the effective reflection point is constant during the experiment.

Hence, observed changes in reflection traveltime are directly related to the translation distance of the transition zone.

Temporal GPR data acquired during the pumping test show a consistent increase in traveltime to the transition zone reflector. The recovery GPR data show a traveltime decrease relative to the maximum drainage profile. The traveltime increase due to pumping is illustrated in Figure 2-5 where the transition zone reflection (labeled X-X') occurs later in time (i.e. further down the section) on the maximum drawdown profile. Small-scale features along the transition zone reflector are due to localized variations in drainage and interference with diffractions from shallow sources.

To quantify the movement of the transition zone reflection, the time difference between the first arrival (i.e., the direct air wave) and the transition zone reflection was determined to an accuracy of ±0.5 ns. The direct air wave has a constant traveltime for a fixed antennae offset distance, providing a standard zero-time reference. To calculate the vertical movement of the transition zone reflection, the background pre-pumping traveltime of this reflection was subtracted from its traveltime during pumping and recovery. This procedure yields a relative time difference from background data analogous to water level drawdown versus static water level. The traveltime differences were converted into equivalent drawdown distance, Δh^{TZ}, of the transition zone reflection using the following equation given by Endres et al. (2000):

$$\Delta h^{TZ} = \left\{ \frac{\left(v^{TZ}\right)^2}{2\left[\left(v^{TZ}\right)^2\left(t^{TZ}\right)^2 - (\Delta x)^2\right]^{1/2}} \right\} \times \left\{ \left(t^{TZ} \times \Delta t^{TZ}\right) - \frac{(\Delta x)^2\left(\Delta t^{TZ}\right)^2}{2\left[\left(v^{TZ}\right)^2\left(t^{TZ}\right)^2 - (\Delta x)^2\right]} \right\} \qquad (1)$$

where v^{TZ} is the normal move-out velocity of the residually saturated material, t^{TZ} is the traveltime of the transition zone reflection in the pre-pumping profiles, Δt^{TZ} is the change in traveltime of the transition zone reflection during the experiment and Δx is the antennae separation (0.5 m).

Figure 2-6 gives a plan view of Δh^{TZ} calculated for various times during the test. The drawdown portion of the test is displayed in Figure 2-6a – g. It is clear that the transition zone reflection becomes depressed around the pumping well. This depression becomes deeper and grows spatially with increased duration of pumping. The transition zone has been affected across almost the entire study area by the end of the pumping portion of the test. The growth of this GPR-imaged "drainage cone" is similar in shape to that expected of the water table during a pumping test. The recovery of

the transition zone (Figure 2-6h – j) is also similar to what would be expected of water table, becoming more shallow with time.

The lowering of regional water levels is also reflected in the plan view of the GPR-derived drainage cone, where a significant portion of Figure 2-6j remains at least 0.10 m below the background level of the transition zone reflector. However, portions in the northern half of the study site have returned to background levels. This area of the site is the home of a pine forest and it is possible that the root zone of this forest draws water up and maintains moisture within the unsaturated zone.

The data presented in Figure 2-6 shows local variations in drainage during the pumping test. These localized variations are a result of differential drainage due to small-scale changes in aquifer properties. It is reasonable to expect that these variations would also affect the potentiometric data, however, it would be difficult to detect these heterogeneity effects with traditional observation wells, given their sparse spatial sampling. The spatial sampling of GPR far surpasses that which could be obtained through traditional observation well methods and allows the imaging of these heterogeneities.

2.5 Comparison of Field Measurements

For the purpose of comparing the various types of measurements acquired as part of the pumping test, drawdowns relative to their pre-pumping level were determined and plotted versus time for each method (Figure 2-7). We will first compare the measurements of the transition zone response. The direct observations of the vertical movement of the transition zone were obtained from the neutron logging displacement of the 50% saturation point. The choice of the 50% saturation point was an arbitrary one; however, the simple translation of the transition zone during the test implies that movement of a reference saturation in the moisture profile will quantify that translation.

GPR-derived transition zone drawdown is the average of all GPR-estimated drawdown between 1 and 2 m from the pumping well. This averaging was done for noise suppression and gives a GPR-derived drawdown estimate for a radial distance of 1.5 m from the pumping well. Error bars for the GPR-derived drawdown on Figure 2-7 are an estimate of the potential uncertainty in this quantity due to ±0.5 ns accuracy in determining reflection traveltimes.

It is clear from Figure 2-7 that the neutron- and GPR-derived transition zone drawdowns are very similar to each other during both pumping and recovery. Further, both transition zone drawdowns are about 0.25 m below their pre-pumping levels after five days of recovery, a result of the regional

decline in water level. The only major difference between the two quantities occurs at 9900 minutes, immediately prior to pump shut-off, when the GPR data has a significantly high level of noise interference. The minor discrepancies between the responses could be the result of localized aquifer heterogeneities or the small difference in radial distances from the well (i.e., 1 m for the neutron logging versus 1.5 m for the effective GPR sampling point). The close similarity between these two independent measures of transition zone movement supports our assumption (based on the invariant transition zone shape and thickness observed on the neuron logs) that the measured changes in reflection traveltime are directly related to the translation distance of the transition zone.

For a comparison between the hydraulic head data and the transition zone behaviour, the water level data from well WD1A, located 1.5 from the pumping well, is shown on Figure 2-7; this well is screened about 3.2 m below the surface. The detailed temporal monitoring performed in well WD1B, located 3 m from the pumping well, is also provide so that rapid early-time variation in the hydraulic head measurements can be observed. The dissimilarity in drawdown between these two observation wells is expected due to the different distances from the pumping well.

It is obvious from Figure 2-7 that the transition zone drawdown differs from that of the hydraulic head levels. It is delayed relative to hydraulic head drawdown, indicating a lag in the response of the transition zone to a decline in the hydraulic heads. Throughout much of the latter portion of the pumping test, the hydraulic head drawdown measured in WD1A is 0.18 m greater than the transition zone drawdown. A similar experiment at this site by Endres et al. (2000) found a consistent 0.20 m difference between the GPR-derived transition zone and hydraulic head drawdowns after about 1600 minutes of pumping. In addition, laboratory experiments have identified 0.20 m pressure head difference between wetting and drainage curves for Borden sand (Nwankwor et al., 1984), suggesting that the observed difference between the transition zone and hydraulic head drawdowns is related to the entry pressure required to start drainage.

The difference between the transition zone and hydraulic head drawdown is less during recovery, about 0.12 m very early into recovery and approximately 0.08 m once the transition zone equilibrated with the recovery rate after about 1500 minutes. The smaller difference in hydraulic head and transition zone drawdowns during recovery indicates that imbibition of the aquifer material occurs more rapidly than drainage, perhaps due to the water wet nature of most aquifer materials.

Looking back to the water content profiles in Figure 2-4, it is seen that the thickness of the transition zone does not significantly change during pumping. Thus, the time lag in the transition

zone response is not due to excess water being stored in the transition zone but due to excess storage within an extended tension-saturated capillary fringe.

An interesting transient feature is present in the neutron-derived transition zone data on Figure 2-7 just before 10,000 minutes (60 minutes into recovery). At this time, the 50% saturation point in the transition zone had declined 0.02 m below the position it held immediately prior to pump shut-off. By 120 minutes into recovery, this point had returned to the same depth it was at prior to pump shut-off. This indicates that although drawdown of the hydraulic heads had ceased and recovery had started, the downward movement of the transition zone continued for some time, possibly for 60 minutes. The cause of this transient phenomenon is currently not well understood.

2.6 Aquifer Drainage

The GPR-derived transition zone drawdowns were used to estimate the drainage cone volume (i.e., the drained aquifer volume); a GPR estimate of the drained water volume was obtained by multiplying the drainage cone volume by the specific yield of the aquifer. A number of different methods were used to derive the drainage cone volume. Initially, drainage cone volume estimates based on a single distance-drawdown relationship were used; this approach suppresses the effects of small-scale drainage variations. Three different functions (i.e., 2nd and 3rd order polynomials and a logarithmic function) were fitted to the GPR-derived transition zone drawdown. Correlations of the fitted functions ranged from $R2 = 0.65$ to 0.76 with the 3rd order polynomial consistently providing the best-fitting function. The cone volumes were obtained by integrating these functions with respect to radial distance.

Two methods were used to incorporate information about aquifer heterogeneity obtained from the GPR data into the estimated drainage cone volume. The first method used a system of concentric elemental annular segments that are centered about the origin of the GPR profile lines. Figure 2-8 illustrates the definition of these segments. Where a gap in GPR coverage existed, the neighbouring elemental annular segments were extended to fill the gap. The area of the element was multiplied by the GPR-derived transition zone drawdown for the sample point to obtain the elemental drained volume; the drained aquifer volume was computed by summing the drained volume of the elements. The second method used the SURFER software package to interpolate the GPR-derived transition zone drawdown samples onto a rectangular 1 m by 1 m grid covering a 100 m by 100 m area. The drained aquifer volume was also determined using the software package.

These drained aquifer volumes were converted into drained water volumes using a laboratory-determined long-term specific yield of 0.30 for the medium-fine sand at the Borden test site given by Nwankwor et al. (1984). The neutron logging data shows that the drained portion of the aquifer attains residual saturation as the water content profiles translates downwards. Hence, this specific yield value is appropriate for these calculations. Figure 2-9 presents the actual pumped water volume and the drained water volume obtained from the different methods; Figure 2-10 shows the calculated drained water volumes as a percentage of the pumped water volume.

The volumes based on the best-fitting functions yield low estimates of drained water volume. With the exception of the high value at 116 hours, these estimates based on the best-fitting functions only account for an average of 50% of the actual pumped water volume.

The elemental annular segment method provided a larger estimate of drained water volume. At 20 hours of pumping, the drained water estimate is nearly 70% of the pumped volume and 63% of the pumped water can be accounted for at the end of the pumping portion of the test. Overall, the average drained volume estimate is 58% of the actual pumped volume. It should be noted that a maximum radial distance of 49 m was used in these calculations. Beyond this distance, the volume of the annular segments would have been based on the drawdown of one GPR line; this would produce an unacceptably large elemental segment in light of the degree of aquifer heterogeneity observed at the site. Hence, this method will underestimate the drained water volume. However, simple calculation suggests that it is unlikely the extra drainage volume beyond 49 m could account for the missing water.

The average drained water volume based on the interpolated GPR-derived transition zone drawdown data is 65% of the actual pumped water, with 80% of the water being accounted for at the end of the test. This method was allowed to predict drainage occurring beyond the extent of the GPR lines and still underestimates the pumped water volume by a significant amount.

The results of this study suggest that small-scale differential drainage due to aquifer heterogeneity is an important factor when assessing drained water volume from this aquifer. The estimates based on best-fitting functions that attenuate heterogeneity effects are consistently lower than the elemental annular segment and interpolated grid methods that incorporate small-scale drainage information. However, there is a significant discrepancy between the GPR-estimated drained water volume and the actual pumped water volume. An analysis of potential uncertainties in the GPR-estimated drained water volume (e.g., traveltime errors and EM wave velocity variation) could not explain the difference.

Further, it is improbable that the discrepancy between the estimated drainage and actual pumped volumes can be accounted for by release of water from elastic storage. Endres et al. (2000) investigated this possibility; they concluded that a specific storage about 20 times larger than that determined by Nwankwor et al. (1984, 1992) would be required to produce the unaccounted water. This value of specific storage would be exceptionally large for this type aquifer material.

Another potential source of additional non-drainage water is leakage from the underlying aquitard. Fractures have been identified in the underlying aquitard in the vicinity of the pumping test site (Morrison, 1998; Mosad, 1999). Sand lenses have also been observed in this aquitard unit. Further, there is evidence that the aquifer is laterally discontinuous to the north of the test site. One or all of these factors could provide sufficient leakage to account for the water volume discrepancy.

2.7 Conclusions

While a previous study by Endres et al. (2000) demonstrated that GPR is capable of providing detailed images of pumping-induced dewatering in unconfined aquifers, the drained water volume estimates derived from the GPR data were significantly smaller than the actual pumped water volume. Among the potential causes cited for these discrepancies were the following: small-scale variations in dewatering were not adequately characterized; and behaviour of the transition zone reflection event did not accurately portray changes in the water content profile. To further examine these potential causes, a seven-day pumping and five-day recovery test was performed at the site used by Endres et al. (2000). The spatial coverage of GPR profiling in this new test was significantly increased over that used by Endres et al. (2000). In addition, a neutron moisture probe was used to directly observe changes in the water content profile, allowing a comparison between its response and the behaviour of the transition zone reflection.

It was observed on the neutron logs that the water content profile underwent a simple translation downwards and upwards in response to pumping and recovery, respectively. Hence, the shape and thickness of the transition zone was not significantly altered during the experiment. These conditions imply that the traveltime changes of the GPR transition zone reflection are directly related to the translation distance of the transition zone. This conclusion is strongly supported by the close similarity between the neutron- and GPR-derived transition zone drawdowns observed in this experiment.

A comparison of the transition zone and hydraulic head drawdown clearly shows that drainage is delayed relative to hydraulic drawdown. Further, at a 1 to 2 m radial distance, there is a consistent

0.18 m difference between the transition zone and hydraulic head drawdowns during pumping that is likely a manifestation of the entry pressure needed to initiate drainage. This delayed drainage results in excess water storage within an extended capillary fringe. The difference between transition zone and hydraulic head drawdowns is less during recovery, suggesting that imbibition occurs more rapidly than drainage.

A number of different methods were used to estimate the drained water volume from the GPR-derived transition zone drawdown information. Estimates obtained from methods that incorporate small-scale drainage information were consistently greater than estimates acquired from methods that suppress heterogeneity effects. However, there is a significant discrepancy between the GPR-estimated drained water volume and the actual pumped water volume. It is quite possible that a substantial amount of water enters the unconfined aquifer through a leaky underlying aquitard.

It is apparent from this study that information from GPR images can be used to accurately describe changes in the water content profile due to pumping and recovery. While a method for incorporating GPR-derived information into pumping test analyses is yet to be determined, it is clear that this non-invasive technique should have an important role in the characterization of unconfined aquifers.

2.8 Acknowledgements

This work was partially supported by an Individual Research Grant to Dr. Endres from the Natural Sciences and Research Council of Canada. I would like to thank the many individuals that provided assistance during this work.

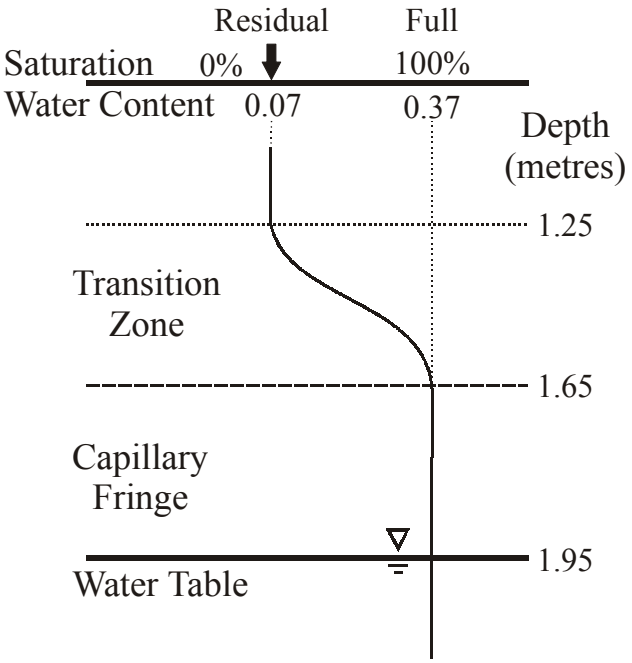

Figure 2-1 - Soil moisture profile at the test site prior to starting the pumping test.

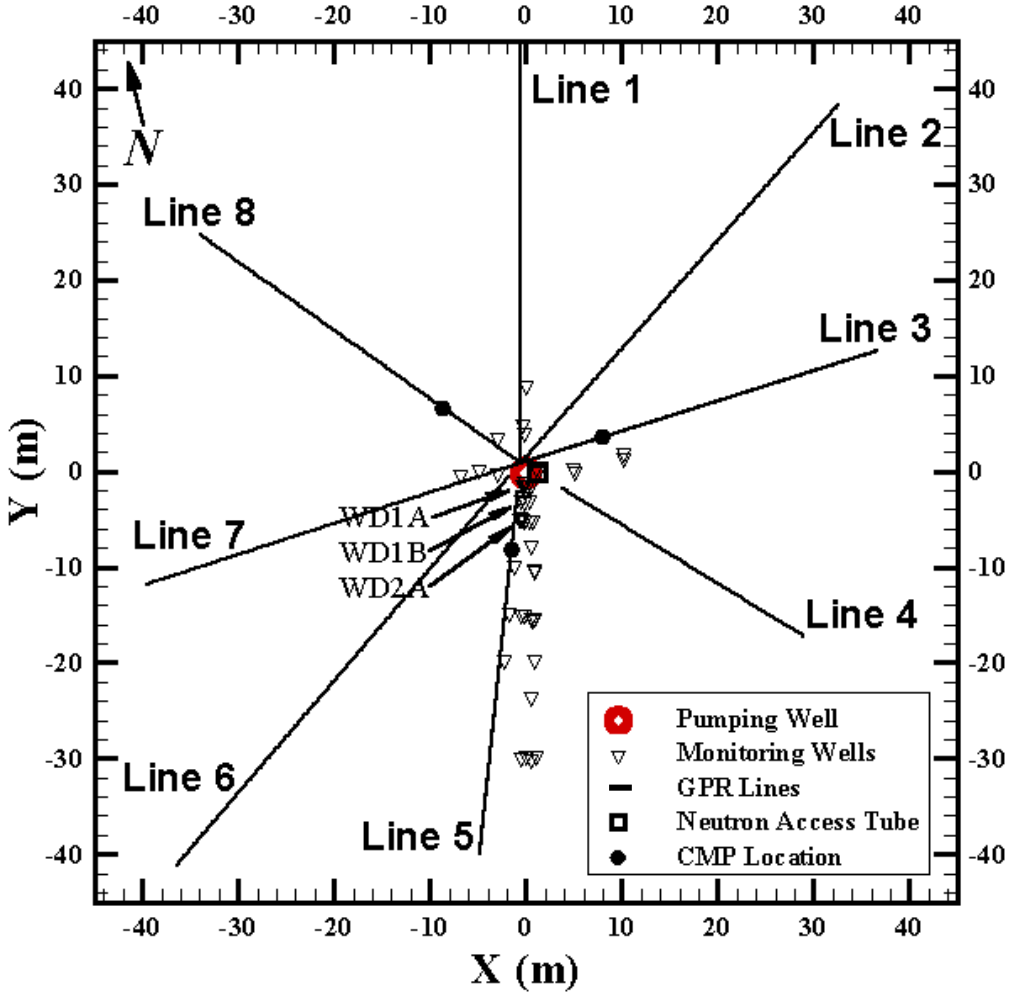

Figure 2-2 - Layout of existing instrumentation and GPR profile lines at the pumping test site at CFB Borden.

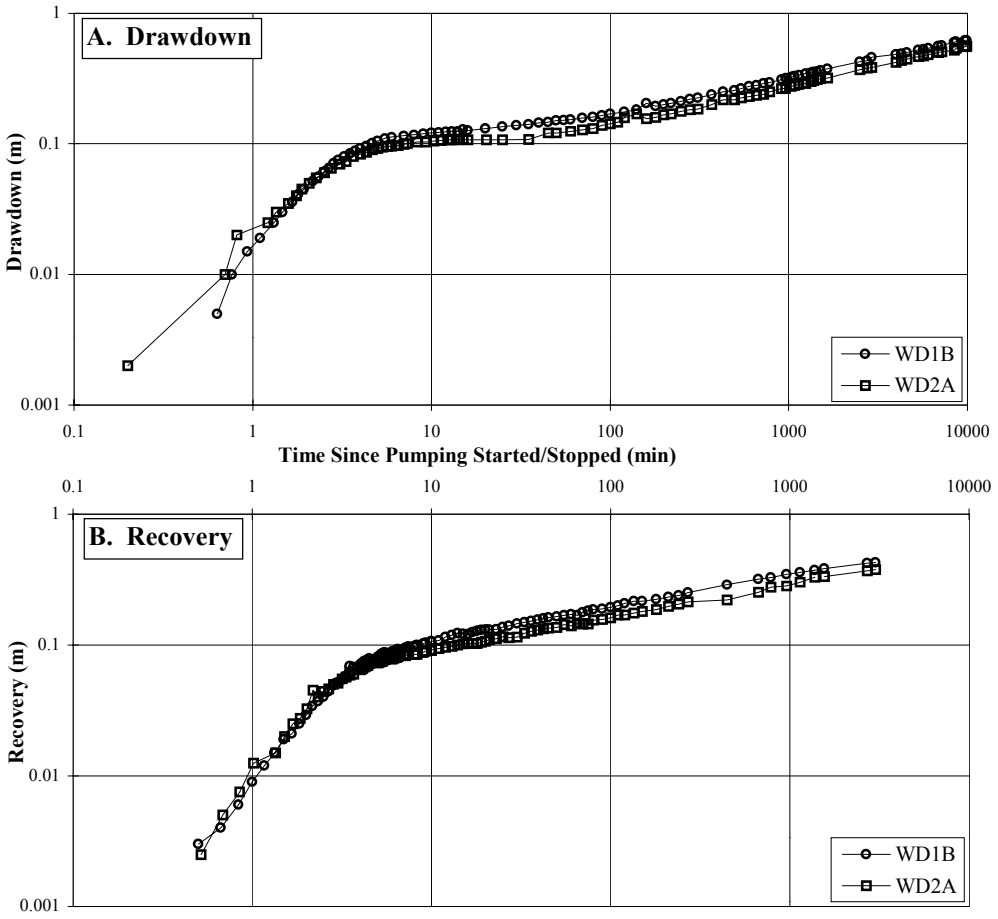

Figure 2-3 - A. Drawdown of hydraulic head levels. B. Recovery of hydraulic head levels.

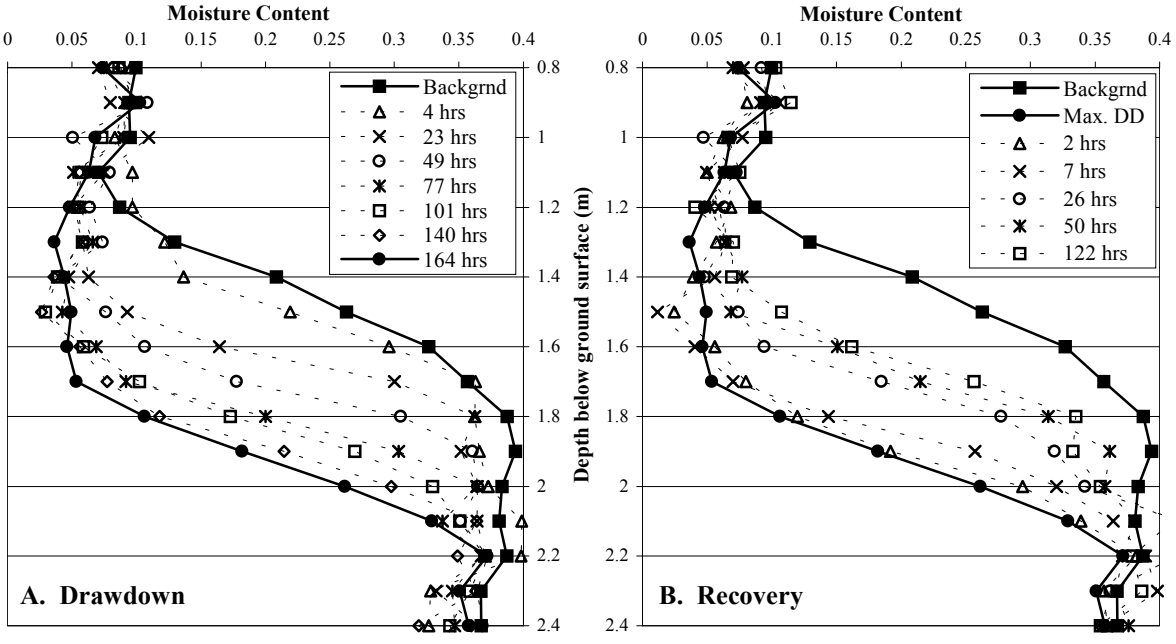

Figure 2-4 - Temporal water content profiles obtained through neutron logging in a sealed observation well at 1 m distance from the pumping well. A. Drawdown profiles. B. Recovery profiles.

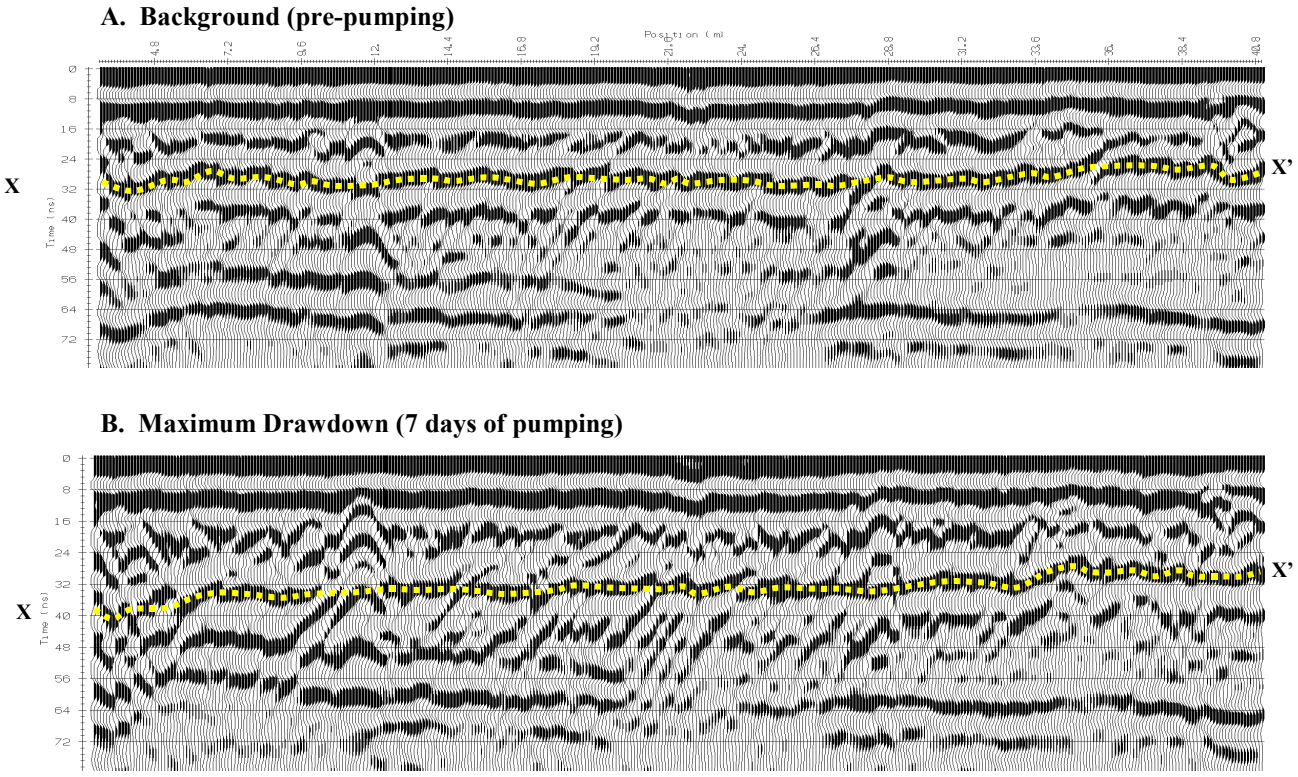

Figure 2-5 - GPR profiles on line 5. Event X-X' is the reflection from the transition zone. A. Background (pre-pumping) profile. B. Profile obtained immediately prior to pump shut-off, after seven days of pumping. (Pump is located 3 m off left side of figure.)

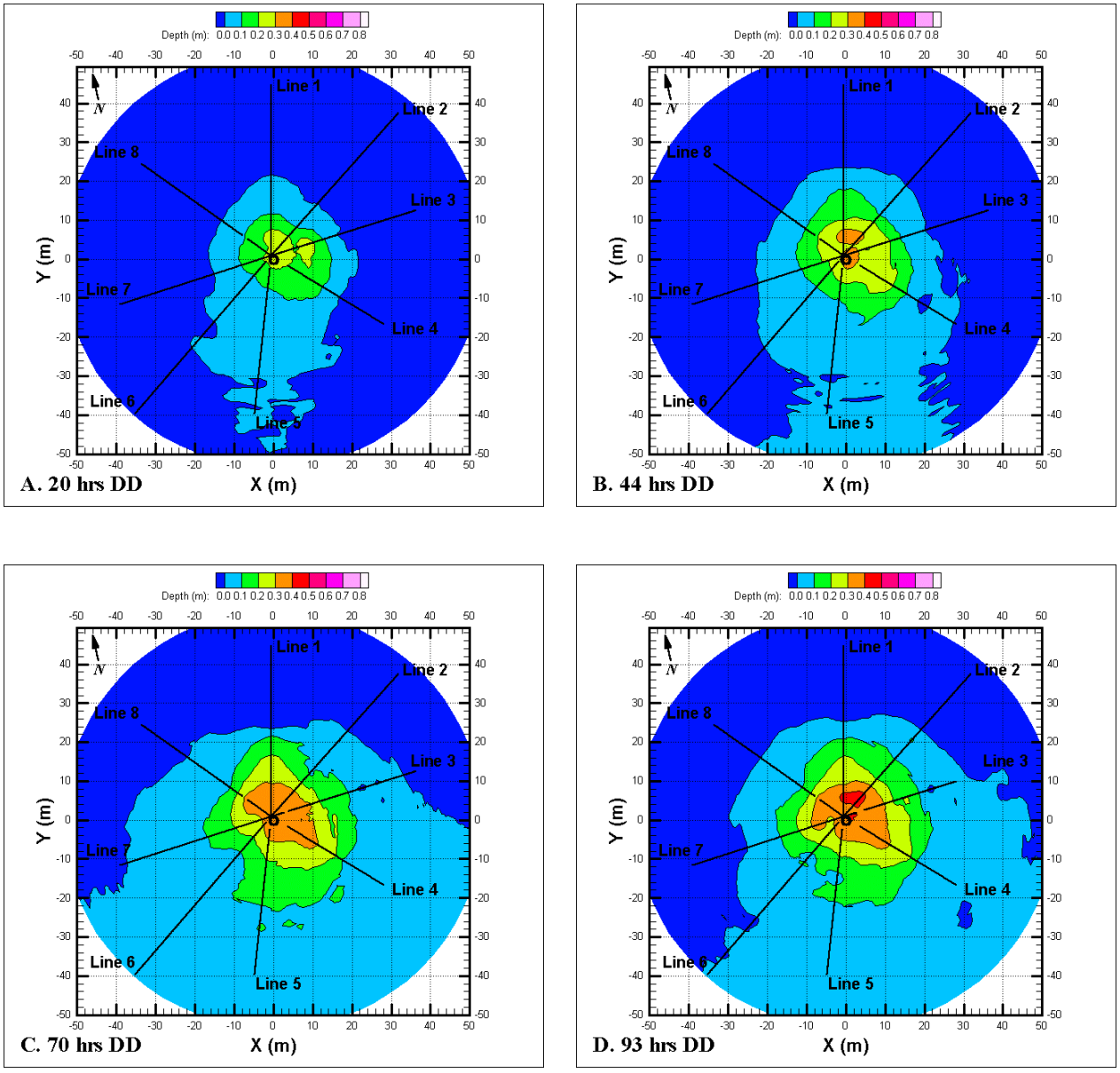

Figure 2-6 - Plan view of GPR-derived drainage cone at different times of pumping and recovery.

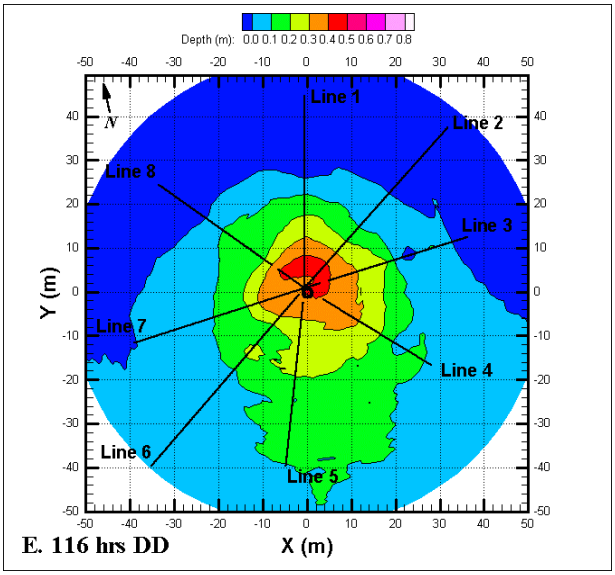

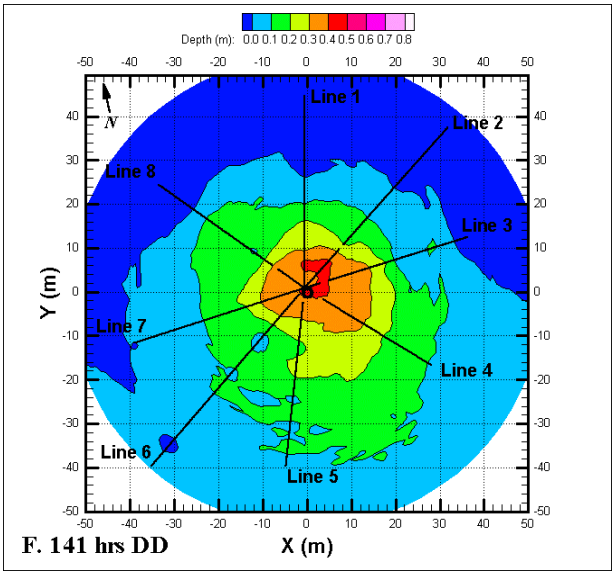

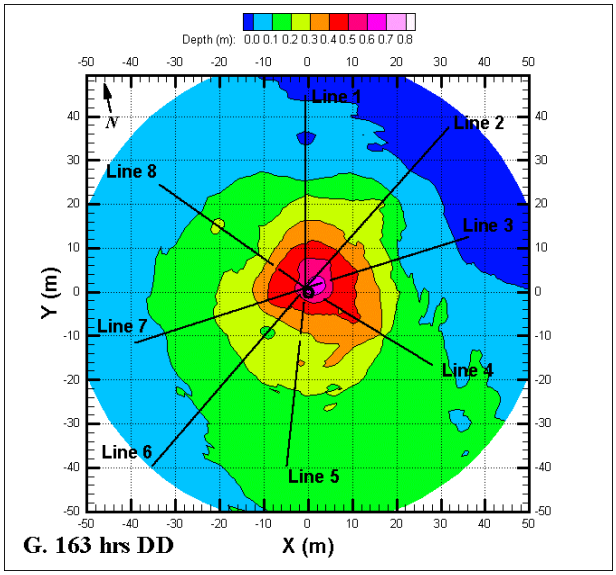

Figure 2-6 (Cont.'d) - E - G

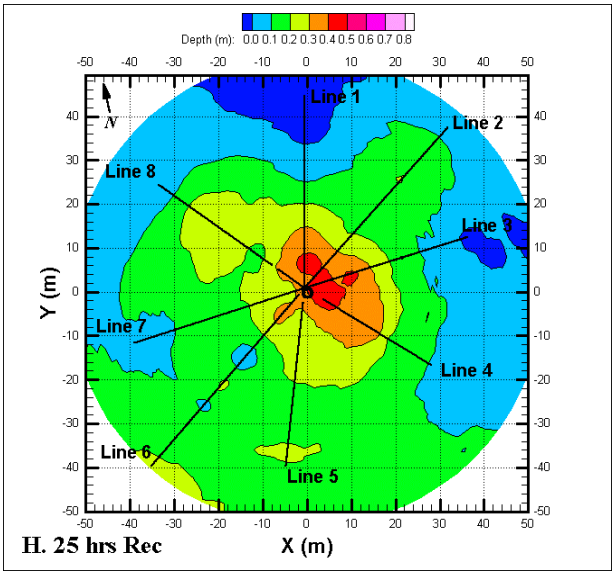

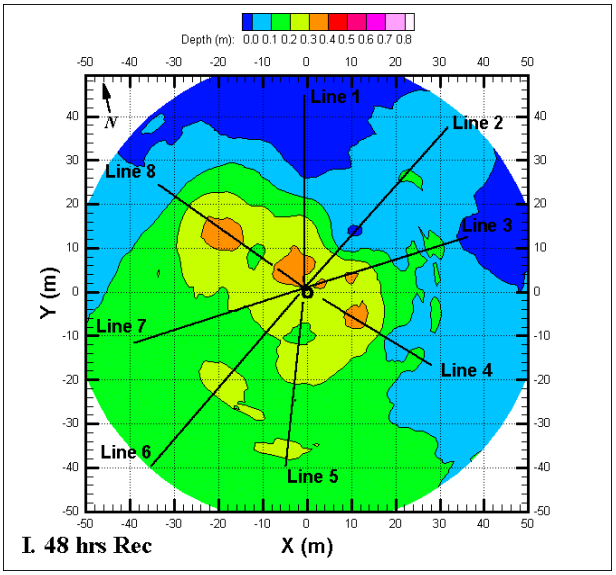

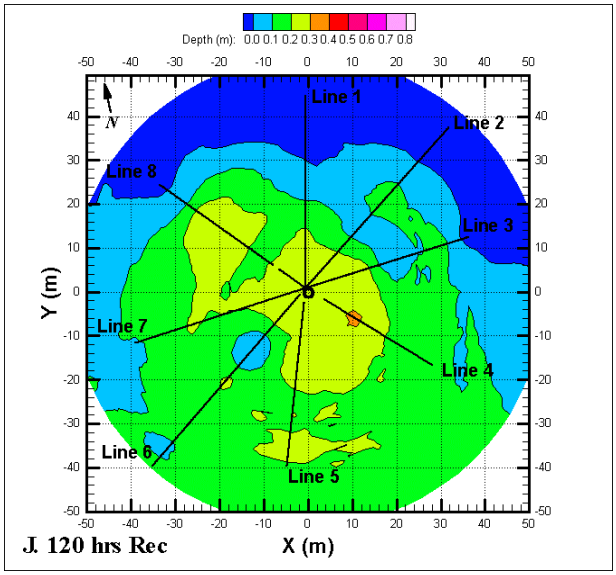

Figure 2-6 (Cont.'d) - H - J

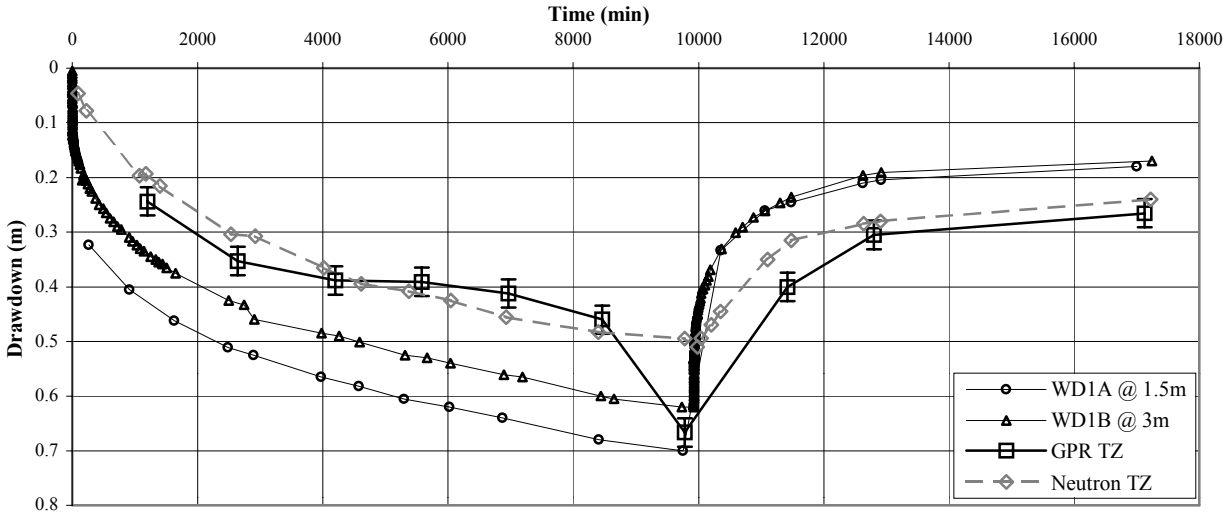

Figure 2-7 - Drawdown and recovery of hydraulic head levels and the transition zone. Pump was shut off and recovery began at 9900 minutes. Error bars correspond to traveltime picking uncertainty of ± 0.5 ns.

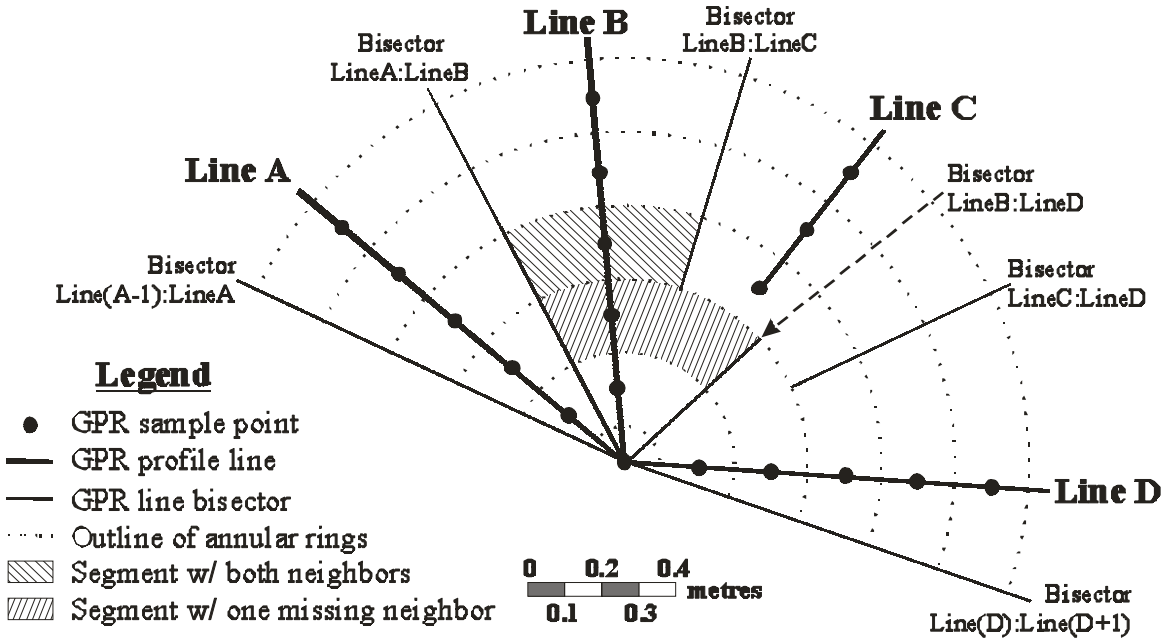

Figure 2-8 - Representation of how annular volume segments were defined. Bisectors were placed between GPR profile lines. Volume was calculated between the nearest neighbouring bisectors, based on drawdown at a particular data point being the average drawdown between the previous and next point on that profile line.

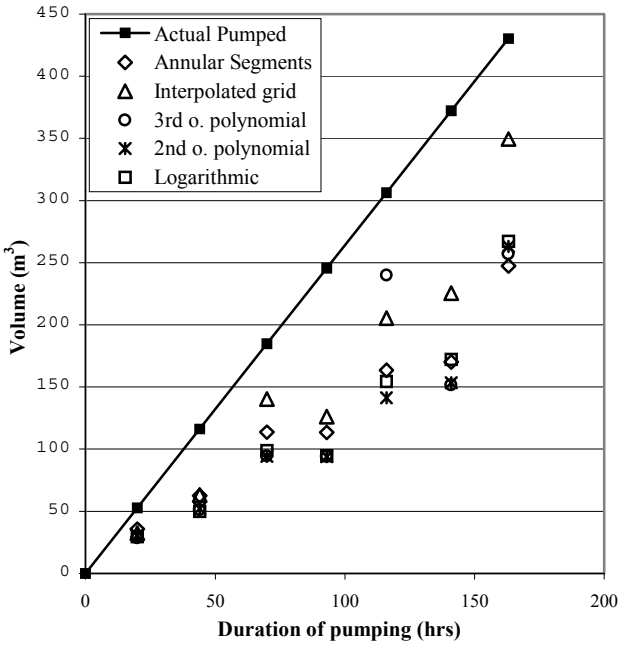

Figure 2-9 - Actual pumped water volume and estimated drained water volumes.

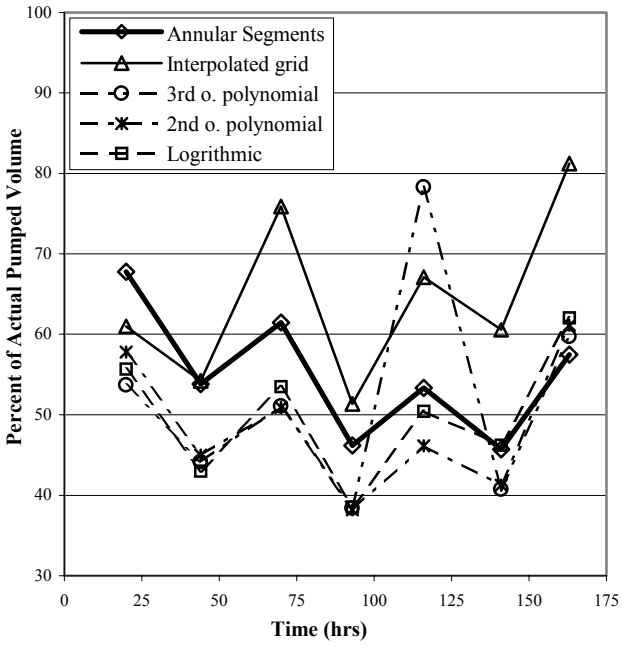

Figure 2-10 - Estimated drained water volumes as a percentage of actual pumped water volume.

Chapter 3
A Detailed Study of Pumping-Induced Drainage and Recovery in the Unconfined Borden Aquifer

Abstract

A seven-day pumping test and five-day recovery test was performed in the unconfined aquifer at Canadian Forces Base Borden in Ontario, Canada. Hydraulic head levels were intensively monitored in eleven observation wells and the moisture content profile was frequently logged at six locations of increasing radial distance from the pumping well.

The hydraulic head levels behaved in a manner typical of unconfined aquifers. Downward vertical gradients were seen to form rapidly after pumping began, reaching maximum values within ten minutes; a slow decline followed, with significant gradients remaining after seven days. Vertical gradients were minimal at a distance of 15 m. The moisture content profile responded to pumping within 480 minutes, essentially translating downward with very little change in shape or thickness. This indicates that no excess storage was formed within the transition zone. During pumping however, the capillary fringe extends significantly; this extension grows with increased pumping and persists throughout the entire test. The extension of the capillary fringe is greatest near the pumping well and decreases radially. This represents a significant volume of excess storage above the water table, extending to a radial distance of between 20 and 25 m. A relationship between the hydraulic gradient and the capillary fringe extension is unclear. These results suggest that the volume-balance method of calculating specific yield (Nwankwor et al., 1984, 1992) using late-time hydraulic head data will not accurately describe drainage occurring above the water table.

During recovery, the hydraulic head levels recovered nearly all of the pumping-induced drawdown within 4200 minutes. Behaviour of the vertical hydraulic gradient during recovery showed a rapid reversal into an upward gradient, again reaching a maximum within 10 minutes followed by a slow decline. No significant gradients existed at 15 m. The transition zone translated upwards, without significant or consistent variations in thickness or shape. However, while the water levels recovered almost completely to their pre-pumping elevations, the transition zone appeared to stabilize approximately 0.20 m below its background position. It is suggested that this lack of full recovery is a result of the air-entry pressure of the aquifer material and that the static transition zone/capillary fringe configuration will slowly be recovered through horizontal flow above the water table.

3.1 Introduction

Unconfined aquifers are often characterized by the analyses of pumping test data. The type-curve analyses provide reasonable estimates of transmissivity and storativity. Moench (1994) stated that careful analyses can provide reasonable estimates of aquifer parameters (i.e., transmissivity, storativity, hydraulic conductivity, specific yield) through type-curve procedures. However, in practice, unreasonably low values of specific yield are often obtained.

Accurate values of specific yield are important to properly quantify the potentially extractable volume of water from an unconfined aquifer; the source of this water is predominantly drainage from above the water table. It has been proposed that the poor estimates of specific yield are a result of inadequately incorporating pumping-induced drainage into the analytical solutions used for analyses (Nwankwor et al., 1984, 1992). Moench (1995) and Moench et al. (2001) proposed revised analytical solutions incorporating mechanisms that allow for the gradual release of water from above the water table. While this approach is an improvement over the previous models, it involves the use of empirical parameters to approximate drainage. The ideal solution to the analysis of unconfined aquifer test data would be based on a description of the physical processes and mechanisms involved in pumping-induced drainage and subsequent imbibition. To do this, in-situ observations of drainage and recovery are required.

Drainage processes occurring during a pumping test in an unconfined aquifer are poorly understood. The processes occurring above the water table during recovery are essentially unknown. However, the analytical type-curve solutions for drawdown are also used in the analysis of data from aquifer recovery tests. A better understanding of these drainage and imbibition processes at the field-scale could lead to improved solutions for analyzing pumping and recovery test data.

Presently, field-scale data on pumping-induced drainage are limited; recovery-induced imbibition data are non-existent. Nwankwor et al. (1992) performed pumping tests during which hydraulic head and moisture content data were acquired; aquifer recovery was not monitored. Moisture content data were obtained directly through a gamma attenuation technique and gravimetric water content analyses performed on soil cores obtained during pumping. While these data provided useful information on pumping-induced drainage, the tests were of too short a duration to observe the longer-term relationships between drainage and hydraulic drawdown. An increase in the aerial and vertical sampling density of moisture content would provide much needed resolution as well.

Earlier work by Endres et al. (2000) demonstrated that aquifer drainage could be imaged using GPR; however, their results raised issues regarding the quantification of aquifer response from GPR

data. Chapter 2 outlined a seven-day pumping test at the same site as Nwankwor et al. (1984, 1992) with the goal of using non-invasive ground penetrating radar (GPR) techniques to monitor drawdown and recovery. GPR was used to define a pumping-induced drainage cone. The volume of water extracted from the drainage cone was calculated from previously published values of specific yield for the aquifer (Nwankwor et al., 1992); the volume of drained water was less than the pumped water volume. One of the reasons proposed for this disagreement was that there is an incomplete understanding of unsaturated drainage. The recovery of the test outlined in Chapter 2 showed that recovery of the transition zone was not complete after five days; lack of full recovery was also reflected in the GPR images.

To further investigate the spatial and temporal variations of moisture content in the unconfined Borden aquifer, a second seven-day pumping and five-day recovery test was designed. Increased in-situ instrumentation allowed for an increased sampling density of the moisture content profile, both spatially and with depth. The behaviour of the hydraulic head levels were intensively monitored as well. The goal of the experiment was to observe drainage and imbibition characteristics in the context of pumping test analyses and to study the relationship between the unsaturated and saturated zones during pumping and recovery.

3.2 Site Description

A well instrumented pumping test site at Canadian Forces Base Borden, near Barrie, Ontario was used to conduct the pumping and recovery test. This site was used for the test discussed in Chapter 2 and has been the focus of several other experiments (Nwankwor et al., 1984, 1992; Endres et al., 2000).

The unconfined aquifer is composed primarily of medium-grained sand of glacio-deltaic or glacio-fluvial origin. It can be locally very heterogeneous due to the presence of lenses and beds of fine-, medium-, and coarse-grained sand (MacFarlane et al., 1983). Significant spatial variability in hydraulic conductivity also exists among discontinuous beds and lenses up to several metres in length (Sudicky, 1986). The aquifer is approximately 9 m thick; it is underlain by a clayey silt aquitard. At the time of the test in August, 2001, the initial water table depth was 2.75 m, giving an initial saturated aquifer thickness of about 6.25 m. The transition zone from residual water content (0.07) to full saturation (0.37) extends for approximately 0.4 m overtop of a capillary fringe that is 0.3 m thick (Nwankwor et al., 1984). Figure 3-1 is a schematic diagram that shows the static water content profile for this site denoting the different zones.

The pumping well at the site has a 0.13 m inner diameter (ID) with a stainless steel slotted telescopic screen over the bottom 3.65 m of the aquifer. Forty-two observation wells are distributed at various distances from the pumping well; these wells are screened over 0.35 m intervals at various depths within the aquifer. While all wells were monitored, the present experiment will focus on a set of intensely monitored wells trending southward from the centrally located pumping well. These particular wells were selected because they could provide hydraulic gradient information in the proximity of newly installed moisture content instrumentation.

For the present experiment, six neutron moisture probe access tubes were installed for monitoring the water content profile during pumping and recovery. These holes were drilled to depths of approximately 4 m and fitted with sealed 0.05 m ID PVC casings. These access tubes were placed at various distances from the pumping well (1, 3, 5, 10, 15 and 20 m) along the southward trending transect of observation wells. Figure 3-2a displays a plan view of the wells and access tubes; Figure 3-2b shows a cross-section of the southern transect.

A series of eight GPR profile lines were arranged radially from a point located 1 m from the pumping well. This offset was required to minimize interference by the steel pumping well with the GPR signal. Three of these lines were monitored in detail, while data on the remaining five was acquired for a spatial view of drainage.

3.3 Field Methods

The pumping test was performed for 7 days at a constant discharge rate of 40 ± 1 l/min; the subsequent recovery was monitored for 5 days. Hydraulic head levels were measured in 11 observation wells trending southward from the pumping well using a pressure transducer and data logging system, providing water level drawdowns accurate to 0.007 m. Measurements of hydraulic head were made in the remaining 31 wells to gain a spatial view of the cone of depression using an electrical acoustic sounder accurate to 0.005 m. These measurements were made twice daily, either immediately prior to or immediately after neutron moisture content logging and GPR profiling.

Water content distribution was measured through the access tubes using a Campbell Pacific Nuclear (CPN) Corporation 503DR thermal neutron probe. This tool emits high-energy neutrons from a 50mCi Americium-241/Berylium source and counts the number of thermal neutrons moderated en-route to a detector over a user specified time interval. A linear field calibration (described in Appendix D) was used to convert the neutron count readings into water content. Neutron logging was performed from a depth of about 1.25 m to 3.5 m below ground surface at a

sampling interval of 0.05 m. This logging interval provided complete coverage of the transition zone throughout the entire experiment.

GPR profiling and common mid-point (CMP) surveys were performed to image the transition zone reflector. These data were collected in a manner similar to that described in Chapter 2. Unfortunately, equipment problems and varying surface conditions resulted in poor images of the static background transition zone upon which subsequent analyses are based. Thus, the discussion of GPR results will be necessarily brief.

3.4 Experimental Results

3.4.1 Pumping Test

3.4.1.1 Hydraulic Head Data and Hydraulic Gradients

The time-drawdown data for the deep-shallow observation well pairs located in the immediate vicinity of the neutron access tubes is shown on Figure 3-3 (and is also included in Appendix B and on the accompanying CD-ROM). The response observed in all wells is a typical three-phase curve for unconfined aquifers. The magnitude and timing of drawdown varies systematically with both depth and radial distance; nearby deep wells show an earlier and greater response than shallow and distant wells. Type-curve analyses of the data using the Neuman (1974) solution gave aquifer parameters consistent with those obtained by Nwankwor et al. (1984, 1992) (see Appendix E).

Figure 3-4 shows the vertical hydraulic gradients for the deep-shallow well pairs during the pumping test. Prior to the test, vertical gradients were zero. For the pairs up to 5 m distance, a downward gradient develops immediately and reaches a maximum value within the first 10 minutes of pumping. The gradients slowly decrease throughout the remainder of the pumping test with significant gradients remaining at the end of pumping on day 7 to at least 5 m; at 1 and 5 m, the vertical gradients remained 80% and 40% of their respective early-time maximums. The magnitude of the gradient decreases with radial distance, being very small at 15 m.

3.4.1.2 Moisture Content Data

Selected moisture content profiles obtained before and during the pumping test for the six access tubes are given in Figure 3-5a-f. Raw moisture content data, the transformation process to moisture content and potential error are included in Appendix D and on the accompanying CD-ROM. The background profiles show the transition zone thickness to be between 0.40 and 0.45 m, which is

comparable to the thickness of 0.40 m given by Nwankwor et al. (1992). Comparison of background hydraulic head levels and the base of the background transition zone profile gives a static pre-pumping capillary fringe thickness of between 0.30 and 0.35 m, again consistent with the thickness of 0.30 m given by Nwankwor et al. (1992).

Drawdown of the transition zone was observed at all locations, up to 20 m from the pumping well. It can be seen in Figure 3-5 that drainage begins within 480 minutes and continues throughout most of the pumping test. The moisture content profiles obtained during pumping appear to translate downwards without significant changes in shape or thickness relative to the background profile. There is a minor deviation at the lower moisture content, θ_w, range ($0.07 \leq \theta_w \leq 0.15$) at the top of the transition zone where this portion of the profile is shifted to slightly higher θ_w values. This feature persists up to 2200 minutes, gradually receding back with time to the residual θ_w level. Hence, the transition zone appears to essentially drain fully to residual saturation at later times (i.e., after 2200 minutes).

Figure 3-5a and c (at 1 and 5 m, respectively) show the effect of rainfall on the unsaturated zone – the level of residual saturation is elevated at 10,560 minutes of pumping, followed by a decrease with depth before the top of the transition zone. This is a result of a rainfall event increasing the near-surface moisture content as it infiltrates through the unsaturated zone. At no time was this effect seen to merge with the top of the transition zone, indicating that the transition zone was not affected by rainwater infiltration during the pumping test. This rainfall effect was not observed at the other radial distances, possibly because of near-surface heterogeneities and ground cover.

To further examine potential variations in the transition zone during pumping, the drawdown of three immediate θ_w values were determined (i.e., θ_w = 0.16, 0.22 and 0.28, representing 30%, 50% and 70% of full water saturation, respectively); the results are displayed in Figure 3-6a-f. The drawdowns of the three saturation levels are consistent with each other, although at some radial distances, the less saturated portion of the transition zone (30% saturation) has a slightly greater drawdown than the higher values of θ_w, indicating a possible contraction of the transition zone. However, this variability is not consistent at all locations. The behaviour showing nearly equal drawdown supports the suggestion that the moisture content profiles are translating downward with only minor variations in shape.

Figure 3-6 shows that the magnitude of drawdown of the transition zone decreases with increasing distance from the pumping well. The drawdown rate during the first 4000 minutes of pumping also decreases with distance. The declining rate is most significant at the sites close to the

pumping well. A nearly constant drawdown rate occurs during the first 4000 minutes at 20 m. Between 6000 to 8000 minutes of pumping, the drawdown rate is very slow and may be approaching a quasi-steady state.

3.4.2 Recovery Test

3.4.2.1 Hydraulic Head Data and Hydraulic Gradients

Time-drawdown data for the recovery of the hydraulic head levels is shown in Figure 3-7. As was the case during pumping, the deep observation wells closer to the pumping well show an earlier and greater response than the shallower and more distant wells. A temporal comparison of the hydraulic head data for the pumping and recovery test clearly shows systematic differences with radial distance and depth. In some cases, such as at 15 meters, these differences are substantial. The differences are particularly obvious during intermediate times (i.e., between 5 and 1000 minutes). Where the drawdown curves show a flattening (i.e., slower rate of drawdown) during this time period, the recovery figures continue to rise (i.e., continue to recover); the difference is greater for the shallow wells.

Vertical hydraulic gradients for the recovery portion of the experiment are displayed in Figure 3-8. The vertical gradients responded to the cessation of pumping very quickly (i.e., within 1 minute). The downward gradients are rapidly reversed into upward gradients. A maximum upward gradient occurs within 10 minutes, after which they slowly diminish until the end of recovery monitoring. The magnitudes of the upward gradients are smaller than the corresponding downward gradients observed during pumping; at 1, 3 and 5 m, the upward gradients are 20, 40 and 50% of the maximum pumping gradient, respectively. The vertical gradients decrease with radial distance and are essentially zero at 15 m.

3.4.2.2 Moisture Content Data

Moisture content profiles obtained during the recovery test are shown in Figure 3-9a-f. In a manner analogous to drawdown, the moisture content profiles translate upwards without significant changes in shape or thickness relative to the background profile. However, comparison with the initial pre-pumping background profile clearly shows that recovery is incomplete after 5 days. Also, the zone of slightly higher θ_w values seen near the beginning of pumping at the top of the transition zone, reoccurs during recovery at similar elevations; this similar behaviour in both tests indicates that the likely cause is vertical heterogeneity in the aquifer material.

The infiltrating rainfall event noted in the moisture content profiles from the pumping test at radial distances of 1 and 5 m (Figures 3-5a and c) is also observed during recovery (Figures 3-9a and c). While this event appears to slightly elevate the residual water content, it does not affect the overall observations of the transition zone response during recovery.

As was done for the pumping data, the recovery of three immediate θ_w values in the transition zone (representing 30%, 50% and 70% of full water saturation) were determined; the results are displayed in Figure 3-10a-f. The responses of the three saturation levels are again consistent with each other, following the same temporal trend for each radial distance. This behaviour is further evidence that the transition zone translates upwards with only minor variations in shape and thickness.

The magnitude of recovery relative to the maximum drawdown decreases with increasing radial distance. Also, the rate of recovery lessens significantly up to about 4000 minutes. Again, this effect is most significant at the sites close to the pumping well. After about 4000 minutes, very little recovery occurs as the quasi-steady state is established.

3.4.3 GPR Data

The GPR data acquired as part of this experiment was analyzed in a manner similar to that outlined in Chapter 2. Post-processing of the data showed that background pre-pumping GPR profiles were of poor quality. Attempts were made to quantify the magnitude of transition zone drawdown, however, due to the poor quality background data, it was not possible to obtain conclusive quantitative results. Regardless, the raw GPR data is provided on the CD included with this thesis and a summary of the GPR files is included in Appendix G.

3.5 Comparison of Hydraulic Head And Moisture Content Data

The combined temporal hydraulic head and moisture content data for each radial distance having a shallow and deep observation well pair are shown in Figure 3-11a-d. To illustrate the relationships between these two different data sets, they are displayed in terms of both elevation and drawdown relative to their initial static conditions. Since the transition zone translates vertically with only minor variations in shape and thickness, the θ_w= 0.22 (i.e., 50% of full water saturation) position on the moisture content profiles is used to illustrate the drawdown and recovery of the transition zone. It should be noted that the data displayed on Figure 3-11a contains hydraulic head data from a distance of 1.5 m from the pumping well while the moisture content data is from a location 1 m from the

pumping well. While this makes direct comparisons of these data sources less meaningful, they remain illustrative of the processes occurring.

In addition, the observation well pairs were used to estimate the drawdown and elevation of the water table (i.e., the surface at which pore pressure is equal to atmospheric pressure). Assuming that no vertical gradients existed prior to pumping, the water table drawdown, Δh^{wt}, could be calculated from the hydraulic head data following the procedure of Endres et al. (2000):

$$\Delta h^{wt} = (\Delta h^{u} - m d^{u}) / (1 - m) \qquad [1]$$

where Δh^{u} is the drawdown in the upper observation well and d^{u} is the depth below the static water table to the screen of the upper well. The vertical hydraulic gradient, m, is given by:

$$m = (\Delta h^{b} - \Delta h^{u}) / \Delta l \qquad [2]$$

where Δh^{b} is the drawdown in the lower observation well and Δl is the vertical separation between the screened intervals of the well pair. The elevation of the water table could then be calculated using the static water elevations in the observation wells.

Let us first consider the pumping portion of the experiment (i.e., 0 – 10,710 min.) for each radial distance. It can be seen that the drawdown rates for the transition zone, hydraulic head levels and the water table are greatest at early times and progressively decrease with increased pumping. While all drawdown rates are high during the early stages of pumping, the hydraulic head data has a larger rate, leading to greater drawdown at any given time and radial distance. The drawdown difference increases significantly up to about 1000 minutes. This early difference is maintained and slowly increases throughout the remainder of the pumping test. The difference is greatest near to the pumping well and decreases radially.

Since the moisture content profile translates downwards with little change in shape, the difference in drawdown between it and the water table must result in an extension of the capillary fringe. This extension must result in what Nwankwor et al. (1984) termed excess storage. The extension has been quantified in Figure 3-12 as the difference between the drawdown of the projected water table and the 80% saturation point (i.e., $\theta_w = 0.31$) in the transition zone. Calculating the capillary fringe extension based on the drawdown of the 80% saturation point is appropriate because the transition zone translated downward – all values of saturation experienced nearly the same magnitude of drawdown. We can see that up to 15 m distance, there has been extension by 480 minutes. This extension increases with time, more so for locations close to the pumping well. It appears that the extension continually increases until the end of pumping, although at a rate much slower after about 8000

minutes. There is irregularity in the magnitude of capillary fringe extension, resulting from variability in the measurements of moisture content.

Now lets consider the recovery portion of the experiment (i.e., 10,710 – 19,500 min.) in Figure 3-11a-d. Similar to that during pumping, the recovery rate of the hydraulic head levels and water table is greater than the transition zone at all radial distances. The rates are highest at the beginning of recovery and at about 15,000 minutes (i.e., about 4300 minutes of recovery), the hydraulic head levels appear to still be slowly rising; the transition zone appears to be approaching a quasi-static state. Again, this different rate leads to greater recovery of the hydraulic head levels and water table than the transition zone; the result is a compression of the transition zone (Figure 3-13) and a corresponding loss of excess storage.

By about 15,000 minutes, the deep wells at 1.5 and 3 m radial distance have fully recovered all of the hydraulic drawdown they experienced during pumping; the shallow wells remain about 0.05 m below their pre-pumping levels. At distances greater than 5 m, all hydraulic head levels have recovered to about 0.05 m of the pre-pumping levels. Figure 3-11 shows that the transition zone has not even recovered half of its pumping-induced drawdown. At all radial distances, the transition zone appears to have recovered to a level about 0.20 m below its initial pre-pumping elevation.

The spatial relationship between the hydraulic head and moisture content data is given by the distance-drawdown and distance-recovery data shown in Figures 3-14 and 3-15, respectively. The hydraulic data from 36 spatially distributed observation wells are displayed on these figures; some of the differences in hydraulic drawdown at similar radial distances are a result of textural heterogeneities across the site. The differential drawdown is again visible on this figure; the hydraulic drawdown is greater than transition zone drawdown. It is also obvious that the differential is less at greater distances from the pumping well. It is expected that at some distance the drawdown of the transition zone and hydraulic head levels will be equal throughout pumping. In an attempt to estimate this distance of equal drawdown, 2^{nd} order polynomial functions were fit to the transition zone and shallow observation well data. At the time intervals shown on Figure 3-14, the functions consistently intersect between 20 and 25 m, implying that differential drawdown is zero at distances beyond this point.

The spatial relationship during recovery is somewhat different than that during drawdown. At 200 minutes of recovery, the hydraulic head levels have risen to nearly the same elevation across the entire site. After this time, it appears to rise at almost the same rate at all radial distances. Most

recovery of the transition zone has occurred between 1500 and 4300 minutes. The transition zone has risen to about 0.20 m from its pre-pumping level and appears to have stabilized.

3.6 Discussion and Conclusions

Observations from the present experiment provide some insight into the drainage and imbibition processes occurring above the water table as a result of aquifer pumping. The importance of these observations to the analysis of unconfined aquifer pumping and recovery test data may be significant. There are several implications of the current observations.

The moisture content profile translated downward with no significant change in transition zone shape or thickness during the pumping test. This behaviour has a number of implications for aquifer drainage during pumping. First, this downward translation with little transition zone variation indicates that there is minimal excess storage in the unsaturated zone. This observation is counter to the suggestion by Grimestad (2002) that significant quantities of excess moisture become more or less permanently trapped within the unsaturated zone. It also conflicts with results of Nwankwor et al. (1992) that showed excess storage forming within the transition zone as well as the capillary fringe. Second, drainage to residual saturation occurs simultaneously with the translation of the transition zone. Hence, the specific yield for the drained aquifer material is equal to the difference between full and residual volumetric water contents, the commonly used definition of this quantity (e.g., Fetter, 2001). This behaviour is inconsistent with the time-increasing effective value of specific yield proposed by Nwankwor et al. (1984).

The transition zone begins its downward translation with the start of pumping. While there is no moisture profile data before 480 minutes, this conclusion is supported by the projection of the transition zone time-drawdown curves through the origin in Figure 3-6a-f. If this translation were delayed relative to the start of pumping, these curves would be displaced to the right (i.e., later in time). This observation becomes more apparent with increasing radial distance where the drawdown rate decreases. Nwankwor et al. (1992) showed that downward vertical gradients in the unsaturated zone formed within 9 minutes of pumping, which also supports the hypothesis that drainage begins nearly instantaneously. The instantaneous drainage behaviour implies that there is no threshold pressure drawdown required to initiate drainage as hypothesized by Endres et al. (2000).

Comparison of the transition zone and hydraulic time-drawdown data shows several similarities. The moisture content profile and hydraulic head levels undergo a progressive increase in drawdown

during pumping. The rates of both drawdowns are largest at early times and gradually slow. At very late times, the drawdown rates are very slow and may be approaching a quasi-steady state.

There are also some notable differences between the transition zone and hydraulic head drawdowns. At early times, the drawdown rate is significantly greater for the hydraulic head levels than for the transition zone. This rate differential leads to less transition zone drawdown (relative to the hydraulic head drawdown) for the unconfined aquifer. Further, significant differential drawdown is maintained throughout the entire duration of the pumping test.

The differential drawdown between the transition zone and hydraulic head levels can be accounted for by an extension of the capillary fringe (i.e., zone of tension saturation). This extension results in the formation of excess capillary fringe storage also identified by Nwankwor and co-authors (1985, 1992). The present results show that excess capillary fringe storage progressively increases at early- and intermediate-times. Further, it does not diminish at late-times and may be stabilizing at a quasi-steady state. However, Nwankwor and co-authors (1985, 1992) determined that the excess capillary fringe storage decreases significantly in the intermediate stages of pumping and essentially disappears at about 1500 minutes. The persistent excess capillary fringe storage identified in the present experiment is at odds with the findings of these previous researchers.

The region of excess capillary fringe storage is not limited to the immediate vicinity of the pumping well (this paper assumes the immediate vicinity to represent a radial distance up to 5 m from the pumping well). While its magnitude is small, differential drawdown and the resultant excess storage is evident to a radial distance of 15 m. At large radial distances, even a small amount of extension will correspond to a large total volume of excess storage.

The persistence of the excess capillary fringe storage means that even long-term drawdowns of hydraulic head from shallow wells may not accurately describe the drainage occurring in the transition zone. Therefore, determining the specific yield using the volume-balance method with shallow well data (proposed by Nwankwor et al., 1984) may not properly quantify drainage above the water table at any time during a pumping test. Caution must be taken when using this approach.

It is commonly assumed that vertical hydraulic gradients have a significant effect on drainage in unconfined aquifers. Let us first examine the nature of the vertical gradients that occurred during pumping. In this experiment, a vertical gradient quickly formed after the start of pumping and rapidly reached a maximum within 10 minutes. While the magnitude of the vertical gradient decreased, it remained until the end of the pumping test, when it was still a significant fraction of its maximum value. This condition indicates that significant vertical flow exists within the saturated zone in the

vicinity of the pumping well throughout the test. Our observations differ from those of Nwankwor et al. (1992); they found the gradient at 5 m radial distance decreased by almost 90% after 1000 minutes of pumping and trended towards lower values. Contrary to the present observations, they suggested that at 5 m from the pumping well and at late times of pumping, flow within the aquifer is predominantly in a horizontal direction.

A direct relationship between the vertical gradients in the saturated zone and the excess capillary fringe storage is difficult to discern from this experimental data. While the magnitudes of both quantities decrease with radial distance, their temporal behaviours at a given distance vary significantly. Again, this observation differs from the claim by Nwankwor and co-authors (1985, 1992) that the temporal response of vertical gradients and excess capillary fringe storage are similar. In addition, excess capillary fringe storage occurs at a radial distance of 15 m where vertical gradients are essentially zero. The formation of this excess storage with a lack of vertical gradient suggests that horizontal flow within the unsaturated zone may be a significant component of drainage at greater distances from the pumping well.

The recovery portion of this experiment also provided a number of interesting results. A comparison of temporal hydraulic head data for the pumping and recovery test clearly shows systematic differences with radial distance and depth. In some cases, such as at 15 meters, these differences are substantial. However, these differences are not unexpected given the differences in driving force in these two types of tests. In particular, pumping-induced drawdown is driven by the extraction of water from the pumping well; recovery is driven by hydraulic gradients between the drawdown cone and regions of the aquifer beyond the zone of influence. These observations have implications for the analysis of recovery data from unconfined aquifers since it is commonly assumed that solutions based on the pumping portion of the test can be used with recovery data (Kruseman and de Ridder, 2000).

The recovery of the moisture content profile behaves in a comparable way as during drawdown; it is essentially an upward translation without significant variations in transition zone shape and thickness. The degree of recovery for the moisture profile appears to stabilize at a quasi-steady state level that is significantly less than that of the hydraulic data (which recovered to within 0.04 m of their background levels). To at least 15 meters radial distance, this quasi-steady state level is 0.17 to 0.20 m below its pre-pumping elevation. This recovery deficit is similar to the 0.20 m pressure difference between experimental drainage and imbibition curves for Borden aquifer material obtained

by Nwankwor et al. (1984). The similarity suggests that the mechanisms responsible for hysteresis in drainage-imbibition curves also affects the degree of moisture profile recovery.

Similar to the pumping phase, there is a differential in the rates of recovery of the hydraulic head levels and the transition zone; the hydraulic head levels move at a higher rate. This rate differential leads to a compression of the capillary fringe to a thickness less than its static pre-pumping value. The amount of compression is significant in the vicinity of the pumping well, up to 0.15 m. This compression is likely to have some impact on the analyses of recovery data, however, the impact is unclear at this time.

A rapid reversal of the vertical hydraulic gradient from downward to upward occurred very soon after the initiation of recovery. This upward gradient reaches a maximum within 10 minutes of recovery, followed by a slow decline; the gradient is larger near to the pumping well and decreases with radial distance. Similar to the pumping test, the upward gradient persists throughout the duration of recovery monitoring up to a radial distance of 5 m. Beyond 5 m, there is essentially no vertical gradient but the moisture content profile needs to recover 0.20 m of pumping drawdown. Without the presence of a vertical gradient, it is speculated that the recovery will be driven by horizontal flow above the water table. It is also likely that horizontal flow will assist in the long-term recovery of hydraulic head levels beyond 5 m distance.

It has become obvious that accurate characterization of moisture profile drainage and recovery is important in understanding the response of an unconfined aquifer to pumping. Moench and co-authors (1995, 2001) provided solutions incorporating the gradual release of water from above the water table. These models require empirical parameters to describe this gradual drainage. Ultimately, it would be desirable to incorporate an explicit description of the physical processes of drainage in porous media into unconfined aquifer pumping test solutions. While many observations on both drainage and recovery of the moisture content profile have been made in the present paper, further analyses are required to determine how these observations are related to the response of the saturated zone and how they fit into the context of unconfined aquifer pumping test analyses.

3.7 Acknowledgements

This work was partially supported by Individual Research Grants to Dr. Endres and Dr. Rudolph from the Natural Sciences and Research Council of Canada. I would like to thank the many individuals that provided assistance during this work.

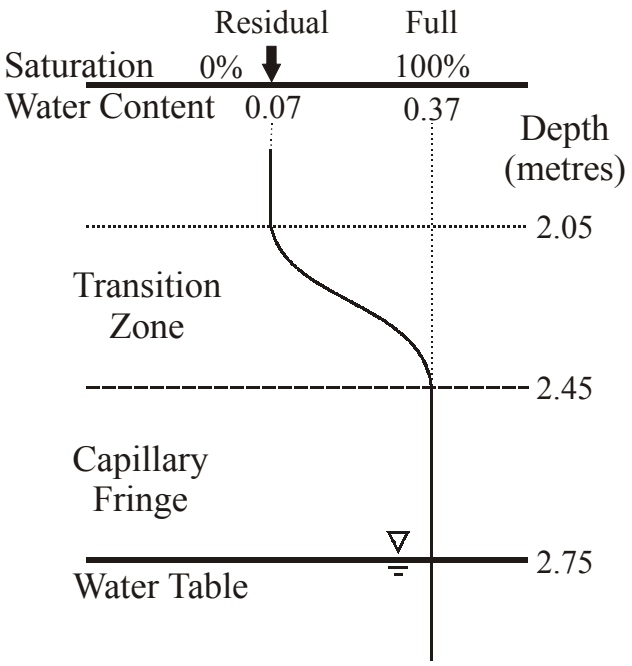

Figure 3-1 - Static equilibrium configuration of the water table, capillary fringe and transition zone.

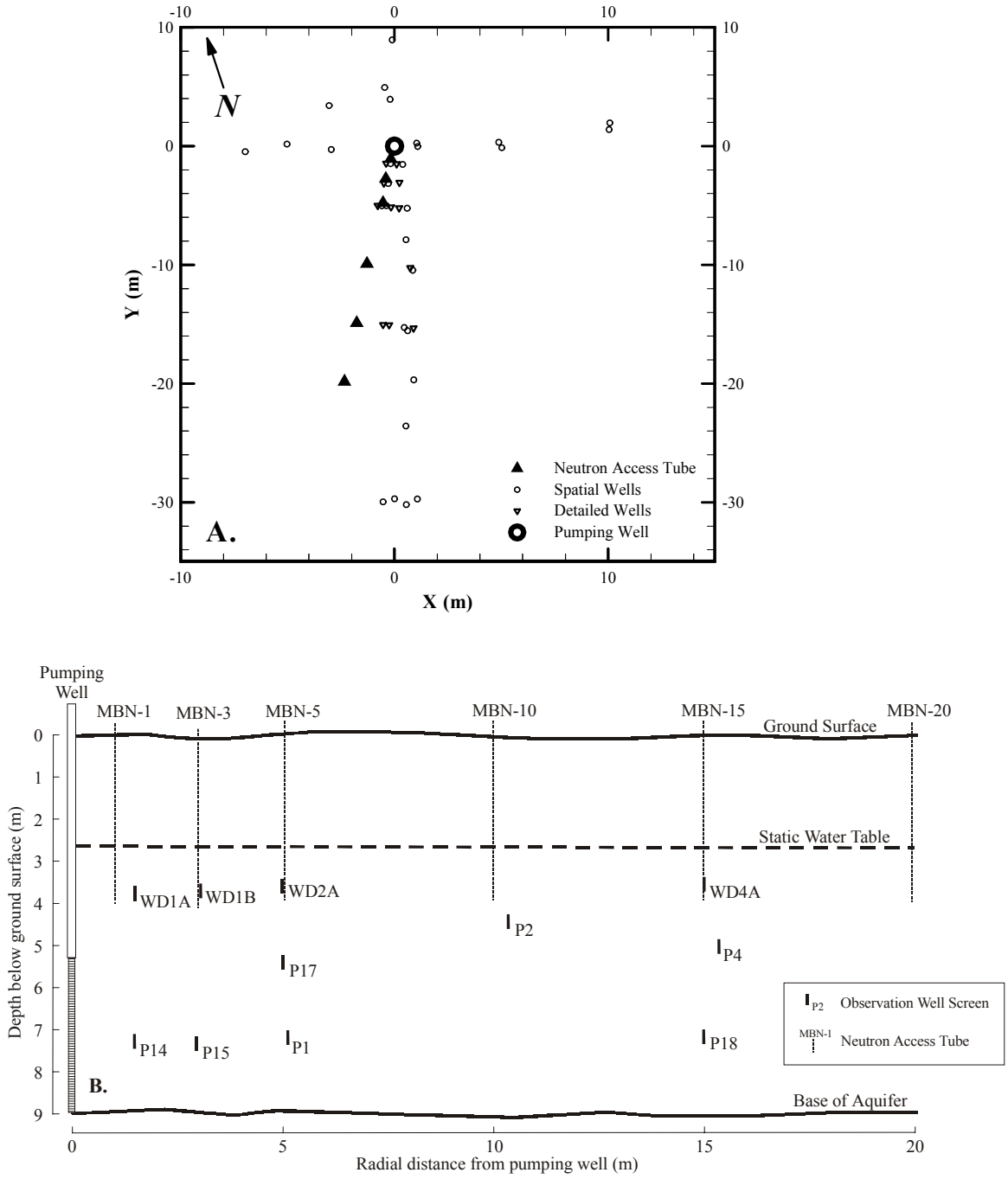

Figure 3-2 - A. Plan view of CFB Borden pumping test site. B. Cross section of the aquifer and instrumentation southward from the pumping well.

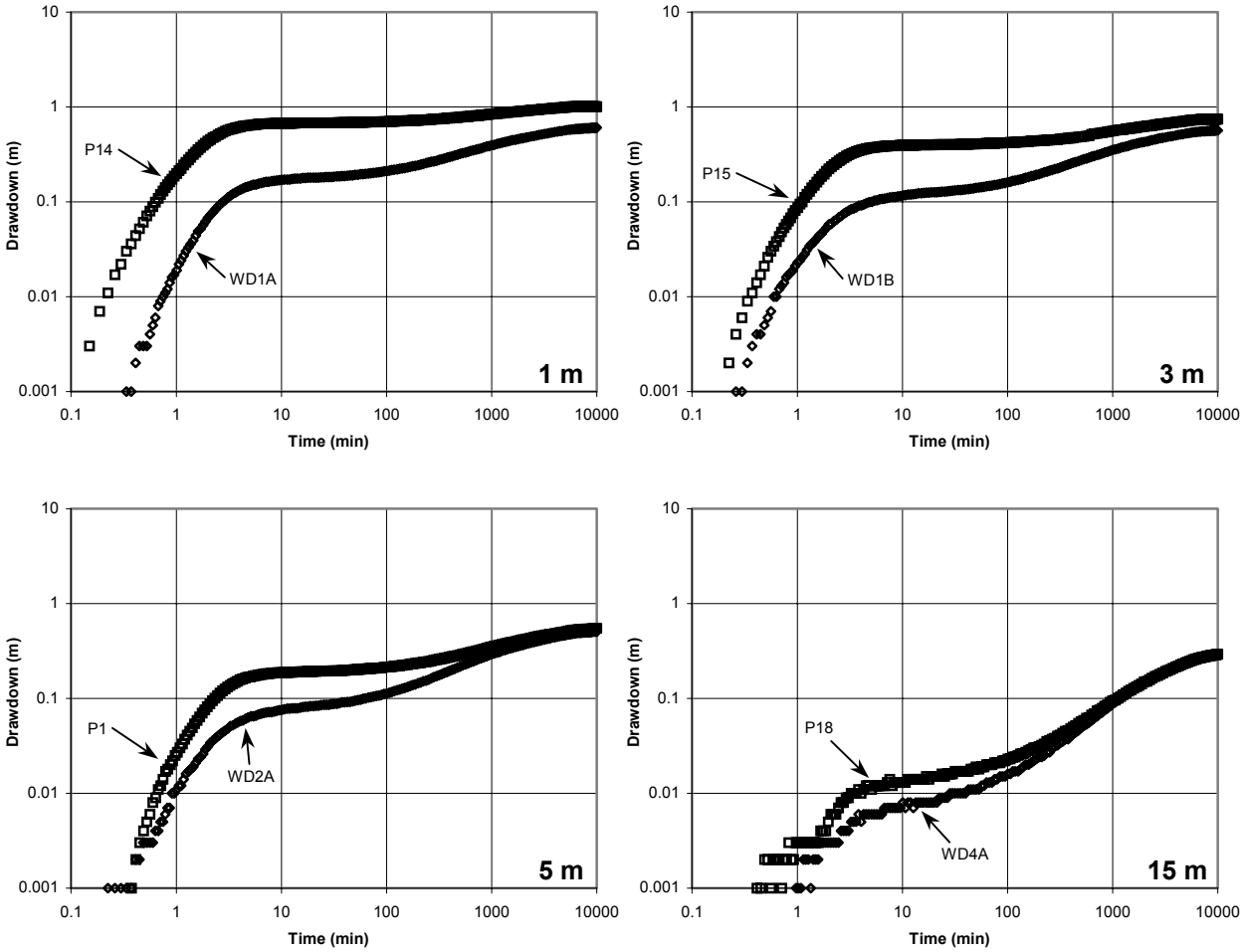

Figure 3-3 – Hydraulic head drawdown in various observation wells.

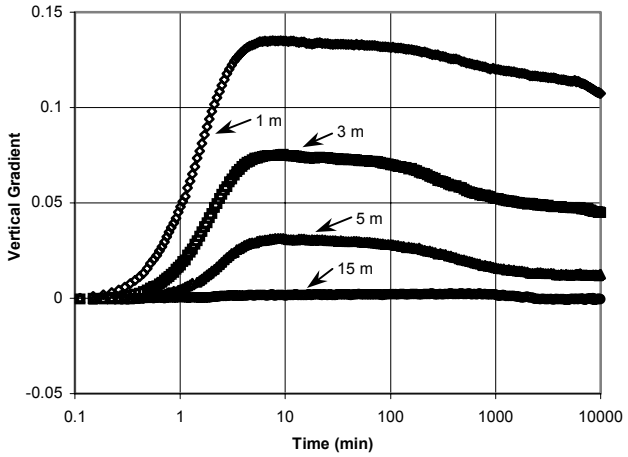

Figure 3-4 -Vertical hydraulic gradients during drawdown (positive is a downward gradient).

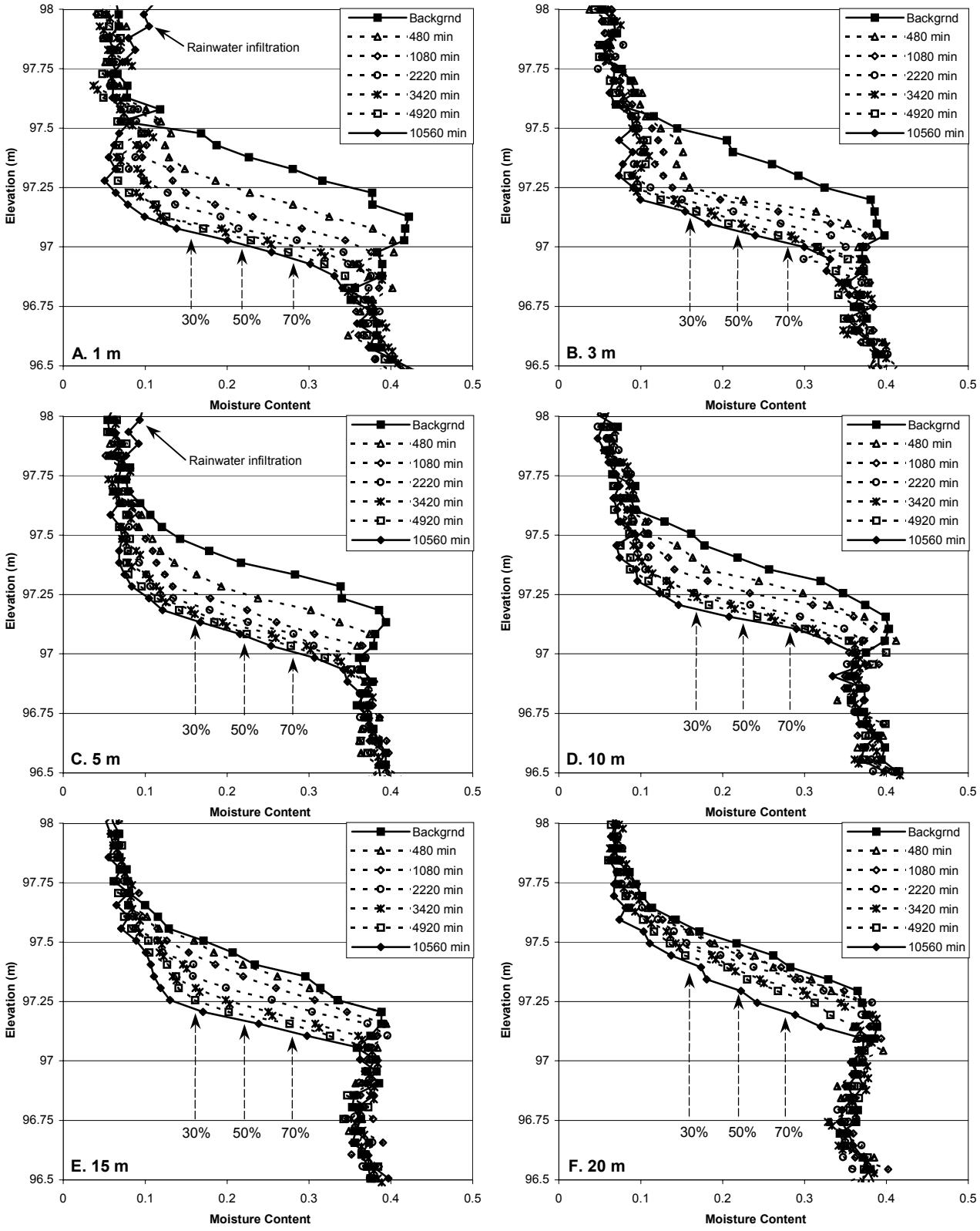

Figure 3-5 A - F - Moisture content distribution at selected times during pumping.

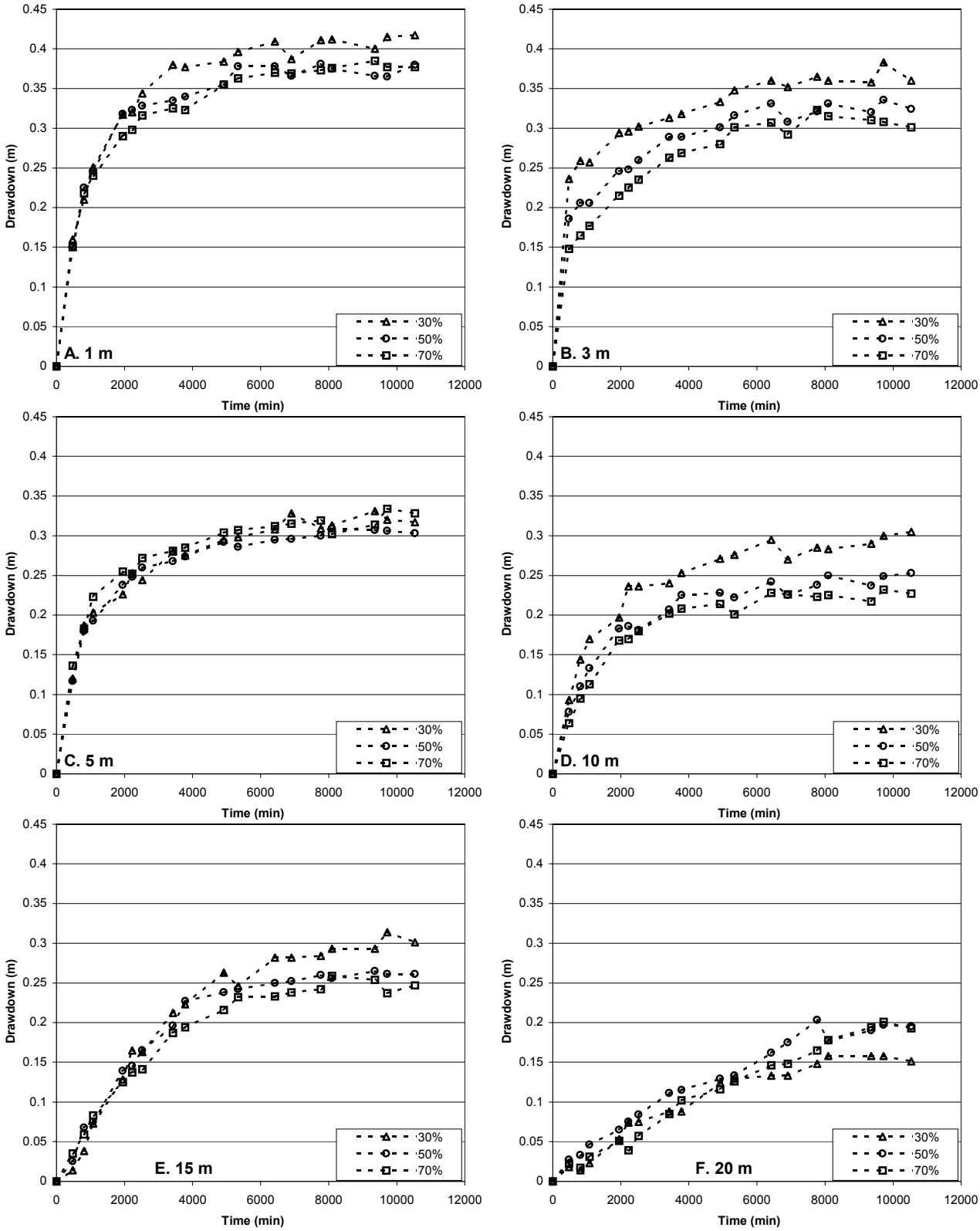

Figure 3-6 A - F - Drawdown of various saturation points within the transition zone.

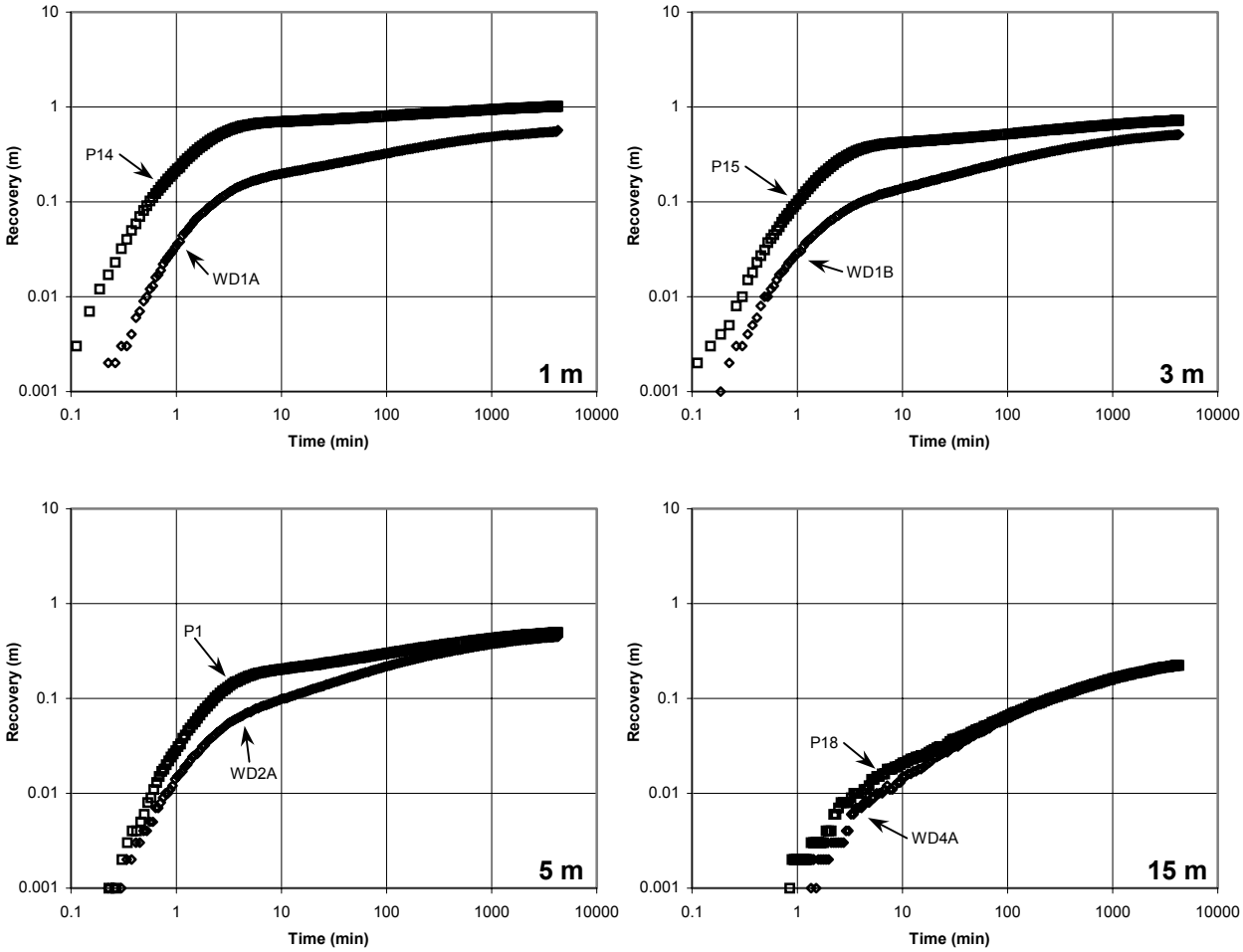

Figure 3-7 – Hydraulic head recovery in various observation wells.

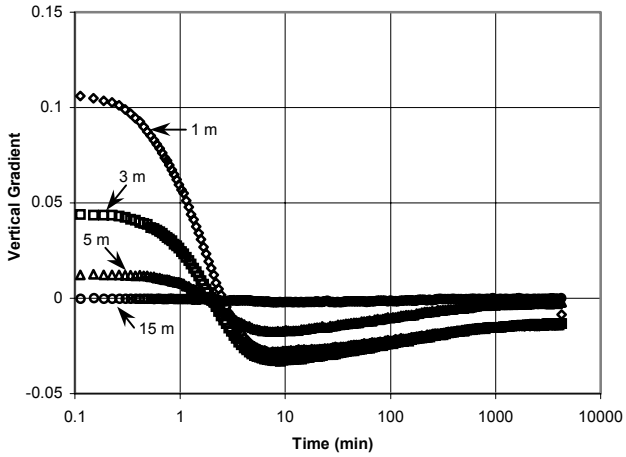

Figure 3-8 - Vertical hydraulic gradients during recovery (positive is a downward gradient).

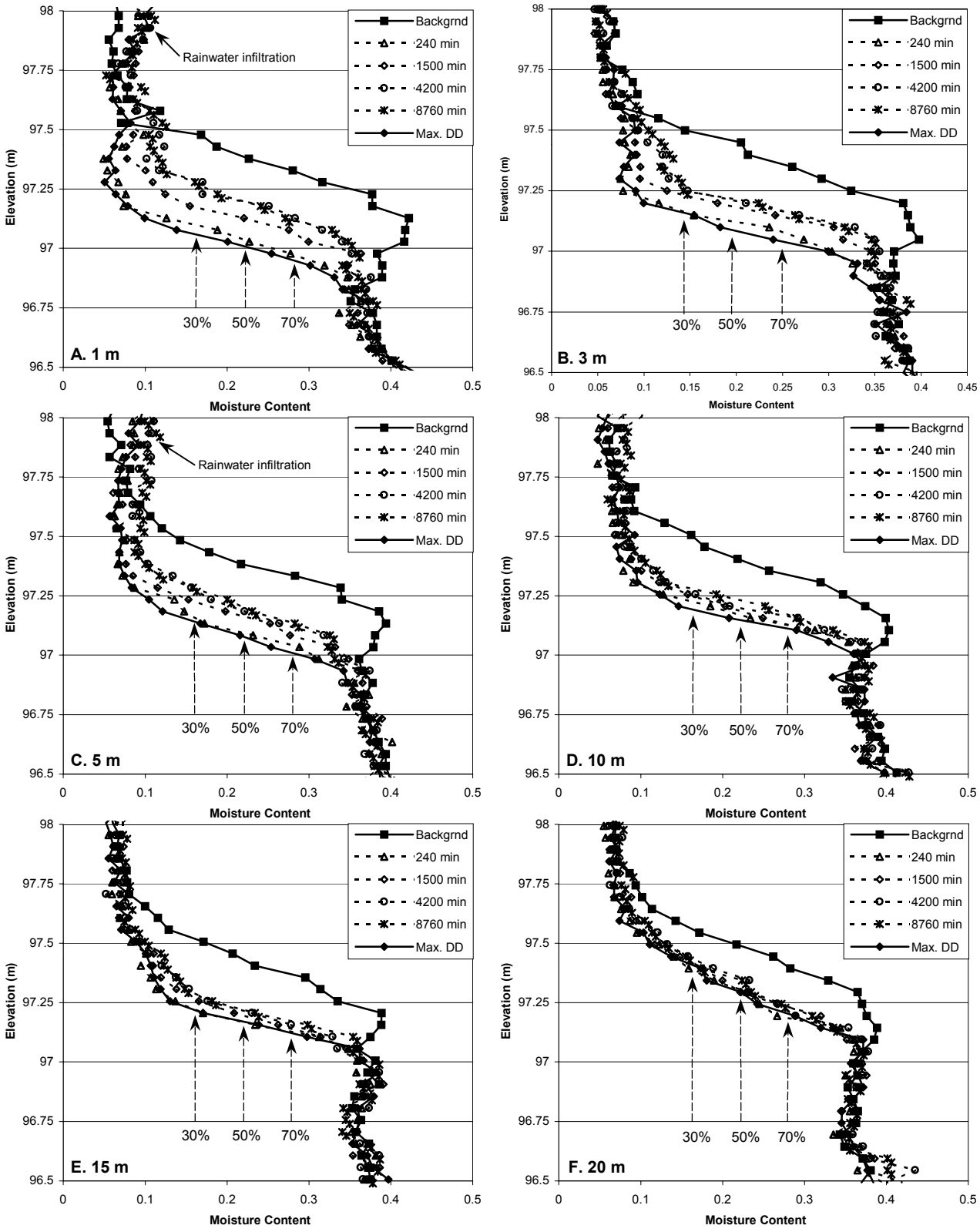

Figure 3-9 A-F - Moisture content distribution at selected times during recovery.

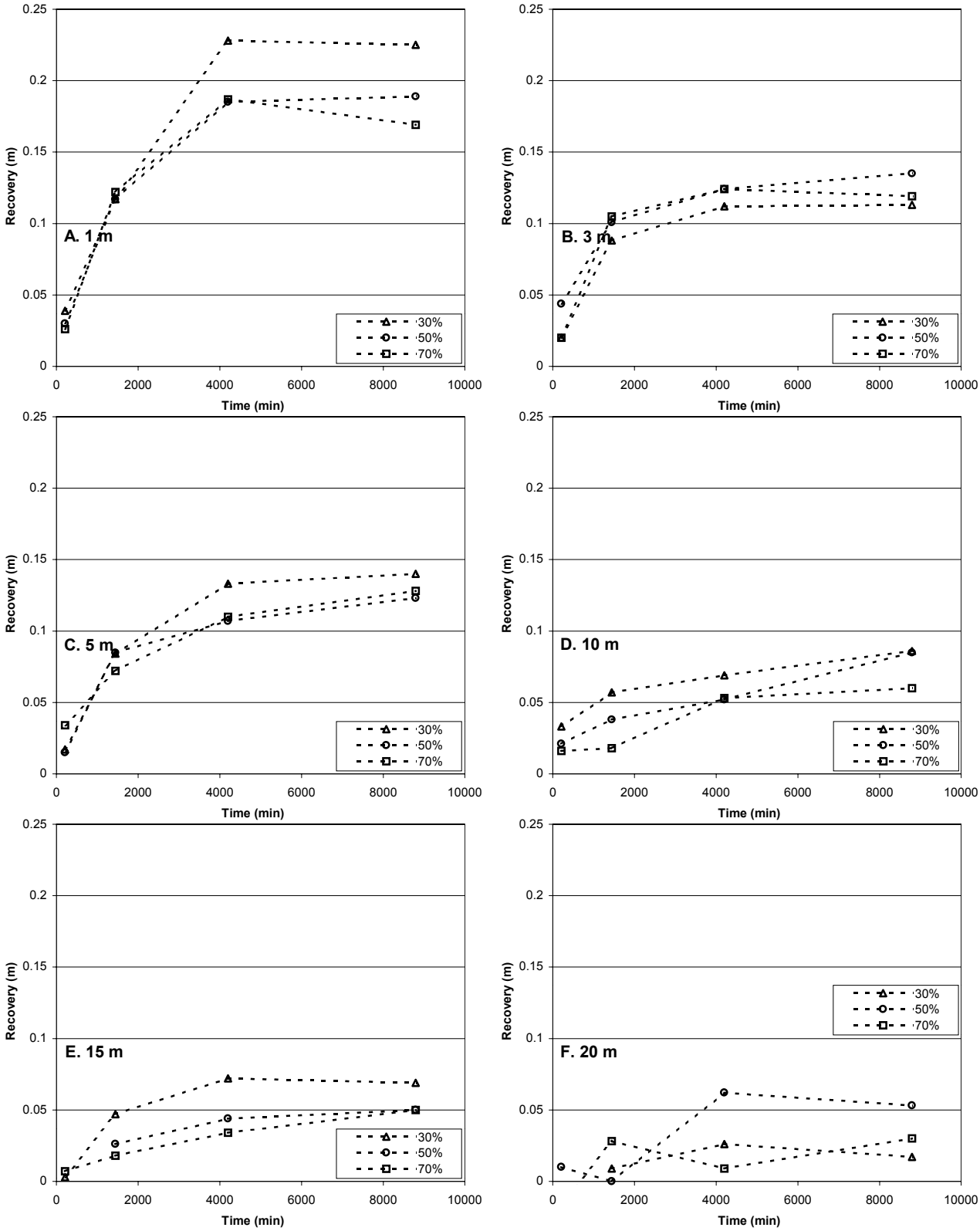

Figure 3-10 A-F - Recovery of various saturation points within the transition zone.

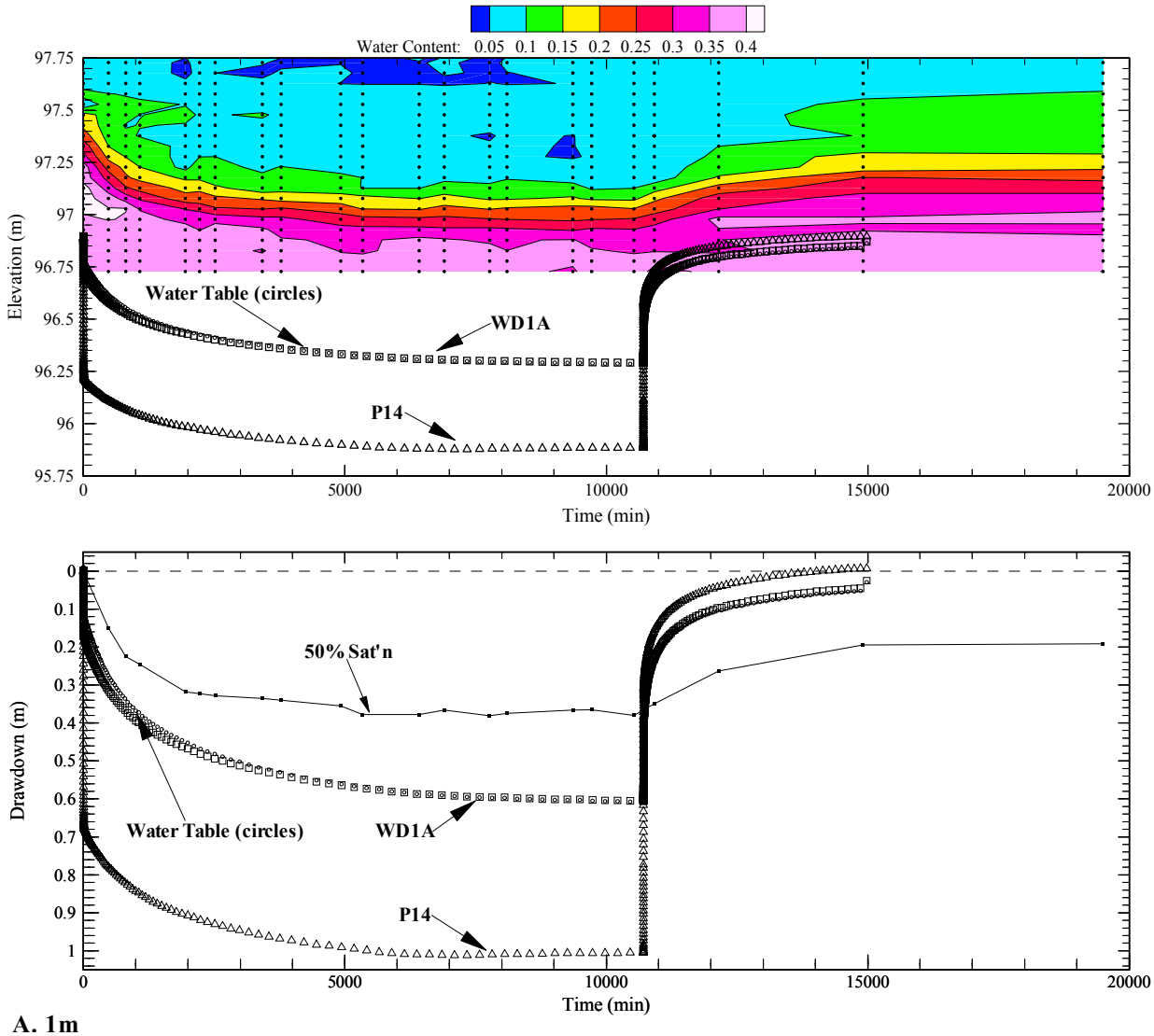

A. 1m

Figure 3-11 A - Top panel: Subsurface moisture content distribution (contoured) and elevation of hydraulic head through pumping and recovery. Lower panel: Drawdown of hydraulic head and 50% saturation point in transition zone throughout pumping and recovery.

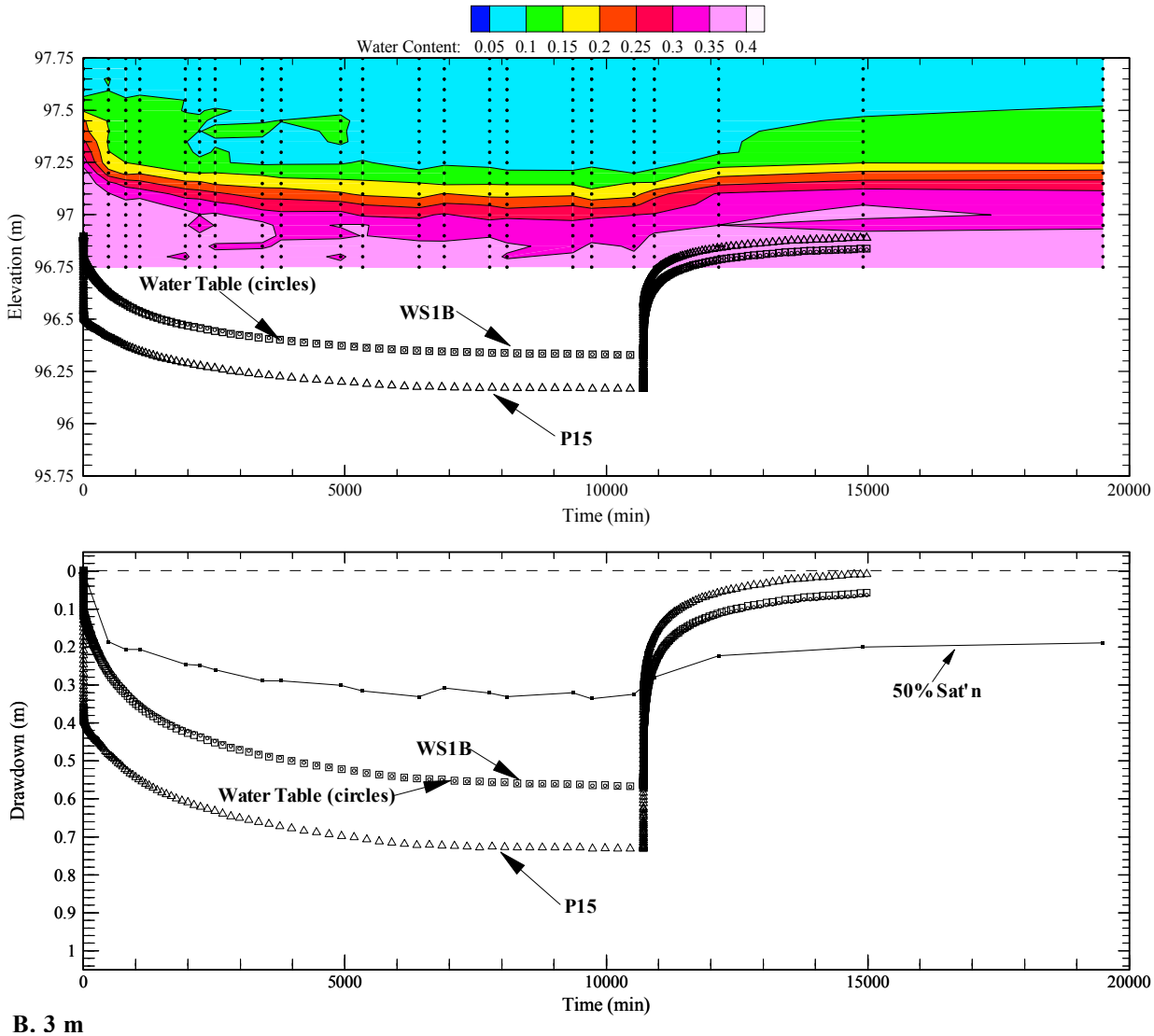

B. 3 m

Figure 3-11 B - Top panel: Subsurface moisture content distribution (contoured) and elevation of hydraulic head through pumping and recovery. Lower panel: Drawdown of hydraulic head and 50% saturation point in transition zone throughout pumping and recovery.

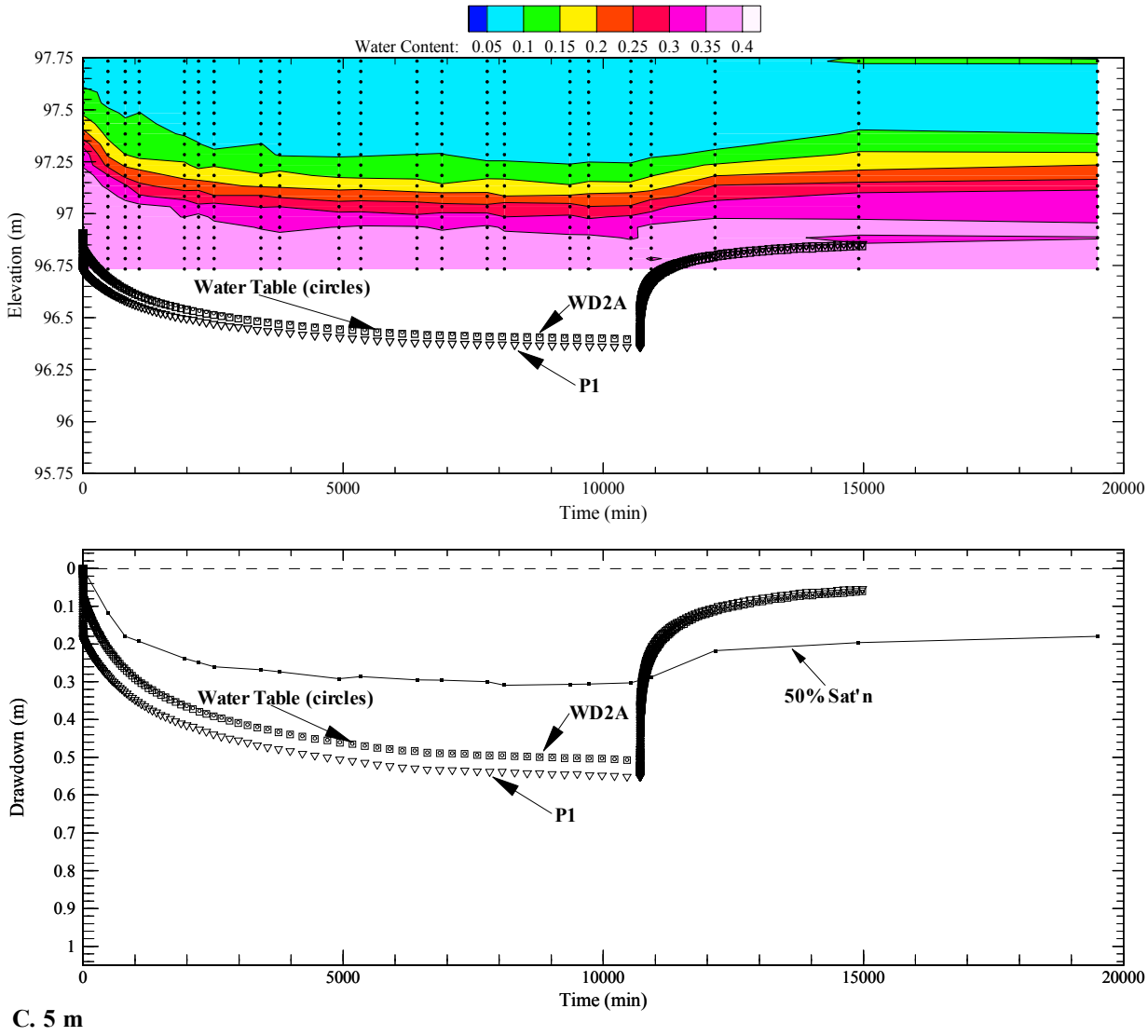

C. 5 m

Figure 3-11 C - Top panel: Subsurface moisture content distribution (contoured) and elevation of hydraulic head through pumping and recovery. Lower panel: Drawdown of hydraulic head and 50% saturation point in transition zone throughout pumping and recovery.

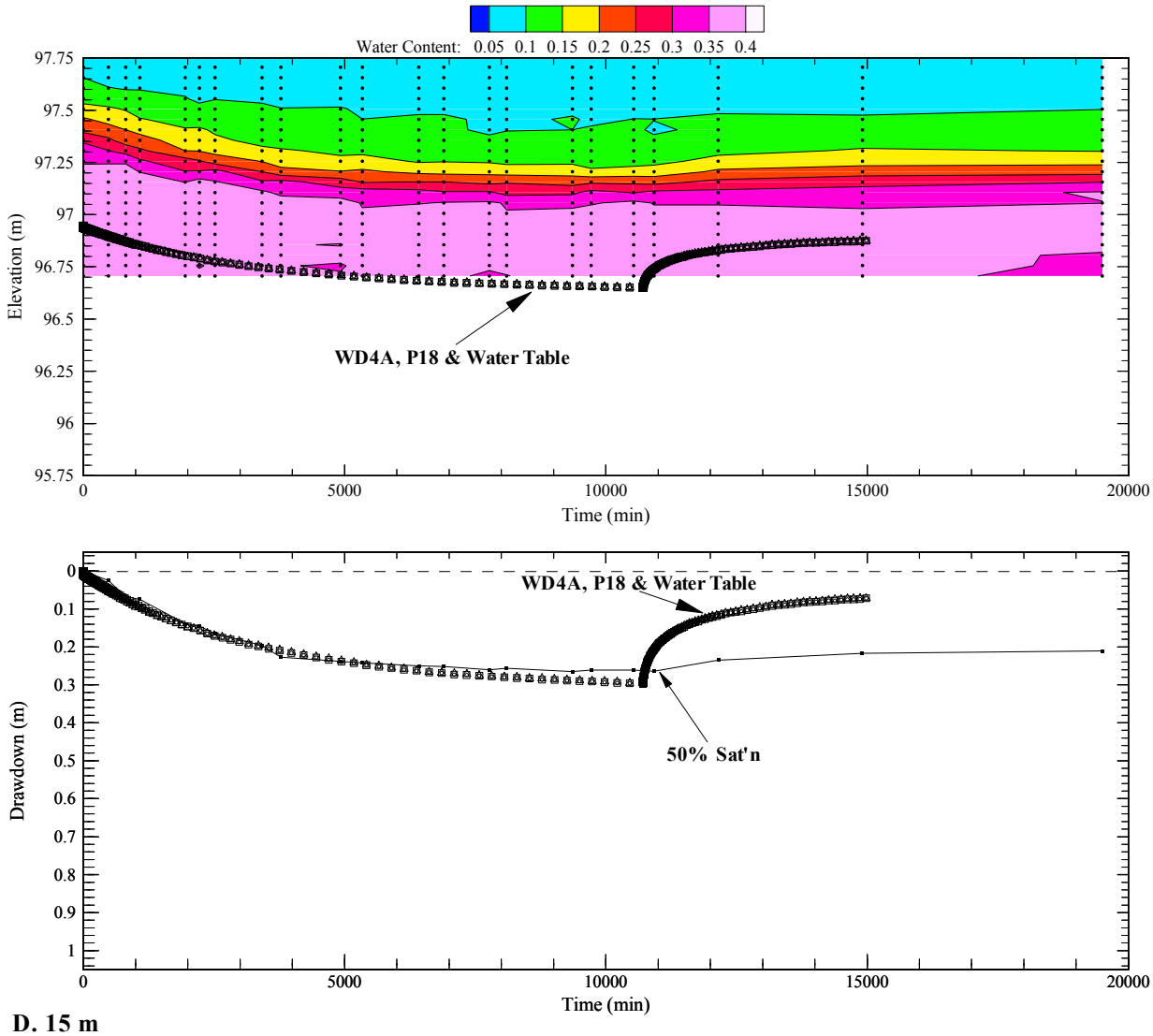

D. 15 m

Figure 3-11 D - Top panel: Subsurface moisture content distribution (contoured) and elevation of hydraulic head through pumping and recovery. Lower panel: Drawdown of hydraulic head and 50% saturation point in transition zone throughout pumping and recovery.

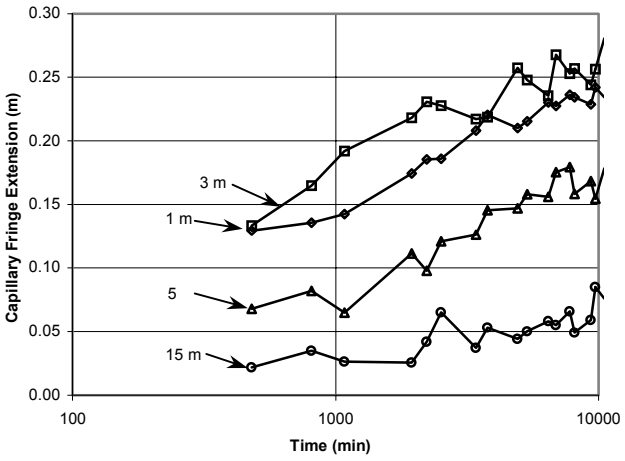

Figure 3-12 - Extension of the capillary fringe during pumping.

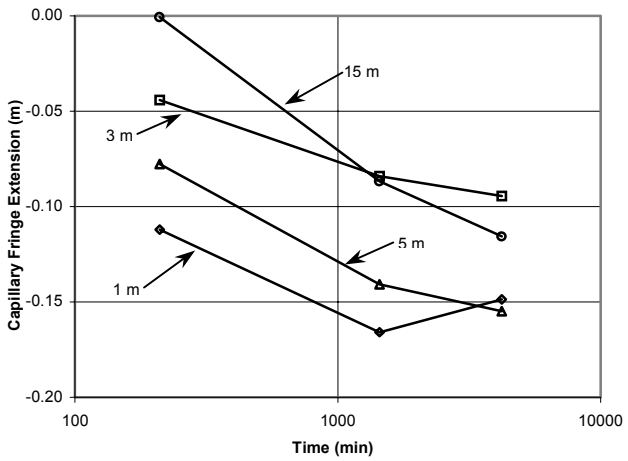

Figure 3-13 - Compression of the capillary fringe during aquifer recovery. (Compression is measured from the static background thickness of the capillary fringe).

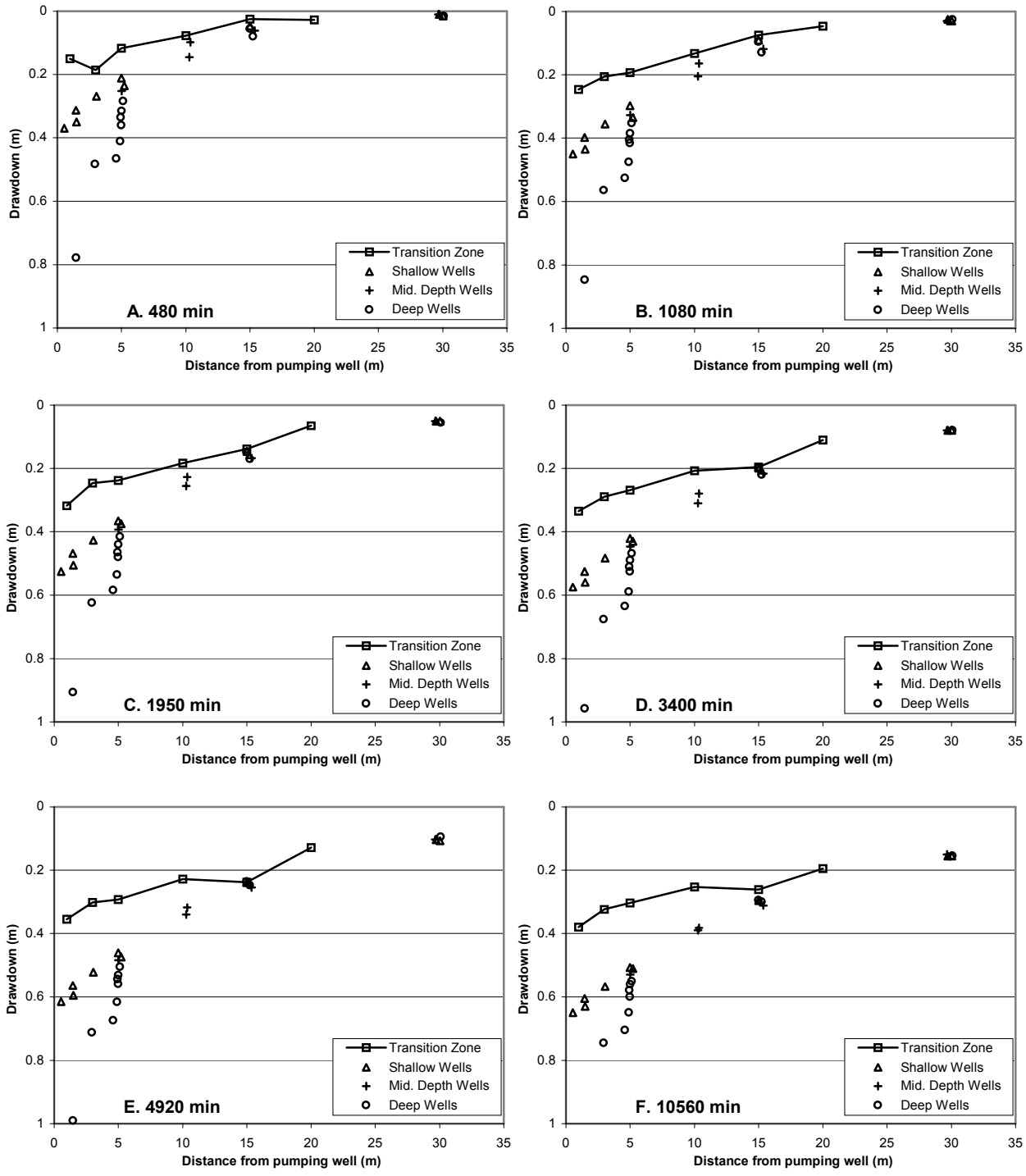

Figure 3-14 A-F - Distance vs. drawdown of hydraulic heads and transition zone at various times during pumping.

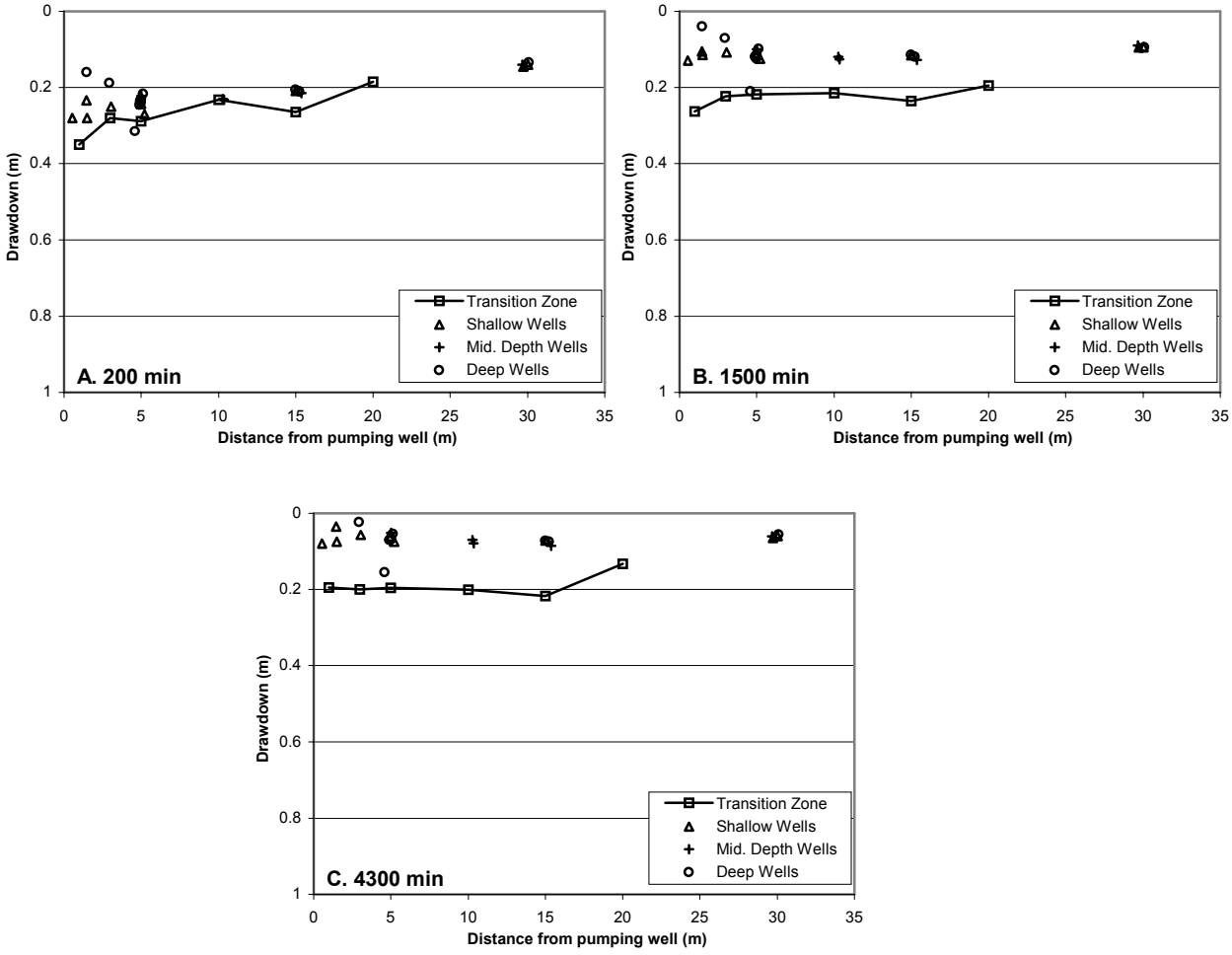

Figure 3-15 A-C - Distance vs. drawdown of hydraulic heads and transition zone at various times during recovery.

Chapter 4
Summary

The research performed as part of this M.Sc. thesis project involved the observation of hydraulic head and moisture content variations during two aquifer pumping and recovery tests. Data for both the downward and upward movement of the moisture content profile were obtained directly through neutron logging techniques and indirectly through GPR imaging techniques. These data were compared with traditional hydraulic head measurements obtained during drawdown and recovery. The data sets show facets of aquifer response that have implications for the analyses of unconfined aquifer tests.

The focus of the first pumping test was to evaluate the use of GPR in characterizing pumping-induced drainage and recovery. Following from Endres et al. (2000), this experiment confirmed that GPR does provide a detailed image of soil moisture changes during drainage and subsequent recovery. Moisture content data from neutron logging showed that the transition zone essentially translated downward with the decline of the hydraulic head levels and back upward during recovery, with little change in the profile shape or thickness. GPR-derived drawdown and recovery estimates were very similar to those for the transition zone as identified by neutron logging. These observations supported the hypothesis that the observed traveltime differences of the GPR reflection (identified as originating from the transition zone) provide a quantifiable measure of the vertical translation of the transition zone.

The rate of translation of the transition zone was slower than the rate of decline of the hydraulic head data. The difference in the rates of drawdown lead to an extension of the capillary fringe, originally observed by Nwankwor et al. (1992). The necessary result of such a capillary fringe extension is the formation of excess storage of water above the water table. However, this excess storage was confined to the capillary fringe; the translational behaviour of the transition zone indicates that the formation of excess storage in the residually- and variably-saturated zones did not occur.

To evaluate the performance of GPR in measuring pumping-induced drawdown, a drainage cone was estimated from the GPR profile data. The drainage cone was defined in two ways: 1) assuming a single drainage-radial distance relationship, and, 2) incorporating spatial information about differential drainage. The volume of water drained from this cone was calculated using previously published values of specific yield (Nwankwor et al., 1984, 1992). Analyses of the various GPR-

derived drainage volumes showed the drainage cone to be of insufficient volume to supply all of the pumped water. Endres et al. (2000) came to the same conclusion based on a similar analysis, although the present experiment was able to account for a larger volume of water. In particular, those estimates that included some measure of heterogeneity were able to account for a larger proportion of the pumped water. Hence, it appears that drainage heterogeneity is important in the unconfined Borden aquifer and, as such, would be a significant factor in calculating specific yield through the volume-balance method of Nwankwor et al. (1984, 1992). However, there was still a significant water deficit; this could have been due to more heterogeneities that would require increased spatial GPR coverage, or because drawdown at large radial distances is small and difficult to quantify using GPR. It is also possible that leakage from the underlying aquitard provided additional water to the aquifer, as suggested by Grimestad (2002).

The recovery of the moisture content profile showed an upward translation, similar to the downward translation during pumping. GPR data again provided a reasonable estimate of the movement of the transition zone. After five days of recovery, the transition zone and GPR-derived recovery levels were between 0.25 and 0.28 m below their pre-pumping levels. The hydraulic head levels had not returned to their pre-pumping elevations either; they remained about 0.17 m low as well. It was determined that the lack of full recovery was a result of a regional lowering of the water table.

While the results from the first pumping test were positive, questions about drainage at greater distances from the pumping well arose. A second pumping test was designed with the addition of six access tubes for obtaining moisture content data up to a 20 m radial distance. Unfortunately, the GPR data was of limited use due to poor quality background pre-pumping profiles, but the second pumping test did provide a significantly improved data set, both temporally and spatially, for observing hydraulic heads and moisture content distribution during pumping and recovery.

As in the first test, the moisture content profile underwent a downward translation at all monitoring locations. Minor observed variations in the moisture content profile shape and thickness appear to be due to small-scale aquifer hetereogeneity. There was no evidence of appreciable excess storage within the transition zone during pumping. However, the rate of drawdown of the water table was greater than that of the transition zone. Again this condition lead to capillary fringe extension and the accompanying formation of excess storage in this zone. The thickening of the capillary fringe and formation of excess storage persisted throughout the entire pumping test. This persistence implies that excess storage within the capillary fringe formed, grew and remained for the entire test.

The capillary fringe extension appeared to approach a quasi-steady state after 6000 to 8000 minutes of pumping. These observations are contrary to Nwankwor et al. (1992) who hypothesized that excess storage formed quickly and then dissipated to nearly zero by about 1500 minutes of pumping. The persistence of the excess capillary fringe storage means that long-term drawdowns of hydraulic head from shallow wells will not accurately describe the drainage occurring above the water table. Using the volume-balance method proposed by Nwankwor et al. (1984) to determine the specific yield may not properly quantify drainage at any time during a pumping test.

The extension of the capillary fringe and corresponding increase in excess storage decreased with radial distance. By extrapolating the drawdown of both the transition zone and the shallow observation wells to increasing radial distance, it was determined that no capillary fringe extension or excess storage is expected beyond a distance of 20 to 25 m.

The results of this experiment showed that while vertical gradients existed throughout pumping, by the end of the pumping test they had diminished by 20 and 50% of their maximum early-time values at distances of 1 and 5 m. Nwankwor et al. (1992) showed a much greater loss in vertical gradient; at 5 m, it decreased by approximately 90% in only 1000 minutes of pumping. Capillary fringe extension and excess storage continued to form throughout the time of declining gradients. Also, capillary fringe extension and excess storage occurred where there were essentially zero vertical gradients at all times during pumping. Nwankwor (1985) and Nwankwor et al. (1992) inferred a direct relationship between the vertical hydraulic gradient and the formation of excess storage. However, data from this experiment do not exhibit such a relationship. If there is a relationship between the vertical gradients and the formation of excess storage, it is complex.

Hydraulic head levels recovered to within 0.04 m of their pre-pumping elevations. Near to the pumping well, the deep observation wells recovered to a higher elevation that the shallow wells, but beyond 3 m, hydraulic recovery at all levels within the saturated zone were very similar. The form of hydraulic recovery on a time-recovery plot is different than that during drawdown. The magnitude of recovery at intermediate times is greater during recovery than at similar times during pumping; these differences are more pronounced at greater distances from the pumping well. Typically, recovery data is analyzed using the same solutions as for drawdown. In light of these data, it appears that some care should be taken when using the drawdown solutions to analyze recovery measurements of hydraulic head.

Recovery of the moisture content profile occurred in a manner similar to drawdown; an upward translation of the moisture profile with little change in shape or thickness occurred. This upward

recovery effectively stabilized at a level approximately 0.20 m below its pre-pumping elevation. Laboratory drainage and imbibition experiments performed on samples of Borden sand have shown a pressure difference of 0.20 m between the drainage and wetting processes. It is hypothesized that this difference is reflected in the recovery of the moisture content profile, as a function of the air-entry pressure.

While the moisture content profile appeared to reach a quasi-steady state, there remained small upward hydraulic gradients below the water table in vicinity of pumping well. Thus, while there remained an upward pressure from below the water table, the moisture content profile no longer responded. At distances beyond 5 m, the vertical gradients were effectively zero, resulting in no upward driving force; this is in agreement with the quasi-steady state of the transition zone. It was proposed that horizontal gradients and flow within the vadose zone would drive the remaining recovery of the unsaturated zone to its equilibrium configuration. It is also possible that horizontal flow within the saturated zone will play a role in the full recovery of the hydraulic heads.

The recovery of the hydraulic head levels was much faster than the transition zone. The differential recovery rate lead to a compression of the capillary fringe of approximately 0.15 m. The significance of this compression the analysis of recovery data is not presently known.

The drawdown behaviour of the transition zone at one metre from the pumping well was similar during both pumping tests. GPR provided a good estimate of the transition zone drawdown during the first experiment. Hence, the difference between the hydraulic head drawdown and the drawdown of the GPR transition zone reflection will give an estimate of capillary fringe extension, from which an estimate of excess storage may be made. As was concluded in Test 2, capillary fringe extension is not expected to exist further than 20 to 25 m. Beyond this distance, hydraulic head data will accurately reflect the drawdown of the transition zone and might be used to calibrate GPR drawdown data.

The characterization of pumping-induced drainage and imbibition is far from complete. Another longer-duration pumping test could provide important information on the long-term state of both the water table and unsaturated zones (i.e., whether they are actually approaching a quasi-steady state after 7 days of pumping). Moisture content data at distances greater than 20 m would be useful in constraining the radial extent of capillary fringe extension and corresponding excess storage. Subsequent tests should involve GPR profiling as well. This data would provide additional calibration of the GPR-derived drawdown data where capillary fringe extension and compression occurs. Monitoring of another test should also involve hydraulic head measurements at larger radial distances

from the pumping well. This would allow for better identification of the zone of influence and may also allow for better estimates of the drained water volume.

It would be beneficial to obtain extensive radial and vertical hydraulic head measurements from above the water table both during pumping and recovery. It was proposed that horizontal flow within the unsaturated zone might play a role in drainage and recovery above water table. Hydraulic head data from this zone would be necessary to confirm the suggestion that horizontal flow is a significant factor. Increasing the duration of recovery monitoring of the unsaturated zone would also provide useful information on field-scale imbibition processes. Such information would be necessary for the formulation of analytical solutions to analyze recovery test data. These data would also provide insight into the long-term processes governing the reestablishment of the equilibrium moisture content profile.

Presently, it is unclear how GPR data will be incorporated into aquifer analyses methods. The work presented shows that the GPR data can not be used as a substitute for hydraulic head data – they are measures of different aquifer processes. Chapter 2 analyses showed that the GPR-derived drainage cone was not of sufficient volume to provide all of the water extracted. If this drainage cone were to be used for calculation of specific yield, it would provide an estimate that would be too large. Thus, further research is required to more completely understand unsaturated drainage and its effect on aquifer pumping tests. Recovery data has shown that the simplifying assumption of Dolynchuk (1998) (i.e., that during recovery, the water table rises at a faster rate than the top of the capillary fringe and thus, the water table corresponds with the point of 100% water saturation) is not valid in the unconfined Borden aquifer. Making this assumption and using GPR transition zone recovery data for aquifer analysis would yield inaccurate hydraulic parameters.

Increased knowledge of pumping-induced drainage and imbibition could provide information on the physical processes involved. From this information, it is possible that a solution for unconfined aquifer pumping test analyses could be formulated based on such physical processes rather than the present solutions that rely on empirical constants (Boulton, 1963; Moench, 1995; Moench et al., 2001). Information on imbibition could provide a unique solution for recovery data that is based upon actual observed recovery processes rather than being based on a reversal of pumping conditions.

References

Akindunni, F.F., Gillham, R.W., 1992. Unsaturated and saturated flow in response to pumping of an unconfined aquifer: Numerical investigation of delayed drainage. Ground Water, 30, 873-884.

Barker, R., Moore, J., 1998. The application of time lapse electrical tomography in groundwater studies. The Leading Edge, 18, 1454-1458.

Bevan, M.B., Endres, A.L., Rudolph, D.L., Parkin, G., In submittal. The non-invasive characterization of pumping induced dewatering using ground penetrating radar. Journal of Hydrology.

Birkelo, B.A., Steeples, D.W., Miller, R.D., Sophocleous, M., 1987. Seismic reflection study of a shallow aquifer during a pumping test. Ground Water, 25, 703-709.

Boulton, N.S., 1963. Analysis of data from non-equilibrium pumping tests allowing for delayed yield from storage. Proceedings of the Institution of Civil Engineers, 26, 469-482.

Dolynchuk, J., Lesmes, D., Urzua, A., Kilbridge, C., 1998. Monitoring of groundwater pump test using GPR and electrical resistivity. Proceeding Symposium on the Application of Geophysics to Engineering and Environmental Problems, Chicago, Illinois, USA, 655-664.

Driscoll, F.G., 1986. Groundwater and Wells, 2nd Edition. US Filter/Johnson Screens, St. Paul.

Endres, A.L., Rudolph, D.L., Clement, W.P., 1997. Monitoring of a pumping test in an unconfined aquifer with ground penetrating radar. Proceedings of the Symposium on the Application of Geophysics to Engineering and Environmental Problems, Reno, Nevada, 483-492.

Endres, A.L., Clement, W.P., Rudolph, D.L., 2000. Ground penetrating radar imaging of an aquifer during a pumping test. Ground Water, 38, 566-576.

Fetter, C.W., 2001. Applied Hydrogeology, 4th edition. Prentice-Hall, New Jersey.

Freeze, R.A., Cherry, J.A., 1979. Groundwater. Prentice-Hall, New Jersey.

Grimestad, G., 2002. A reassessment of ground water flow conditions and specific yield at Borden and Cape Cod. Ground Water, 40, 14-24.

Jones, O.R., Schneider, A.D., 1969. Determining specific yield of the Ogallala Aquifer by the neutron method. Water Resources Research, 5, 1267-1272.

Karous, M., Kelly, W.E., Landa, I., Mares, S., Mazac, O., Muller, K., Mullerova, J., 1993. Applied Geophysics in Hydrogeological and Engineering Practice. Eds. W.E. Kelly and S. Mares, Elsevier Science, Amsterdam.

Kroszynski, U.I., Dagan, G., 1975. Well pumping in unconfined aquifers: the influence of the unsaturated zone. Water Resources Research, 11, 479-490.

Kruseman, G.P., de Ridder, N.A., 2000. Analysis and Evaluation of Pumping Test Data, 2nd Edition. ILRI Publication 47, The Netherlands.

MacFarlane, D.S., Cherry, J.A., Gillham, R.W., Sudicky, E.A., 1983. Migration of contaminants in groundwater at a landfill: a case study, 1. Groundwater flow and plume delineation. In: J.A. Cherry (Guest Editor), Migration of Contaminants in Groundwater at a Landfill: A Case Study. Journal of Hydrology, 63, 1-29.

Meyer, W.R., 1962. Use of a neutron moisture probe to determine the storage coefficient of an unconfined aquifer. USGS Professional Paper 450-E, 174-176.

Moench, A.F., 1994. Specific yield as determined by type-curve analysis of aquifer-test data. Ground Water, 32, 949-957.

Moench, A.F., 1995. Combining the Neuman and Boulton models for flow to a well in an unconfined aquifer. Ground Water, 33, 378-384.

Moench, A.F., Garabedian, S.P., LeBlanc, D.R., 2001. Estimation of hydraulic parameters from an unconfined aquifer test conducted in a glacial outwash deposit, Cape Cod, Massachesetts. USGS Professional Paper 1629.

Morrison, W.E., 1998. Hydrogeological controls on flow and fate of PCE DNAPL in a fractured and layered clayey aquitard: A Borden experiment. M.Sc. Thesis, Univ. of Waterloo, Ontario, Canada.

Mosad, H., 1999. Passive field experiments for PCE destruction using KMnO4 in steel in-situ columns in the Borden aquitard. M.Sc. Thesis, Univ. of Waterloo, Ontario, Canada.

Neuman, S.P., 1972. Theory of flow in unconfined aquifers considering delayed response of the water table. Water Resources Research, 8, 1031-1044.

Neuman, S.P., 1974. Effect of partial penetration on flow in unconfined aquifers considering delayed gravity response. Water Resources Research, 10, 303-312.

Nwankwor,G.I., 1985. Delayed yield processes and specific yield in a shallow sand aquifer. Ph.D. Thesis, University of Waterloo, Ontario, Canada.

Nwankwor,G.I., Cherry, J.A., Gillham, R.W., 1984. A comparative study of specific yield determinations for a shallow sand aquifer. Ground Water, 22, 764-772.

Nwankwor, G.I., Gillham, R.W., van der Kamp, G., Akindunni, F.F., 1992. Unsaturated and saturated flow in response to pumping of an unconfined aquifer: field evidence of delayed drainage. Ground Water, 30, 690-700.

Reynolds, J.M., 1997. An Introduction to Applied and Environmental Geophysics. John Wiley & Sons, Toronto.

Sharma, P.V., 1997. Environmental and Engineering Geophysics. Cambridge Univ. Press, Cambridge.

Sherriff, R.E., Geldart, L.P., 1995. Exploration Seismology. Cambridge University Press, Cambridge.

Sudicky, E.A., 1986. A natural gradient experiment on solute transport in a sand aquifer: spatial variability of hydraulic conductivity and its role in the dispersion process. Water Resources Research, 22, 2069-2082.

Tsoflias, G.P., Halihan, T., Sharp, J.M., 2001. Monitoring pumping test response in a fractured aquifer using ground-penetrating radar. Water Resources Research, 37, 1221-1230.

Stannard, D.I., 1990. Tensiometers – theory, construction and use. In: D.M. Nielsen and A.I. Johnson (Eds.) Water and Vadose Zone Monitoring, ASTM STP 1053, 34-51.

Theis, C.V., 1935. The relationship between the lowering of the piezometric surface and the rate and duration of discharge of a well using groundwater storage. EOS Transcripts AGU, 16, 519-524.

Appendix A

Potentiometric Drawdown Data – Test 1, Aug. 2000

Potentiometric Drawdown and Recovery - Test 1 - August, 2000

Elapsed Time (min)	PW1 m H2O	WD1A m H2O	WS1A m H2O	P14 m H2O	WD1 m H2O	WS1B m H2O	WD1B m H2O	P15 m H2O	WD2A m H2O	WS2A m H2O	P16 m H2O	P17 m H2O	P1 m H2O	WD3 m H2O
Drawdown														
0	0	0	0	0	0	0	0	0	0	0	0	0	0	0
280	3.225	0.323	0.292	0.885	0.209	0.251	0.225	0.565	0.19	0.185	0.408	0.262	0.308	-0.525
920	3.26	0.405	0.38	0.945	0.315	0.335	0.32	0.625	0.27	0.27	0.47	0.33	0.373	0.182
1630	3.305	0.462	0.44	0.995	0.38	0.395	0.38	0.675	0.325	0.325	0.515	0.385	0.423	0.24
2510	3.345	0.511	0.485	1.035	0.432	0.445	0.431	0.717	0.371	0.375	0.556	0.43	0.46	0.287
2905	3.355	0.525	0.51	1.05	0.465	0.46	0.445	0.745	0.39	0.39	0.57	0.445	0.478	0.31
3980	3.385	0.565	0.543	1.087	0.505	0.5	0.49	0.768	0.425	0.43	0.603	0.48	0.513	0.344
4585	3.4	0.582	0.563	1.1	0.525	0.519	0.506	0.785	0.45	0.449	0.622	0.5	0.528	0.359
5310	3.435	0.605	0.585	1.125	0.55	0.54	0.53	0.805	0.47	0.465	0.645	0.52	0.548	0.383
6040	3.453	0.62	0.602	1.14	0.62	0.557	0.545	0.82	0.485	0.485	0.66	0.535	0.563	0.4
6890	3.459	0.64	0.622	1.156		0.577	0.566	0.839	0.505	0.503	0.676	0.558	0.582	0.412
8420	3.49	0.68	0.65	1.18	0.625	0.635	0.605	0.875	0.545	0.54	0.715	0.595	0.618	0.45
9770	3.49	0.7	0.68	1.2	0.655	0.635	0.625	0.89	0.56	0.56	0.72	0.61	0.643	0.47
Recovery														
445	0.3	0.333	0.34	0.302	0.375	0.335	0.34	0.303	0.317	0.325	0.295	0.31	0.303	0.32
1140	0.247	0.26	0.265	0.246	0.29	0.265	0.265	0.25	0.24	0.26	0.245	0.252	0.253	0.26
1560	0.23	0.245	0.24	0.215	0.26	0.25	0.245	0.235	0.235	0.255	0.23	0.23	0.233	0.24
2715	0.197	0.21	0.208	0.197	0.214	0.211	0.205	0.2	0.199	0.219	0.215	0.203	0.204	0.202
3000	0.188	0.204	0.204	0.193	0.213	0.203	0.2	0.196	0.192	0.212	0.209	0.197	0.198	0.198
7080	0.175	0.18	0.18	0.175	0.18	0.18	0.176	0.178	0.17	0.175	0.175	0.18	0.18	0.177

Elapsed Time (min)	P2 m H2O	WS3 m H2O	WD4A m H2O	P18 m H2O	P3 m H2O	P4 m H2O	WS4 m H2O	WS5 m H2O	WS6 m H2O	WS7A m H2O	P6 m H2O	P5 m H2O	WS7 m H2O	WD10 m H2O
Drawdown														
0	0	0	0	0	0	0	0	0	0	0	0	0	0	0
280	0.07	0.08	0.055	0.07	0.07	0.06	0.05	0.03	0.02	0.03	0.015	0.02	0.015	0.2
920	0.16	0.145	0.1	0.115	0.11	0.105	0.09	0.061	0.045	0.035	0.035	0.03	0.032	0.3
1630	0.205	0.195	0.14	0.155	0.15	0.14	0.125	0.093	0.07	0.055	0.055	0.05	0.053	0.37
2510	0.249	0.239	0.172	0.186	0.185	0.179	0.165	0.126	0.1	0.076	0.078	0.074	0.084	0.425
2905	0.265	0.255	0.19	0.205	0.195	0.195	0.17	0.138	0.113	0.09	0.09	0.085	0.085	0.445
3980	0.3	0.29	0.22	0.232	0.22	0.22	0.208	0.166	0.14	0.105	0.112	0.112	0.105	0.49
4585	0.315	0.309	0.239	0.245	0.238	0.235	0.227	0.182	0.151	0.123	0.124	0.122	0.12	0.505
5310	0.333	0.325	0.252	0.265	0.26	0.265	0.225	0.198	0.162	0.13	0.135	0.13	0.13	0.532
6040	0.347	0.342	0.267	0.275	0.267	0.265	0.258	0.208	0.175	0.145	0.147	0.143	0.14	0.549
6890	0.36	0.359	0.286	0.294	0.283	0.285	0.276	0.228	0.192	0.16	0.158	0.157	0.16	0.568
8420	0.42	0.391	0.32	0.325	0.33	0.32	0.315	0.278	0.23	0.19	0.21	0.2	0.2	0.63
9770	0.415	0.415	0.34	0.345	0.34	0.335	0.33	0.278	0.245	0.205	0.21	0.205	0.205	0.635
Recovery														
445	0.29	0.3	0.265	0.258	0.256	0.255	0.265	0.243	0.225	0.197	0.198	0.192	0.191	0.37
1140	0.24	0.245	0.226	0.22	0.221	0.22	0.224	0.213	0.202	0.187	0.185	0.18	0.185	0.27
1560	0.225	0.23	0.21	0.205	0.21	0.215	0.21	0.198	0.195	0.18	0.185	0.175	0.18	0.25
2715	0.195	0.198	0.192	0.187	0.187	0.183	0.187	0.184	0.179	0.174	0.172	0.168	0.177	0.203
3000	0.191	0.193	0.188	0.184	0.184	0.182	0.185	0.184	0.178	0.174	0.171	0.167	0.171	0.197
7080	0.175	0.175	0.173	0.173	0.17	0.17	0.175	0.173	0.17	0.168	0.17	0.165	0.168	0.17

Elapsed Time (min)	WS11 m H2O	P19 m H2O	P22 m H2O	WS12 m H2O	WD20 m H2O	WD21 m H2O	P20 m H2O	WS22 m H2O	WD30 m H2O	P21 m H2O	WS31 m H2O	P13 m H2O
Drawdown												
0	0	0	0	0	0	0	0	0	0	0	0	0
280	0.19	0.33	0.125	0.085	0.34	0.155	0.315	0.115	0.157	0.298	0.123	0.335
920	0.27	0.39	0.18	0.15	0.41	0.25	0.375	0.18	0.255	0.355	0.198	0.393
1630	0.33	0.44	0.227	0.2	0.47	0.317	0.42	0.23	0.325	0.405	0.258	0.44
2510	0.38	0.485	0.265	0.245	0.52	0.375	0.47	0.28	0.38	0.445	0.308	0.48

2905	0.395	0.495	0.28	0.26	0.53	0.39	0.48	0.29	0.4	0.46	0.326	0.495
3980	0.44	0.531	0.315	0.297	0.571	0.43	0.514	0.33	0.444	0.497	0.361	0.53
4585	0.457	0.549	0.329	0.314	0.587	0.455	0.531	0.347	0.465	0.512	0.383	0.549
5310	0.475	0.565	0.35	0.33	0.608	0.475	0.55	0.364	0.485	0.535	0.403	0.565
6040	0.495	0.585	0.4	0.349	0.625	0.498	0.569	0.383	0.506	0.547	0.417	0.582
6890	0.51	0.602	0.382	0.366	0.644	0.519	0.585	0.398	0.53	0.554	0.435	0.6
8420	0.56	0.645	0.42	1.265	0.685	0.59	0.62	0.44	0.575	0.605	0.483	0.63
9770	0.565	0.655	0.435	0.42	0.7	0.58	0.64	0.455	0.595	0.62	0.493	0.655
Recovery												
445	0.325	0.3	0.28	0.306	0.32	0.366	0.29	0.31	0.38	0.295	0.323	0.257
1140	0.255	0.235	0.233	0.242	0.253	0.278	0.235	0.245	0.28	0.235	0.253	0.212
1560	0.235	0.22			0.235	0.25	0.215	0.235	0.255	0.22	0.233	0.195
2715	0.199	0.188	0.188	0.192	0.209	0.207	0.188	0.198	0.207	0.191	0.197	0.168
3000	0.192	0.182	0.185	0.188	0.193	0.199	0.184	0.193	0.2	0.189	0.191	0.161
7080	0.17	0.167	0.17	0.17	0.17	0.171	0.163	0.173	0.174	0.17	0.166	0.142

Elapsed Time (min)	WD1B m H2O	Elapsed Time (min)	WS2A m H2O	Elapsed Time (min)	WD1B m H2O	Elapsed Time (min)	WS2A m H2O
Drawdown		**Drawdown**		**Recovery**		**Recovery**	
0	0	0	0	0	0	0	0
0.633333	0.005	0.2	0.002	0.5	0.003	0.516667	0.0025
0.766667	0.01	0.7	0.01	0.666667	0.004	0.683333	0.005
0.933333	0.015	0.816667	0.02	0.833333	0.006	0.85	0.0075
1.1	0.019	1.216667	0.025	1	0.009	1.016667	0.0125
1.316667	0.025	1.35	0.03	1.166667	0.012	1.35	0.015
1.466667	0.03	1.583333	0.035	1.333333	0.015	1.516667	0.02
1.666667	0.036	1.75	0.04	1.5	0.019	1.683333	0.025
1.8	0.041	1.883333	0.045	1.666667	0.021	1.85	0.0275
1.933333	0.045	2.066667	0.05	1.833333	0.025	2.016667	0.0325
2.166667	0.052	2.266667	0.055	2	0.029	2.183333	0.045
2.333333	0.056	2.516667	0.06	2.166667	0.034	2.333333	0.04
2.5	0.061	2.75	0.065	2.333333	0.037	2.5	0.044
2.666667	0.065	3.066667	0.07	2.5	0.04	2.666667	0.046
2.833333	0.071	3.333333	0.073	2.666667	0.044	2.833333	0.05
3	0.075	3.666667	0.08	2.833333	0.049	3	0.051
3.25	0.08	4	0.083	3	0.052	3.166667	0.055
3.5	0.084	4.333333	0.086	3.166667	0.054	3.333333	0.057
3.75	0.088	4.666667	0.09	3.333333	0.058	3.5	0.059
4	0.092	5	0.092	3.5	0.061	3.666667	0.06
4.333333	0.096	5.333333	0.094	3.666667	0.068	3.5	0.062
4.666667	0.101	5.666667	0.095	3.5	0.069	4	0.065
5	0.105	6	0.096	4	0.071	4.1	0.066
5.5	0.11	6.5	0.097	4.1	0.073	4.2	0.068
6	0.113	7	0.099	4.2	0.075	4.3	0.069
7	0.115	7.3	0.1	4.3	0.076	4.4	0.07
8	0.117	8.3	0.103	4.4	0.077	4.5	0.072
9	0.12	9.3	0.103	4.5	0.079	5	0.073
10	0.122	10.3	0.105	5	0.081	5.1	0.074
11	0.123	11.3	0.106	5.1	0.082	5.2	0.075
12	0.124	12.3	0.107	5.2	0.084	5.3	0.075
13	0.125	13	0.107	5.3	0.086	5.4	0.077
14	0.125	14	0.107	5.4	0.087	5.5	0.078
15	0.129	15	0.108	5.5	0.088	6	0.078
16	0.127	16	0.107	6	0.089	6.1	0.08
20	0.131	20.3	0.107	6.1	0.089	6.2	0.08
25	0.136	25	0.107	6.2	0.09	6.3	0.081
30	0.139	35	0.108	6.3	0.091	6.4	0.081
35	0.141	45	0.121	6.4	0.092	6.5	0.082

40	0.145
45	0.147
50	0.151
55	0.152
60	0.154
70	0.158
80	0.161
90	0.165
100	0.17
120	0.176
140	0.183
160	0.205
180	0.195
200	0.2
220	0.205
250	0.212
280	0.22
310	0.225
370	0.238
430	0.25
495	0.257
540	0.265
600	0.275
660	0.281
720	0.29
780	0.295
910	0.31
960	0.317
1030	0.324
1080	0.33
1142	0.335
1248	0.345
1330	0.35
1375	0.355
1440	0.358
1505	0.365
1650	0.375
2500	0.425
2746	0.433
2905	0.46
3980	0.485
4260	0.49
4584	0.501
5315	0.525
5665	0.53
6040	0.54
6890	0.561
7185	0.565
8440	0.6
8650	0.605
9730	0.62
9922	0.62

50	0.121
60	0.125
70	0.128
80	0.131
90	0.139
100	0.143
110	0.147
120	0.159
141	0.17
160	0.156
180	0.16
200	0.167
220	0.17
250	0.178
280	0.183
310	0.185
370	0.2
430	0.218
495	0.218
540	0.225
600	0.23
660	0.236
720	0.24
780	0.25
910	0.265
960	0.265
1030	0.275
1080	0.28
1141	0.285
1245	0.29
1330	0.3
1375	0.305
1440	0.31
1505	0.315
1650	0.32
2500	0.37
2746	0.38
2905	0.385
3980	0.42
4260	0.435
4584	0.445
5315	0.465
5665	0.47
6040	0.48
6890	0.5
7185	0.505
8440	0.52
8650	0.54
9730	0.555
9922	0.556

6.5	0.093
7	0.093
7.15	0.095
7.3	0.096
7.45	0.097
8	0.098
8.15	0.098
8.3	0.1
9	0.102
9.3	0.104
10	0.106
10	0.107
11	0.108
12	0.115
13	0.119
14	0.123
15	0.122
16	0.121
17	0.125
18	0.128
19	0.13
20	0.131
21	0.131
23	0.132
25	0.137
27	0.14
30	0.146
33	0.149
36	0.152
39	0.156
42	0.159
45	0.162
50	0.165
55	0.169
60	0.171
65	0.169
70	0.177
75	0.182
80	0.186
90	0.189
100	0.194
110	0.199
120	0.208
135	0.216
150	0.216
180	0.223
210	0.232
240	0.239
270	0.251
445	0.289
670	0.319
785	0.329
960	0.347
1140	0.359
1380	0.374
1560	0.384
2705	0.424
3000	0.429

7	0.083
7.15	0.083
7.3	0.085
7.45	0.085
8	0.085
8.3	0.085
9	0.088
9.3	0.09
10	0.091
10	0.092
11	0.094
12	0.096
13	0.098
14	0.1
15	0.102
16	0.103
17	0.103
18	0.103
19	0.105
20	0.107
21	0.11
23	0.112
25	0.116
27	0.114
30	0.115
33	0.123
36	0.127
39	0.13
42	0.133
45	0.135
50	0.136
55	0.143
60	0.14
65	0.146
70	0.145
75	0.145
80	0.155
90	0.157
100	0.161
110	0.17
120	0.17
135	0.175
150	0.18
180	0.187
210	0.197
240	0.205
270	0.213
445	0.221
670	0.253
785	0.277
960	0.282
1140	0.303
1380	0.33
1560	0.335
2705	0.371
3000	0.378

Appendix B

Potentiometric Drawdown Data – Test 2, Aug. 2001

Potentiometric Drawdown and Recovery - Test 2 - August, 2001

Elapsed Time (min)	PW1 m H2O	WD1A m H2O	P14 m H2O	WS1B m H2O	P15 m H2O	WD2A m H2O
0	0	0	0	0	0	0
0.0373	0.071	0	-0.001	0	-0.001	0.001
0.0747	0.148	0	0	0	-0.001	0
0.112	0.235	0	0	0	-0.001	0
0.1493	0.304	-0.001	0.003	0	0	0.001
0.1867	0.376	0	0.007	0	0	0
0.224	0.451	0	0.011	0	0.002	0.001
0.2613	0.517	0.001	0.017	0.001	0.004	0.001
0.2987	0.596	0	0.022	0.001	0.006	0.001
0.336	0.654	0.001	0.03	0.002	0.009	0.001
0.3733	0.725	0.001	0.036	0.003	0.011	0.001
0.4107	0.777	0.002	0.044	0.004	0.014	0.002
0.448	0.827	0.003	0.052	0.004	0.017	0.002
0.4853	0.893	0.003	0.061	0.005	0.021	0.003
0.5227	0.953	0.003	0.071	0.006	0.026	0.003
0.56	0.999	0.004	0.08	0.007	0.03	0.003
0.5973	1.054	0.005	0.089	0.01	0.034	0.003
0.6347	1.103	0.006	0.099	0.01	0.038	0.004
0.672	1.158	0.008	0.109	0.012	0.043	0.004
0.7093	1.203	0.009	0.119	0.013	0.048	0.005
0.7467	1.234	0.01	0.13	0.014	0.053	0.005
0.784	1.294	0.011	0.141	0.016	0.058	0.006
0.8235	1.329	0.012	0.151	0.017	0.063	0.007
0.8653	1.38	0.014	0.162	0.018	0.068	0.007
0.9097	1.413	0.016	0.173	0.019	0.075	0.01
0.9567	1.457	0.017	0.186	0.021	0.081	0.01
1.0065	1.502	0.019	0.199	0.023	0.087	0.011
1.0592	1.554	0.022	0.212	0.024	0.095	0.012
1.115	1.598	0.024	0.224	0.026	0.1	0.012
1.1742	1.665	0.027	0.244	0.028	0.111	0.014
1.2368	1.719	0.03	0.26	0.031	0.12	0.016
1.3032	1.769	0.033	0.277	0.034	0.129	0.017
1.3735	1.832	0.036	0.294	0.036	0.14	0.018
1.448	1.903	0.039	0.314	0.038	0.149	0.019
1.527	1.964	0.044	0.333	0.041	0.161	0.021
1.6107	2.026	0.049	0.353	0.044	0.173	0.023
1.6992	2.092	0.052	0.373	0.046	0.185	0.024
1.793	2.143	0.057	0.394	0.05	0.196	0.026
1.8923	2.184	0.062	0.414	0.053	0.209	0.029
1.9977	2.209	0.068	0.435	0.058	0.222	0.031
2.1092	2.232	0.073	0.454	0.059	0.235	0.034
2.2273	2.251	0.078	0.472	0.063	0.246	0.036
2.3525	2.281	0.084	0.49	0.065	0.258	0.038
2.485	2.323	0.09	0.508	0.069	0.27	0.04
2.6255	2.358	0.095	0.524	0.071	0.281	0.042
2.7743	2.389	0.1	0.541	0.075	0.291	0.044
2.9318	2.42	0.105	0.555	0.078	0.303	0.046
3.0987	2.459	0.111	0.569	0.081	0.312	0.048
3.2755	2.48	0.116	0.582	0.084	0.322	0.051
3.4628	2.508	0.121	0.593	0.085	0.33	0.052
3.6612	2.525	0.125	0.603	0.088	0.337	0.054
3.8713	2.543	0.13	0.613	0.091	0.346	0.056
4.094	2.57	0.134	0.622	0.092	0.351	0.058
4.3298	2.577	0.138	0.63	0.094	0.357	0.059
4.5797	2.591	0.142	0.637	0.097	0.362	0.061
4.8443	2.609	0.145	0.642	0.099	0.367	0.063

Elapsed Time (min)	P17 m H2O	P1 m H2O	P2 m H2O	WD4A m H2O	P18 m H2O	P4 (MB4) m H2O
0	0	0	0	0	0	0
0.0375	0.004	0	0.001	0.002	0.001	0.002
0.075	0.004	0	0.001	0	0.001	0
0.1125	0.003	0	0.001	0.002	0.001	0
0.15	0.003	-0.001	0	0.001	0.001	0
0.1875	0.003	-0.001	0.001	0.001	0.001	0
0.225	0.003	0	0	0	0.001	0
0.2625	0.003	0	0.001	0	0.001	0
0.3	0.004	0	0.001	0.001	0.001	0
0.3375	0.004	0	0	0.001	0.001	0
0.375	0.004	0.001	0.001	0	0.001	0
0.4125	0.005	0.002	0.001	0.001	0.001	0
0.45	0.007	0.003	0.002	0.001	0.001	0
0.4875	0.008	0.004	0.002	0.001	0.002	0.001
0.525	0.009	0.005	0.002	0.001	0.002	0.001
0.5625	0.01	0.006	0.002	0.001	0.001	0.001
0.6	0.011	0.008	0.003	0.001	0.002	0.001
0.6375	0.012	0.009	0.003	0.001	0.002	0.001
0.675	0.013	0.011	0.003	0.001	0.002	0.001
0.7125	0.015	0.012	0.003	0.001	0.001	0.002
0.75	0.017	0.014	0.003	0.001	0.002	0.001
0.7895	0.018	0.017	0.003	0.001	0.002	0.002
0.8313	0.02	0.018	0.003	0.001	0.003	0.002
0.8757	0.022	0.02	0.003	0.001	0.002	0.002
0.9227	0.025	0.022	0.004	0.001	0.002	0.002
0.9725	0.025	0.025	0.005	0.001	0.003	0.003
1.0252	0.027	0.027	0.005	0.001	0.003	0.003
1.081	0.031	0.03	0.005	0.001	0.003	0.003
1.1402	0.031	0.033	0.005	0.002	0.003	0.003
1.2028	0.034	0.037	0.006	0.002	0.003	0.004
1.2692	0.038	0.041	0.006	0.002	0.003	0.004
1.3395	0.04	0.045	0.007	0.001	0.003	0.004
1.414	0.044	0.049	0.008	0.002	0.003	0.004
1.493	0.047	0.054	0.009	0.002	0.003	0.004
1.5767	0.053	0.059	0.009	0.002	0.003	0.005
1.6652	0.056	0.064	0.01	0.003	0.004	0.005
1.759	0.062	0.07	0.01	0.003	0.004	0.006
1.8583	0.064	0.076	0.011	0.003	0.004	0.007
1.9637	0.069	0.082	0.012	0.003	0.005	0.007
2.0752	0.073	0.088	0.013	0.003	0.006	0.009
2.1933	0.079	0.095	0.013	0.003	0.006	0.01
2.3185	0.083	0.101	0.014	0.003	0.006	0.011
2.451	0.088	0.107	0.015	0.003	0.007	0.011
2.5915	0.092	0.114	0.016	0.004	0.008	0.012
2.7403	0.097	0.12	0.017	0.004	0.008	0.012
2.8978	0.1	0.126	0.017	0.004	0.009	0.013
3.0647	0.104	0.132	0.018	0.004	0.009	0.014
3.2415	0.108	0.137	0.019	0.005	0.01	0.015
3.4288	0.112	0.143	0.019	0.005	0.01	0.015
3.6272	0.114	0.147	0.02	0.005	0.01	0.016
3.8373	0.118	0.152	0.021	0.006	0.011	0.017
4.06	0.12	0.157	0.021	0.005	0.01	0.016
4.2958	0.123	0.16	0.022	0.006	0.011	0.017
4.5457	0.125	0.164	0.023	0.006	0.012	0.018
4.8103	0.126	0.167	0.023	0.006	0.012	0.018
5.0907	0.127	0.169	0.023	0.006	0.011	0.018

5.1247	2.624	0.148	0.647	0.1	0.371	0.065
5.4215	2.625	0.151	0.652	0.103	0.374	0.065
5.736	2.642	0.152	0.656	0.104	0.377	0.066
6.0692	2.64	0.155	0.659	0.106	0.38	0.068
6.422	2.65	0.158	0.663	0.107	0.382	0.069
6.7958	2.656	0.16	0.664	0.108	0.384	0.07
7.1918	2.657	0.162	0.667	0.11	0.386	0.071
7.6112	2.658	0.163	0.669	0.111	0.387	0.072
8.0555	2.657	0.165	0.67	0.112	0.388	0.072
8.5262	2.659	0.166	0.671	0.112	0.389	0.073
9.0247	2.669	0.167	0.673	0.114	0.391	0.074
9.5527	2.669	0.169	0.674	0.115	0.393	0.075
10.112	2.673	0.17	0.675	0.117	0.393	0.076
10.7045	2.672	0.172	0.676	0.118	0.394	0.077
11.332	2.672	0.172	0.677	0.119	0.394	0.078
11.9968	2.672	0.172	0.677	0.119	0.394	0.078
12.701	2.672	0.174	0.677	0.12	0.395	0.079
13.4468	2.674	0.175	0.677	0.121	0.395	0.079
14.2368	2.674	0.175	0.678	0.123	0.396	0.079
15.0737	2.671	0.175	0.678	0.123	0.396	0.08
15.9602	2.672	0.178	0.678	0.124	0.396	0.081
16.8992	2.671	0.178	0.678	0.125	0.396	0.082
17.8938	2.671	0.179	0.678	0.125	0.397	0.082
18.9475	2.672	0.179	0.679	0.126	0.397	0.083
20.0635	2.671	0.179	0.68	0.126	0.398	0.083
21.2457	2.673	0.179	0.681	0.126	0.399	0.084
22.4978	2.672	0.18	0.68	0.127	0.399	0.084
23.8243	2.67	0.181	0.681	0.128	0.4	0.085
25.2293	2.67	0.181	0.681	0.128	0.4	0.086
26.7177	2.669	0.182	0.681	0.129	0.4	0.086
28.2942	2.669	0.183	0.681	0.13	0.4	0.086
29.964	2.669	0.183	0.682	0.131	0.401	0.087
31.7328	2.669	0.184	0.683	0.132	0.401	0.088
33.6065	2.669	0.185	0.684	0.133	0.401	0.088
35.5912	2.668	0.185	0.684	0.133	0.402	0.089
37.6935	2.669	0.186	0.684	0.134	0.403	0.091
39.9203	2.669	0.187	0.685	0.135	0.403	0.091
42.2792	2.679	0.188	0.686	0.136	0.404	0.092
44.7778	2.679	0.19	0.687	0.137	0.405	0.092
47.4245	2.679	0.19	0.689	0.138	0.406	0.093
50.228	2.678	0.192	0.689	0.14	0.406	0.095
53.1977	2.678	0.192	0.69	0.141	0.407	0.096
56.3433	2.679	0.195	0.691	0.143	0.409	0.097
59.6753	2.679	0.196	0.692	0.144	0.41	0.099
63.2048	2.678	0.197	0.693	0.146	0.411	0.1
66.9433	2.679	0.199	0.695	0.147	0.412	0.102
70.9035	2.689	0.2	0.696	0.148	0.413	0.103
75.0983	2.688	0.202	0.697	0.15	0.414	0.105
79.5417	2.687	0.203	0.697	0.152	0.415	0.106
84.2483	2.688	0.205	0.699	0.154	0.415	0.107
89.2338	2.687	0.206	0.7	0.156	0.417	0.109
94.5147	2.687	0.209	0.702	0.158	0.418	0.111
100.1085	2.688	0.211	0.703	0.161	0.419	0.113
106.0338	2.696	0.212	0.705	0.163	0.421	0.115
112.3102	2.696	0.216	0.707	0.166	0.422	0.117
118.9585	2.698	0.218	0.709	0.168	0.423	0.119
126.0007	2.698	0.219	0.71	0.17	0.425	0.122
133.4602	2.699	0.222	0.712	0.173	0.426	0.124
141.3617	2.698	0.225	0.714	0.175	0.428	0.127

5.3875	0.129	0.172	0.024	0.006	0.012	0.018
5.702	0.131	0.174	0.024	0.006	0.012	0.018
6.0352	0.132	0.176	0.024	0.006	0.012	0.018
6.388	0.134	0.178	0.024	0.006	0.012	0.018
6.7618	0.134	0.179	0.024	0.007	0.012	0.02
7.1578	0.137	0.182	0.025	0.007	0.013	0.02
7.5772	0.138	0.183	0.025	0.007	0.014	0.02
8.0215	0.137	0.184	0.025	0.007	0.012	0.02
8.4922	0.139	0.185	0.025	0.007	0.013	0.02
8.9907	0.14	0.186	0.026	0.007	0.013	0.02
9.5187	0.141	0.187	0.026	0.007	0.013	0.02
10.078	0.141	0.187	0.026	0.008	0.013	0.022
10.6705	0.142	0.187	0.026	0.007	0.013	0.022
11.298	0.142	0.188	0.027	0.008	0.014	0.022
11.9628	0.143	0.188	0.026	0.008	0.014	0.022
12.667	0.143	0.188	0.027	0.007	0.014	0.022
13.4128	0.144	0.19	0.027	0.008	0.014	0.022
14.2028	0.145	0.19	0.027	0.008	0.014	0.022
15.0397	0.145	0.191	0.028	0.008	0.014	0.023
15.9262	0.146	0.191	0.028	0.008	0.014	0.023
16.8652	0.146	0.191	0.028	0.008	0.015	0.023
17.8598	0.146	0.192	0.028	0.008	0.014	0.023
18.9135	0.147	0.192	0.028	0.008	0.015	0.023
20.0295	0.147	0.193	0.028	0.008	0.015	0.023
21.2117	0.147	0.193	0.029	0.008	0.015	0.023
22.4638	0.148	0.194	0.029	0.009	0.015	0.023
23.7903	0.148	0.194	0.029	0.009	0.016	0.024
25.1953	0.148	0.194	0.03	0.009	0.015	0.024
26.6837	0.149	0.194	0.03	0.009	0.016	0.024
28.2602	0.149	0.194	0.03	0.01	0.016	0.024
29.93	0.15	0.195	0.031	0.01	0.016	0.024
31.6988	0.15	0.195	0.031	0.01	0.017	0.025
33.5725	0.152	0.196	0.031	0.01	0.017	0.025
35.5572	0.152	0.196	0.032	0.01	0.017	0.025
37.6595	0.153	0.197	0.033	0.01	0.017	0.025
39.8863	0.154	0.197	0.033	0.01	0.017	0.025
42.2452	0.154	0.198	0.033	0.011	0.017	0.025
44.7438	0.155	0.199	0.034	0.011	0.018	0.025
47.3905	0.155	0.2	0.034	0.011	0.018	0.025
50.194	0.156	0.201	0.035	0.011	0.019	0.026
53.1637	0.158	0.201	0.035	0.011	0.018	0.026
56.3093	0.159	0.202	0.036	0.012	0.019	0.026
59.6413	0.161	0.204	0.037	0.012	0.019	0.026
63.1708	0.161	0.205	0.037	0.013	0.02	0.027
66.9093	0.162	0.206	0.038	0.013	0.02	0.028
70.8695	0.163	0.207	0.038	0.013	0.02	0.027
75.0643	0.164	0.208	0.039	0.014	0.021	0.028
79.5077	0.166	0.208	0.039	0.014	0.021	0.028
84.2143	0.167	0.209	0.04	0.015	0.021	0.029
89.1998	0.168	0.21	0.041	0.015	0.022	0.029
94.4807	0.17	0.212	0.043	0.015	0.022	0.03
100.0745	0.171	0.214	0.043	0.016	0.023	0.03
105.9998	0.173	0.215	0.044	0.016	0.023	0.03
112.2762	0.175	0.216	0.045	0.017	0.024	0.03
118.9245	0.177	0.218	0.046	0.017	0.024	0.031
125.9667	0.178	0.219	0.047	0.017	0.025	0.031
133.4262	0.18	0.221	0.049	0.018	0.026	0.032
141.3277	0.183	0.222	0.05	0.019	0.026	0.033
149.6973	0.185	0.225	0.051	0.02	0.027	0.033

149.7313	2.7	0.227	0.716	0.179	0.429	0.129
158.597	2.711	0.23	0.718	0.182	0.433	0.132
167.988	2.712	0.233	0.72	0.186	0.434	0.135
177.9355	2.712	0.237	0.723	0.188	0.435	0.138
188.4723	2.71	0.239	0.724	0.193	0.437	0.14
199.6335	2.71	0.243	0.726	0.196	0.438	0.145
211.4562	2.71	0.246	0.73	0.2	0.441	0.147
223.9793	2.722	0.25	0.732	0.204	0.443	0.152
237.2445	2.723	0.255	0.735	0.208	0.444	0.154
251.2957	2.721	0.259	0.737	0.212	0.446	0.158
266.1795	2.723	0.263	0.741	0.216	0.448	0.163
281.9452	2.725	0.266	0.744	0.221	0.449	0.168
298.645	2.736	0.271	0.746	0.225	0.452	0.171
316.3345	2.739	0.276	0.751	0.23	0.456	0.175
335.0722	2.741	0.28	0.754	0.235	0.459	0.179
354.92	2.742	0.286	0.757	0.241	0.462	0.185
375.944	2.748	0.292	0.762	0.246	0.465	0.189
398.2137	2.748	0.296	0.766	0.251	0.468	0.195
421.803	2.752	0.301	0.771	0.257	0.475	0.2
446.79	2.764	0.307	0.775	0.262	0.477	0.205
473.2577	2.766	0.313	0.778	0.268	0.482	0.211
501.2935	2.774	0.319	0.783	0.274	0.485	0.216
530.9907	2.774	0.324	0.786	0.28	0.488	0.222
562.4475	2.774	0.33	0.791	0.286	0.492	0.228
595.7682	2.772	0.335	0.795	0.291	0.495	0.233
631.0633	2.773	0.342	0.8	0.298	0.516	0.24
668.4498	2.779	0.347	0.805	0.303	0.521	0.245
708.0517	2.792	0.354	0.81	0.31	0.525	0.252
750	2.792	0.36	0.815	0.316	0.53	0.259
794.434	2.819	0.366	0.82	0.322	0.537	0.264
841.5008	2.827	0.374	0.826	0.329	0.542	0.271
891.3565	2.831	0.381	0.831	0.336	0.548	0.277
944.1663	2.839	0.386	0.838	0.343	0.552	0.284
1000.105	2.846	0.394	0.843	0.35	0.558	0.291
1059.359	2.848	0.398	0.847	0.356	0.564	0.297
1122.124	2.857	0.406	0.854	0.363	0.569	0.304
1188.608	2.862	0.412	0.859	0.37	0.575	0.309
1259.031	2.869	0.419	0.865	0.376	0.58	0.317
1333.627	2.878	0.425	0.871	0.383	0.586	0.322
1412.643	2.882	0.431	0.876	0.389	0.592	0.329
1496.341	2.889	0.437	0.882	0.396	0.598	0.335
1584.999	2.893	0.444	0.887	0.402	0.603	0.341
1678.909	2.895	0.45	0.892	0.408	0.608	0.347
1778.385	2.899	0.456	0.898	0.415	0.614	0.353
1883.754	2.905	0.462	0.903	0.421	0.62	0.36
1995.368	2.913	0.468	0.907	0.427	0.624	0.366
2113.594	2.912	0.475	0.912	0.432	0.631	0.372
2238.826	2.918	0.482	0.919	0.438	0.636	0.379
2371.479	2.922	0.488	0.925	0.445	0.642	0.385
2511.992	2.924	0.494	0.93	0.452	0.647	0.391
2660.83	2.927	0.5	0.935	0.458	0.654	0.397
2818.488	2.938	0.507	0.942	0.465	0.661	0.403
2985.488	2.937	0.512	0.946	0.471	0.665	0.409
3162.383	2.942	0.519	0.952	0.476	0.671	0.415
3349.759	2.945	0.525	0.958	0.483	0.676	0.421
3548.239	2.954	0.53	0.963	0.489	0.681	0.427
3758.479	2.951	0.536	0.968	0.494	0.687	0.434
3981.177	2.954	0.543	0.973	0.5	0.693	0.439
4217.07	2.964	0.549	0.978	0.506	0.699	0.445

158.563	0.187	0.227	0.053	0.02	0.028	0.034
167.954	0.189	0.229	0.055	0.021	0.029	0.035
177.9015	0.191	0.231	0.056	0.022	0.03	0.036
188.4383	0.193	0.234	0.058	0.023	0.03	0.037
199.5995	0.197	0.236	0.059	0.024	0.031	0.038
211.4222	0.199	0.237	0.06	0.024	0.032	0.039
223.9453	0.202	0.24	0.063	0.025	0.033	0.039
237.2105	0.205	0.243	0.065	0.027	0.035	0.04
251.2617	0.208	0.245	0.066	0.027	0.036	0.042
266.1455	0.212	0.249	0.068	0.03	0.037	0.043
281.9112	0.215	0.251	0.071	0.031	0.038	0.045
298.611	0.219	0.255	0.074	0.032	0.04	0.046
316.3005	0.222	0.257	0.077	0.034	0.041	0.048
335.0382	0.227	0.261	0.079	0.035	0.043	0.05
354.886	0.23	0.264	0.081	0.037	0.045	0.052
375.91	0.235	0.268	0.084	0.037	0.046	0.053
398.1797	0.239	0.272	0.087	0.04	0.048	0.055
421.769	0.242	0.276	0.09	0.042	0.05	0.057
446.756	0.248	0.279	0.094	0.044	0.052	0.06
473.2237	0.252	0.283	0.098	0.046	0.055	0.061
501.2595	0.257	0.288	0.102	0.049	0.057	0.064
530.9567	0.262	0.292	0.105	0.051	0.059	0.066
562.4135	0.267	0.297	0.11	0.053	0.062	0.068
595.7342	0.271	0.301	0.114	0.056	0.063	0.07
631.0293	0.278	0.306	0.119	0.059	0.067	0.075
668.4158	0.282	0.31	0.122	0.062	0.069	0.075
708.0177	0.287	0.316	0.127	0.065	0.074	0.08
749.966	0.292	0.32	0.132	0.069	0.076	0.083
794.4	0.298	0.326	0.136	0.071	0.079	0.084
841.4668	0.304	0.331	0.143	0.076	0.083	0.089
891.3225	0.309	0.337	0.146	0.079	0.086	0.093
944.1323	0.316	0.342	0.152	0.084	0.091	0.096
1000.071	0.321	0.348	0.157	0.088	0.095	0.101
1059.325	0.328	0.353	0.164	0.091	0.096	0.119
1122.09	0.334	0.359	0.169	0.096	0.101	0.124
1188.574	0.341	0.364	0.174	0.099	0.105	0.127
1258.997	0.346	0.37	0.18	0.106	0.11	0.132
1333.593	0.352	0.376	0.186	0.11	0.114	0.136
1412.609	0.357	0.381	0.192	0.115	0.119	0.141
1496.307	0.364	0.388	0.197	0.119	0.123	0.146
1584.965	0.37	0.392	0.203	0.125	0.128	0.15
1678.875	0.376	0.398	0.208	0.13	0.133	0.155
1778.351	0.381	0.404	0.214	0.136	0.137	0.16
1883.72	0.388	0.41	0.22	0.141	0.143	0.165
1995.334	0.393	0.415	0.227	0.146	0.149	0.168
2113.56	0.398	0.419	0.233	0.151	0.152	0.173
2238.792	0.404	0.426	0.24	0.157	0.158	0.179
2371.445	0.41	0.432	0.245	0.165	0.164	0.184
2511.958	0.417	0.439	0.251	0.171	0.17	0.19
2660.796	0.422	0.445	0.255	0.176	0.174	0.195
2818.454	0.429	0.45	0.261	0.181	0.18	0.2
2985.454	0.435	0.455	0.268	0.187	0.185	0.206
3162.349	0.44	0.461	0.273	0.194	0.192	0.21
3349.725	0.447	0.468	0.279	0.199	0.197	0.216
3548.205	0.452	0.473	0.285	0.205	0.202	0.222
3758.445	0.458	0.478	0.29	0.21	0.208	0.227
3981.143	0.464	0.483	0.296	0.216	0.214	0.233
4217.036	0.47	0.49	0.302	0.222	0.22	0.238
4457.036	0.475	0.495	0.308	0.228	0.226	0.244

4457.07	2.964	0.555	0.984	0.512	0.703	0.451
4697.07	2.967	0.559	0.987	0.517	0.708	0.455
4937.07	2.975	0.564	0.991	0.522	0.713	0.461
5177.07	2.976	0.569	0.995	0.526	0.716	0.465
5417.07	2.988	0.573	0.999	0.532	0.722	0.47
5657.07	2.997	0.576	1.004	0.536	0.727	0.475
5897.07	3.007	0.581	1.006	0.54	0.73	0.478
6137.07	3.009	0.583	1.009	0.544	0.734	0.482
6377.07	3.007	0.587	1.01	0.546	0.737	0.483
6617.07	3.004	0.588	1.01	0.548	0.736	0.488
6857.07	2.995	0.59	1.011	0.549	0.738	0.489
7097.07	2.998	0.592	1.012	0.552	0.739	0.49
7337.07	2.996	0.594	1.012	0.553	0.741	0.491
7577.07	2.982	0.595	1.011	0.554	0.743	0.494
7817.07	2.978	0.596	1.01	0.556	0.741	0.495
8057.07	2.967	0.596	1.009	0.556	0.742	0.495
8297.07	2.965	0.598	1.009	0.559	0.743	0.497
8537.07	2.953	0.599	1.009	0.56	0.743	0.498
8777.07	2.953	0.6	1.008	0.56	0.743	0.499
9017.07	2.946	0.601	1.007	0.56	0.743	0.5
9257.07	2.935	0.601	1.006	0.561	0.743	0.502
9497.07	2.935	0.601	1.006	0.562	0.743	0.502
9737.07	2.922	0.603	1.006	0.564	0.746	0.503
9977.07	2.923	0.604	1.006	0.564	0.745	0.503
10217.07	2.918	0.604	1.006	0.566	0.746	0.505
10457.07	2.912	0.605	1.005	0.567	0.746	0.507

4697.036	0.479	0.5	0.313	0.234	0.231	0.249
4937.036	0.484	0.505	0.318	0.239	0.236	0.254
5177.036	0.489	0.509	0.324	0.243	0.241	0.259
5417.036	0.494	0.514	0.328	0.248	0.247	0.263
5657.036	0.498	0.519	0.333	0.252	0.25	0.267
5897.036	0.501	0.523	0.338	0.256	0.255	0.271
6137.036	0.505	0.527	0.342	0.26	0.258	0.275
6377.036	0.508	0.529	0.349	0.263	0.262	0.278
6617.036	0.51	0.532	0.351	0.267	0.266	0.281
6857.036	0.512	0.533	0.351	0.269	0.268	0.284
7097.036	0.513	0.534	0.353	0.273	0.27	0.286
7337.036	0.515	0.535	0.357	0.274	0.272	0.288
7577.036	0.517	0.537	0.358	0.276	0.275	0.29
7817.036	0.518	0.538	0.36	0.278	0.277	0.293
8057.036	0.519	0.538	0.36	0.28	0.279	0.293
8297.036	0.52	0.54	0.359	0.282	0.28	0.295
8537.036	0.522	0.542	0.36	0.283	0.283	0.297
8777.036	0.522	0.542	0.361	0.286	0.283	0.3
9017.036	0.523	0.544	0.363	0.287	0.285	0.301
9257.036	0.524	0.545	0.366	0.289	0.287	0.302
9497.036	0.524	0.544	0.367	0.29	0.288	0.303
9737.036	0.526	0.547	0.369	0.291	0.29	0.305
9977.036	0.527	0.548	0.372	0.293	0.291	0.308
10217.04	0.528	0.549	0.376	0.295	0.292	0.307
10457.04	0.529	0.551	0.382	0.296	0.295	0.311

Recovery

Elapsed Time (min)	PW1 m H2O	WD1A m H2O	P14 m H2O	WS1B m H2O	P15 m H2O	WD2A m H2O
0	0	0	0	0	0	0
0.0375	-0.069	0	0	0	0	0
0.075	-0.149	0	-0.001	0	-0.001	0
0.1125	-0.225	0	-0.003	0	-0.002	0
0.15	-0.299	0	-0.007	0	-0.003	-0.001
0.1875	-0.371	0	-0.012	-0.001	-0.004	0
0.225	-0.451	-0.002	-0.017	-0.002	-0.005	-0.001
0.2625	-0.575	-0.002	-0.023	-0.003	-0.008	-0.001
0.3	-0.671	-0.003	-0.032	-0.003	-0.01	-0.001
0.3375	-0.753	-0.003	-0.04	-0.004	-0.015	-0.002
0.375	-0.824	-0.004	-0.05	-0.005	-0.018	-0.002
0.4125	-0.89	-0.006	-0.059	-0.006	-0.023	-0.003
0.45	-0.935	-0.007	-0.07	-0.008	-0.027	-0.003
0.4875	-0.97	-0.009	-0.081	-0.01	-0.031	-0.004
0.525	-1.008	-0.01	-0.091	-0.01	-0.037	-0.004
0.5625	-1.044	-0.012	-0.102	-0.012	-0.041	-0.005
0.6	-1.08	-0.013	-0.111	-0.013	-0.045	-0.005
0.6375	-1.118	-0.016	-0.122	-0.015	-0.05	-0.007
0.675	-1.157	-0.017	-0.132	-0.017	-0.055	-0.007
0.7125	-1.196	-0.019	-0.143	-0.018	-0.061	-0.008
0.75	-1.236	-0.022	-0.152	-0.019	-0.066	-0.009
0.7895	-1.279	-0.024	-0.163	-0.021	-0.071	-0.01
0.8313	-1.32	-0.026	-0.174	-0.023	-0.076	-0.01
0.8757	-1.362	-0.028	-0.185	-0.024	-0.084	-0.011
0.9227	-1.406	-0.03	-0.197	-0.026	-0.089	-0.012
0.9725	-1.451	-0.033	-0.21	-0.028	-0.095	-0.014
1.0252	-1.497	-0.036	-0.223	-0.029	-0.103	-0.015
1.081	-1.529	-0.038	-0.232	-0.03	-0.108	-0.016

Recovery

Elapsed Time (min)	P17 m H2O	P1 m H2O	P2 m H2O	WD4A m H2O	P18 m H2O	P4 (MB4) m H2O
0	0	0	0	0	0	0
0.0382	0.002	0	0	0	0	0
0.0763	0.002	0	0.001	0	0	0
0.1145	0.002	0	0.001	0	0	0
0.1527	0.002	0	0.001	-0.001	0	0
0.1908	0.002	0	0.001	0	0	0.001
0.229	0.001	-0.001	0.001	0	0	0.001
0.2672	0.001	-0.001	0.001	0	0	0
0.3053	0	-0.002	0	0	0	0
0.3435	-0.001	-0.003	0	0	0	0
0.3817	-0.002	-0.004	0	0	0	0
0.4198	-0.004	-0.004	0	0	0	0
0.458	-0.005	-0.005	0	0	0	0
0.4962	-0.006	-0.006	0	0	0	0
0.5343	-0.007	-0.008	-0.001	0	0	0
0.5725	-0.01	-0.009	-0.001	0	-0.001	0
0.6107	-0.011	-0.011	-0.001	0	0	0
0.6488	-0.013	-0.013	-0.002	0	0	-0.001
0.687	-0.015	-0.015	-0.002	0	-0.001	-0.001
0.7252	-0.017	-0.017	-0.002	0	-0.001	-0.001
0.7633	-0.018	-0.018	-0.003	0	-0.001	-0.001
0.8028	-0.02	-0.02	-0.003	-0.001	-0.001	-0.001
0.8447	-0.022	-0.022	-0.003	-0.001	-0.001	-0.001
0.889	-0.024	-0.024	-0.003	-0.001	-0.002	-0.002
0.936	-0.026	-0.026	-0.003	-0.001	-0.002	-0.002
0.9858	-0.028	-0.028	-0.004	-0.001	-0.002	-0.001
1.0385	-0.032	-0.031	-0.005	-0.001	-0.002	-0.002
1.0943	-0.032	-0.033	-0.005	-0.001	-0.002	-0.002

1.1402	-1.597	-0.044	-0.252	-0.034	-0.119	-0.017
1.2028	-1.646	-0.047	-0.268	-0.037	-0.128	-0.019
1.2692	-1.696	-0.05	-0.285	-0.039	-0.137	-0.02
1.3395	-1.747	-0.055	-0.3	-0.041	-0.147	-0.022
1.414	-1.798	-0.059	-0.318	-0.044	-0.157	-0.024
1.493	-1.849	-0.064	-0.336	-0.046	-0.167	-0.025
1.5767	-1.899	-0.068	-0.353	-0.049	-0.179	-0.026
1.6652	-1.95	-0.072	-0.372	-0.051	-0.188	-0.028
1.759	-2.001	-0.076	-0.389	-0.055	-0.201	-0.031
1.8583	-2.051	-0.079	-0.407	-0.058	-0.211	-0.032
1.9637	-2.098	-0.085	-0.426	-0.061	-0.223	-0.035
2.0752	-2.146	-0.09	-0.444	-0.064	-0.235	-0.037
2.1933	-2.193	-0.093	-0.463	-0.066	-0.246	-0.039
2.3185	-2.238	-0.098	-0.48	-0.07	-0.259	-0.041
2.451	-2.282	-0.104	-0.498	-0.072	-0.27	-0.044
2.5915	-2.324	-0.109	-0.514	-0.076	-0.282	-0.046
2.7403	-2.364	-0.113	-0.53	-0.079	-0.292	-0.048
2.8978	-2.402	-0.118	-0.546	-0.082	-0.304	-0.051
3.0647	-2.438	-0.123	-0.561	-0.085	-0.313	-0.054
3.2415	-2.472	-0.128	-0.574	-0.088	-0.324	-0.056
3.4288	-2.503	-0.132	-0.588	-0.091	-0.333	-0.058
3.6272	-2.531	-0.138	-0.601	-0.093	-0.342	-0.06
3.8373	-2.559	-0.143	-0.612	-0.097	-0.351	-0.062
4.06	-2.584	-0.146	-0.623	-0.099	-0.359	-0.064
4.2958	-2.605	-0.15	-0.633	-0.102	-0.366	-0.066
4.5457	-2.626	-0.154	-0.642	-0.105	-0.373	-0.069
4.8103	-2.642	-0.158	-0.65	-0.107	-0.379	-0.071
5.0907	-2.657	-0.162	-0.657	-0.11	-0.385	-0.072
5.3875	-2.671	-0.166	-0.664	-0.112	-0.389	-0.075
5.702	-2.683	-0.169	-0.669	-0.116	-0.394	-0.078
6.0352	-2.693	-0.172	-0.675	-0.119	-0.399	-0.079
6.388	-2.701	-0.176	-0.679	-0.12	-0.402	-0.082
6.7618	-2.709	-0.178	-0.683	-0.123	-0.405	-0.084
7.1578	-2.716	-0.181	-0.688	-0.125	-0.409	-0.085
7.5772	-2.721	-0.185	-0.69	-0.127	-0.411	-0.087
8.0215	-2.726	-0.188	-0.694	-0.129	-0.414	-0.089
8.4922	-2.73	-0.191	-0.696	-0.132	-0.416	-0.092
8.9907	-2.733	-0.192	-0.698	-0.133	-0.419	-0.093
9.5187	-2.737	-0.196	-0.7	-0.137	-0.421	-0.096
10.078	-2.739	-0.198	-0.702	-0.139	-0.422	-0.099
10.6705	-2.742	-0.2	-0.704	-0.141	-0.424	-0.1
11.298	-2.745	-0.203	-0.706	-0.144	-0.426	-0.101
11.9628	-2.747	-0.205	-0.709	-0.146	-0.428	-0.104
12.667	-2.749	-0.208	-0.711	-0.148	-0.429	-0.106
13.4128	-2.752	-0.211	-0.712	-0.15	-0.431	-0.108
14.2028	-2.753	-0.213	-0.715	-0.152	-0.434	-0.111
15.0397	-2.755	-0.215	-0.716	-0.156	-0.436	-0.113
15.9262	-2.758	-0.218	-0.72	-0.159	-0.438	-0.115
16.8652	-2.8	-0.22	-0.722	-0.161	-0.44	-0.118
17.8598	-2.763	-0.223	-0.723	-0.164	-0.441	-0.12
18.9135	-2.766	-0.227	-0.728	-0.167	-0.443	-0.123
20.0295	-2.768	-0.229	-0.73	-0.169	-0.446	-0.126
21.2117	-2.771	-0.232	-0.732	-0.172	-0.448	-0.128
22.4638	-2.772	-0.234	-0.734	-0.174	-0.449	-0.131
23.7903	-2.775	-0.237	-0.736	-0.179	-0.452	-0.133
25.1953	-2.777	-0.239	-0.738	-0.181	-0.454	-0.135
26.6837	-2.778	-0.242	-0.741	-0.184	-0.457	-0.14
28.2602	-2.781	-0.246	-0.743	-0.186	-0.459	-0.141
29.93	-2.784	-0.249	-0.745	-0.19	-0.462	-0.145

1.1535	-0.04	-0.038	-0.006	-0.001	-0.002	-0.002
1.2162	-0.042	-0.041	-0.006	-0.001	-0.002	-0.004
1.2825	-0.045	-0.046	-0.007	-0.001	-0.002	-0.004
1.3528	-0.048	-0.049	-0.007	-0.001	-0.003	-0.004
1.4273	-0.053	-0.053	-0.008	-0.002	-0.003	-0.004
1.5063	-0.055	-0.057	-0.009	-0.001	-0.003	-0.004
1.59	-0.059	-0.062	-0.01	-0.002	-0.003	-0.005
1.6785	-0.063	-0.067	-0.01	-0.002	-0.003	-0.006
1.7723	-0.068	-0.073	-0.011	-0.002	-0.003	-0.007
1.8717	-0.071	-0.078	-0.012	-0.002	-0.004	-0.007
1.977	-0.076	-0.083	-0.013	-0.002	-0.004	-0.007
2.0885	-0.079	-0.089	-0.014	-0.003	-0.004	-0.008
2.2067	-0.083	-0.095	-0.015	-0.003	-0.006	-0.009
2.3318	-0.089	-0.102	-0.016	-0.003	-0.006	-0.009
2.4643	-0.092	-0.107	-0.017	-0.003	-0.007	-0.01
2.6048	-0.097	-0.114	-0.017	-0.003	-0.008	-0.011
2.7537	-0.1	-0.12	-0.018	-0.003	-0.008	-0.011
2.9112	-0.104	-0.125	-0.019	-0.004	-0.008	-0.011
3.078	-0.108	-0.131	-0.02	-0.004	-0.008	-0.012
3.2548	-0.113	-0.137	-0.021	-0.006	-0.009	-0.013
3.4422	-0.117	-0.144	-0.022	-0.006	-0.01	-0.014
3.6405	-0.12	-0.149	-0.023	-0.007	-0.01	-0.014
3.8507	-0.124	-0.152	-0.024	-0.007	-0.01	-0.015
4.0733	-0.126	-0.157	-0.024	-0.007	-0.01	-0.016
4.3092	-0.129	-0.163	-0.025	-0.008	-0.011	-0.017
4.559	-0.133	-0.166	-0.026	-0.008	-0.011	-0.018
4.8237	-0.135	-0.171	-0.028	-0.008	-0.012	-0.018
5.104	-0.14	-0.174	-0.03	-0.009	-0.014	-0.019
5.4008	-0.142	-0.178	-0.031	-0.009	-0.014	-0.019
5.7153	-0.144	-0.182	-0.031	-0.01	-0.015	-0.02
6.0485	-0.147	-0.185	-0.031	-0.01	-0.015	-0.02
6.4013	-0.148	-0.187	-0.033	-0.01	-0.016	-0.021
6.7752	-0.15	-0.19	-0.034	-0.011	-0.016	-0.022
7.1712	-0.152	-0.192	-0.035	-0.012	-0.018	-0.023
7.5905	-0.154	-0.194	-0.036	-0.011	-0.018	-0.023
8.0348	-0.156	-0.196	-0.037	-0.011	-0.018	-0.023
8.5055	-0.158	-0.198	-0.038	-0.012	-0.019	-0.024
9.004	-0.161	-0.2	-0.038	-0.013	-0.019	-0.025
9.532	-0.162	-0.202	-0.039	-0.013	-0.02	-0.025
10.0913	-0.164	-0.203	-0.041	-0.015	-0.021	-0.025
10.6838	-0.166	-0.205	-0.042	-0.015	-0.021	-0.025
11.3113	-0.168	-0.207	-0.044	-0.016	-0.022	-0.026
11.9762	-0.169	-0.209	-0.044	-0.016	-0.023	-0.027
12.6803	-0.171	-0.211	-0.045	-0.017	-0.023	-0.028
13.4262	-0.173	-0.213	-0.046	-0.017	-0.024	-0.028
14.2162	-0.175	-0.214	-0.048	-0.018	-0.024	-0.029
15.053	-0.176	-0.216	-0.049	-0.018	-0.025	-0.031
15.9395	-0.178	-0.218	-0.052	-0.019	-0.025	-0.032
16.8785	-0.181	-0.219	-0.052	-0.02	-0.026	-0.032
17.8732	-0.184	-0.221	-0.053	-0.021	-0.027	-0.032
18.9268	-0.185	-0.223	-0.055	-0.022	-0.028	-0.033
20.0428	-0.188	-0.225	-0.057	-0.024	-0.029	-0.034
21.225	-0.19	-0.227	-0.059	-0.024	-0.03	-0.035
22.4772	-0.192	-0.228	-0.059	-0.025	-0.031	-0.036
23.8037	-0.195	-0.232	-0.061	-0.026	-0.031	-0.037
25.2087	-0.196	-0.234	-0.063	-0.027	-0.031	-0.037
26.697	-0.198	-0.236	-0.065	-0.027	-0.033	-0.039
28.2735	-0.201	-0.238	-0.066	-0.029	-0.035	-0.039
29.9433	-0.205	-0.241	-0.068	-0.03	-0.037	-0.04

31.6988	-2.786	-0.252	-0.749	-0.193	-0.463	-0.148
33.5725	-2.789	-0.255	-0.751	-0.197	-0.466	-0.15
35.5572	-2.792	-0.258	-0.754	-0.2	-0.468	-0.154
37.6595	-2.794	-0.26	-0.756	-0.203	-0.47	-0.158
39.8863	-2.796	-0.265	-0.759	-0.207	-0.473	-0.16
42.2452	-2.798	-0.268	-0.761	-0.21	-0.476	-0.164
44.7438	-2.8	-0.271	-0.763	-0.213	-0.479	-0.167
47.3905	-2.804	-0.274	-0.766	-0.217	-0.481	-0.17
50.194	-2.806	-0.278	-0.77	-0.221	-0.484	-0.173
53.1637	-2.809	-0.281	-0.772	-0.224	-0.487	-0.177
56.3093	-2.812	-0.286	-0.775	-0.229	-0.489	-0.181
59.6413	-2.816	-0.288	-0.778	-0.232	-0.492	-0.184
63.1708	-2.818	-0.293	-0.782	-0.235	-0.496	-0.188
66.9093	-2.821	-0.296	-0.783	-0.239	-0.498	-0.19
70.8695	-2.824	-0.3	-0.788	-0.243	-0.501	-0.195
75.0643	-2.827	-0.303	-0.79	-0.247	-0.503	-0.199
79.5077	-2.83	-0.307	-0.793	-0.251	-0.507	-0.202
84.2143	-2.834	-0.31	-0.797	-0.254	-0.51	-0.206
89.1998	-2.837	-0.315	-0.799	-0.259	-0.512	-0.209
94.4807	-2.839	-0.319	-0.802	-0.263	-0.516	-0.214
100.0745	-2.843	-0.322	-0.806	-0.268	-0.519	-0.217
105.9998	-2.846	-0.326	-0.81	-0.271	-0.523	-0.221
112.2762	-2.849	-0.331	-0.812	-0.275	-0.525	-0.224
118.9245	-2.853	-0.334	-0.816	-0.28	-0.529	-0.228
125.9667	-2.857	-0.339	-0.818	-0.283	-0.531	-0.233
133.4262	-2.859	-0.342	-0.822	-0.288	-0.536	-0.236
141.3277	-2.863	-0.346	-0.826	-0.292	-0.538	-0.24
149.6973	-2.866	-0.351	-0.83	-0.295	-0.542	-0.244
158.563	-2.87	-0.355	-0.832	-0.3	-0.544	-0.248
167.954	-2.872	-0.359	-0.836	-0.305	-0.548	-0.251
177.9015	-2.877	-0.363	-0.839	-0.309	-0.551	-0.256
188.4383	-2.88	-0.367	-0.842	-0.313	-0.554	-0.26
199.5995	-2.884	-0.371	-0.845	-0.317	-0.558	-0.264
211.4222	-2.887	-0.375	-0.85	-0.322	-0.562	-0.269
223.9453	-2.891	-0.38	-0.852	-0.326	-0.565	-0.272
237.2105	-2.894	-0.385	-0.857	-0.33	-0.569	-0.276
251.2617	-2.898	-0.388	-0.859	-0.335	-0.572	-0.28
266.1455	-2.901	-0.393	-0.863	-0.339	-0.575	-0.283
281.9112	-2.905	-0.396	-0.866	-0.344	-0.578	-0.289
298.611	-2.908	-0.4	-0.87	-0.347	-0.582	-0.292
316.3005	-2.912	-0.405	-0.874	-0.351	-0.586	-0.296
335.0382	-2.915	-0.409	-0.877	-0.356	-0.589	-0.299
354.886	-2.919	-0.414	-0.88	-0.361	-0.592	-0.304
375.91	-2.923	-0.418	-0.884	-0.365	-0.595	-0.307
398.1797	-2.925	-0.421	-0.887	-0.369	-0.599	-0.311
421.769	-2.929	-0.426	-0.891	-0.373	-0.602	-0.316
446.756	-2.932	-0.429	-0.895	-0.377	-0.605	-0.32
473.2237	-2.935	-0.434	-0.898	-0.382	-0.609	-0.323
501.2595	-2.939	-0.438	-0.901	-0.385	-0.613	-0.326
530.9567	-2.944	-0.441	-0.904	-0.39	-0.616	-0.331
562.4135	-2.946	-0.447	-0.908	-0.394	-0.619	-0.334
595.7342	-2.95	-0.45	-0.911	-0.398	-0.623	-0.338
631.0293	-2.953	-0.454	-0.915	-0.402	-0.626	-0.343
668.4158	-2.956	-0.458	-0.918	-0.405	-0.628	-0.346
708.0177	-2.959	-0.461	-0.922	-0.41	-0.633	-0.351
749.966	-2.964	-0.466	-0.926	-0.414	-0.636	-0.354
794.4	-2.967	-0.47	-0.929	-0.417	-0.64	-0.358
841.4668	-2.971	-0.474	-0.932	-0.421	-0.642	-0.36
891.3225	-2.974	-0.478	-0.936	-0.425	-0.646	-0.365

31.7122	-0.205	-0.242	-0.07	-0.031	-0.037	-0.041
33.5858	-0.209	-0.244	-0.073	-0.031	-0.038	-0.042
35.5705	-0.212	-0.247	-0.074	-0.033	-0.039	-0.044
37.6728	-0.214	-0.25	-0.076	-0.035	-0.04	-0.046
39.8997	-0.217	-0.252	-0.078	-0.036	-0.041	-0.046
42.2585	-0.22	-0.255	-0.08	-0.037	-0.042	-0.047
44.7572	-0.223	-0.257	-0.082	-0.039	-0.044	-0.048
47.4038	-0.226	-0.26	-0.085	-0.04	-0.045	-0.05
50.2073	-0.228	-0.263	-0.087	-0.042	-0.047	-0.052
53.177	-0.232	-0.265	-0.089	-0.043	-0.048	-0.053
56.3227	-0.234	-0.269	-0.092	-0.044	-0.049	-0.054
59.6547	-0.237	-0.271	-0.094	-0.045	-0.051	-0.056
63.1842	-0.241	-0.274	-0.095	-0.047	-0.052	-0.057
66.9227	-0.244	-0.277	-0.098	-0.048	-0.053	-0.059
70.8828	-0.247	-0.279	-0.101	-0.051	-0.056	-0.06
75.0777	-0.25	-0.282	-0.103	-0.053	-0.057	-0.062
79.521	-0.253	-0.286	-0.106	-0.055	-0.059	-0.064
84.2277	-0.256	-0.289	-0.108	-0.056	-0.06	-0.066
89.2132	-0.259	-0.291	-0.11	-0.058	-0.062	-0.067
94.494	-0.263	-0.294	-0.113	-0.059	-0.064	-0.069
100.0878	-0.266	-0.298	-0.116	-0.062	-0.066	-0.071
106.0132	-0.27	-0.301	-0.119	-0.063	-0.068	-0.073
112.2895	-0.272	-0.304	-0.121	-0.065	-0.07	-0.075
118.9378	-0.276	-0.307	-0.125	-0.067	-0.072	-0.077
125.98	-0.278	-0.31	-0.128	-0.069	-0.073	-0.078
133.4395	-0.284	-0.313	-0.13	-0.071	-0.075	-0.081
141.341	-0.286	-0.316	-0.133	-0.074	-0.077	-0.082
149.7107	-0.29	-0.32	-0.136	-0.076	-0.079	-0.084
158.5763	-0.293	-0.323	-0.138	-0.078	-0.081	-0.086
167.9673	-0.297	-0.327	-0.141	-0.08	-0.084	-0.089
177.9148	-0.3	-0.329	-0.144	-0.083	-0.087	-0.091
188.4517	-0.304	-0.333	-0.147	-0.085	-0.087	-0.093
199.6128	-0.307	-0.335	-0.15	-0.087	-0.089	-0.096
211.4355	-0.311	-0.339	-0.153	-0.089	-0.091	-0.097
223.9587	-0.315	-0.342	-0.156	-0.091	-0.094	-0.099
237.2238	-0.318	-0.346	-0.159	-0.094	-0.096	-0.102
251.275	-0.321	-0.348	-0.162	-0.096	-0.099	-0.104
266.1588	-0.325	-0.352	-0.165	-0.099	-0.101	-0.106
281.9245	-0.329	-0.355	-0.168	-0.102	-0.103	-0.109
298.6243	-0.332	-0.359	-0.171	-0.105	-0.105	-0.11
316.3138	-0.335	-0.362	-0.173	-0.107	-0.108	-0.113
335.0515	-0.34	-0.365	-0.177	-0.109	-0.11	-0.116
354.8993	-0.344	-0.369	-0.18	-0.112	-0.113	-0.118
375.9233	-0.347	-0.372	-0.182	-0.114	-0.115	-0.12
398.193	-0.35	-0.376	-0.185	-0.117	-0.117	-0.123
421.7823	-0.354	-0.379	-0.189	-0.119	-0.12	-0.124
446.7693	-0.357	-0.382	-0.192	-0.122	-0.123	-0.127
473.237	-0.361	-0.385	-0.195	-0.125	-0.126	-0.13
501.2728	-0.364	-0.389	-0.198	-0.127	-0.129	-0.132
530.97	-0.368	-0.392	-0.202	-0.13	-0.131	-0.135
562.4268	-0.371	-0.396	-0.205	-0.133	-0.134	-0.138
595.7475	-0.375	-0.399	-0.208	-0.136	-0.136	-0.139
631.0427	-0.378	-0.402	-0.212	-0.139	-0.139	-0.142
668.4292	-0.382	-0.405	-0.214	-0.141	-0.142	-0.145
708.031	-0.385	-0.409	-0.218	-0.144	-0.144	-0.147
749.9793	-0.388	-0.411	-0.221	-0.146	-0.147	-0.149
794.4133	-0.392	-0.415	-0.224	-0.149	-0.15	-0.153
841.4802	-0.395	-0.418	-0.227	-0.153	-0.153	-0.156
891.3358	-0.4	-0.422	-0.231	-0.156	-0.157	-0.158

944.1323	-2.977	-0.481	-0.939	-0.43	-0.65	-0.369
1000.071	-2.98	-0.486	-0.943	-0.433	-0.654	-0.372
1059.325	-2.985	-0.489	-0.946	-0.437	-0.657	-0.377
1122.09	-2.988	-0.494	-0.949	-0.44	-0.661	-0.38
1188.574	-2.991	-0.496	-0.952	-0.444	-0.663	-0.383
1258.997	-2.994	-0.5	-0.957	-0.448	-0.667	-0.386
1333.593	-2.997	-0.503	-0.959	-0.451	-0.669	-0.389
1412.609	-3	-0.508	-0.963	-0.455	-0.673	-0.393
1496.307	-3.004	-0.499	-0.965	-0.459	-0.676	-0.396
1584.965	-3.007	-0.503	-0.968	-0.462	-0.679	-0.4
1678.875	-3.01	-0.507	-0.972	-0.465	-0.682	-0.402
1778.351	-3.012	-0.509	-0.974	-0.468	-0.684	-0.405
1883.72	-3.016	-0.511	-0.977	-0.471	-0.688	-0.408
1995.334	-3.018	-0.515	-0.979	-0.475	-0.69	-0.411
2113.56	-3.02	-0.518	-0.983	-0.478	-0.694	-0.414
2233.56	-3.024	-0.521	-0.985	-0.48	-0.695	-0.418
2353.56	-3.027	-0.523	-0.988	-0.484	-0.698	-0.42
2473.56	-3.03	-0.527	-0.992	-0.486	-0.702	-0.423
2593.56	-3.032	-0.528	-0.993	-0.489	-0.704	-0.426
2713.56	-3.034	-0.531	-0.995	-0.492	-0.707	-0.427
2833.56	-3.037	-0.534	-0.998	-0.493	-0.709	-0.429
2953.56	-3.039	-0.536	-0.999	-0.495	-0.71	-0.432
3073.56	-3.04	-0.537	-1.001	-0.498	-0.711	-0.434
3193.56	-3.041	-0.539	-1.002	-0.499	-0.713	-0.435
3313.56	-3.043	-0.542	-1.004	-0.5	-0.715	-0.435
3433.56	-3.044	-0.542	-1.006	-0.502	-0.715	-0.438
3553.56	-3.046	-0.544	-1.006	-0.503	-0.716	-0.439
3673.56	-3.047	-0.545	-1.008	-0.504	-0.718	-0.44
3793.56	-3.048	-0.546	-1.009	-0.505	-0.719	-0.441
3913.56	-3.049	-0.548	-1.011	-0.506	-0.721	-0.442
4033.56	-3.051	-0.549	-1.011	-0.507	-0.722	-0.444
4153.56	-3.051	-0.55	-1.012	-0.509	-0.722	-0.445
4273.56	-3.052	-0.57	-1.012	-0.51	-0.723	-0.446

944.1457	-0.402	-0.425	-0.233	-0.159	-0.158	-0.16
1000.085	-0.407	-0.429	-0.236	-0.161	-0.162	-0.164
1059.338	-0.409	-0.432	-0.24	-0.163	-0.164	-0.167
1122.103	-0.414	-0.436	-0.243	-0.167	-0.167	-0.169
1188.587	-0.416	-0.439	-0.246	-0.169	-0.17	-0.172
1259.01	-0.42	-0.442	-0.248	-0.172	-0.172	-0.175
1333.606	-0.422	-0.445	-0.252	-0.175	-0.176	-0.177
1412.622	-0.426	-0.447	-0.253	-0.177	-0.178	-0.179
1496.32	-0.429	-0.452	-0.256	-0.18	-0.18	-0.183
1584.978	-0.434	-0.454	-0.26	-0.184	-0.184	-0.187
1678.889	-0.436	-0.457	-0.262	-0.186	-0.185	-0.189
1778.364	-0.439	-0.46	-0.265	-0.188	-0.188	-0.192
1883.734	-0.442	-0.463	-0.268	-0.19	-0.191	-0.195
1995.347	-0.444	-0.466	-0.272	-0.193	-0.193	-0.196
2113.574	-0.448	-0.469	-0.275	-0.195	-0.196	-0.198
2233.574	-0.45	-0.471	-0.278	-0.198	-0.199	-0.201
2353.574	-0.453	-0.474	-0.28	-0.201	-0.201	-0.204
2473.574	-0.456	-0.476	-0.283	-0.204	-0.205	-0.207
2593.574	-0.458	-0.479	-0.285	-0.206	-0.206	-0.209
2713.574	-0.461	-0.481	-0.287	-0.207	-0.208	-0.211
2833.574	-0.462	-0.482	-0.289	-0.209	-0.209	-0.213
2953.574	-0.465	-0.485	-0.29	-0.211	-0.212	-0.215
3073.574	-0.466	-0.487	-0.292	-0.213	-0.213	-0.217
3193.574	-0.468	-0.489	-0.293	-0.214	-0.215	-0.217
3313.574	-0.469	-0.49	-0.295	-0.215	-0.215	-0.217
3433.574	-0.47	-0.49	-0.296	-0.216	-0.216	-0.219
3553.574	-0.472	-0.491	-0.298	-0.218	-0.218	-0.219
3673.574	-0.473	-0.492	-0.299	-0.218	-0.22	-0.22
3793.574	-0.473	-0.494	-0.301	-0.22	-0.22	-0.223
3913.574	-0.475	-0.496	-0.301	-0.221	-0.222	-0.224
4033.574	-0.477	-0.496	-0.303	-0.221	-0.222	-0.224
4153.574	-0.478	-0.497	-0.303	-0.222	-0.223	-0.224
4273.574	-0.478	-0.497	-0.303	-0.224	-0.223	-0.225

Elapsed Time (min)	WS1A m H2O	WD1 m H2O	WD1B m H2O	WS2A m H2O	P16 m H2O	WD2 m H2O	WD3 m H2O	WS3 m H2O	P3 m H2O	WS5 m H2O	WS7A m H2O	P6 m H2O	P5 m H2O	WS7 m H2O
Drawdown														
0	0	0	0	0	0	0	0	0	0	0	0	0	0	0
480	0.32	0.35	dry	0.23	0.41	0.235	0.02	0.05	0.08	0.025	0.015	0.01	0.015	0.01
1080	0.47	0.435	dry	0.31	0.475	0.335	0.08	0.075	0.13	0.05	0.03	0.03	0.025	0.025
1950	0.485	0.505	dry	0.38	0.535	0.375	0.125	dry	0.17	0.09	0.05	0.05	0.055	0.05
2610	0.525	0.535	dry	0.41	0.565	0.42	0.135	dry	0.195	0.12	0.07	0.065	0.07	0.065
3420	0.55	0.56	dry	0.44	0.59	0.43	dry	dry	0.22	0.14	0.08	0.08	0.08	0.08
3855	0.565	0.565	dry	0.45	0.6	0.445	dry	dry	0.23	0.15	0.09	0.09	0.09	0.085
4920	dry	0.595	dry	0.473	0.617	0.474	dry	dry	0.248	dry	0.107	0.103	0.095	0.104
5400	dry	0.605	dry	0.48	0.62	0.465	dry	dry	0.255	dry	0.105	0.11	0.105	0.105
6375	dry	0.62	dry	dry	0.635	0.485	dry	dry	0.27	dry	0.115	0.12	0.12	0.12
6750	dry	0.62	dry	dry	0.637	0.485	dry	dry	0.275	dry	0.125	0.13	0.13	0.125
7770	dry	0.62	dry	dry	0.645	0.5	dry	dry	0.28	dry	0.135	0.135	0.135	0.135
8070	dry	0.625	dry	dry	0.645	0.505	dry	dry	0.285	dry	0.138	0.138	0.138	0.14
9345	dry	0.63	dry	dry	0.645	0.5	dry	dry	0.29	dry	0.145	0.145	0.14	0.145
9720	dry	0.63	dry	dry	0.65	0.505	dry	dry	0.295	dry	0.145	0.145	0.145	0.15
10530	dry	0.63	dry	dry	0.65	0.51	dry	dry	0.3	dry	0.155	0.15	0.155	0.155
Recovery														
150	0.29	0.28	dry	0.28	0.245	0.27	dry	dry	0.21	dry	0.14	0.14	0.135	0.145
1440	0.125	0.115	dry	0.13	0.12	0.125	dry	dry	0.12	0.12	0.095	0.09	0.095	0.095
4430	0.07	0.075	dry	0.075	0.07	0.075	dry	dry	0.075	0.07	0.06	0.06	0.055	0.065

Potentiometric Drawdown and Recovery - Test 2 - August, 2001

8750	0.062	0.078	0.055	0.065	0.07	0.065	dry	0.075	-0.925	0.065	0.06	0.055	0.06	0.065

Elapsed Time (min)	WD10 m H2O	WS11 m H2O	P19 m H2O	P22 m H2O	WS12 m H2O	WS14 m H2O	WD20 m H2O	P20 m H2O	WS22 m H2O	WS23 m H2O	WD30 m H2O	P21 m H2O	WS31 m H2O	P13 m H2O
Drawdown														
0	0	0	0	0	0	0	0	0	0	0	0	0	0	0
480	0.28	0.24	0.36	0.145	0.12	0.01	0.37	0.335	0.14	0	dry	0.315	0.18	0.465
1095	dry	0.32	0.415	0.205	0.17	0.055	0.45	0.405	0.215	-0.035	dry	0.385	0.26	0.525
1935	dry	0.385	0.48	0.255	0.225	0.085	0.525	0.465	0.275	-0.02	dry	0.44	dry	0.585
2595	dry	0.42	0.505	0.285	0.255	0.1	0.57	0.5	0.305	-0.015	dry	0.47	dry	0.615
3420	dry	0.445	0.525	0.31	0.285	0.12	0.575	0.51	0.33	-0.01	dry	0.49	dry	0.635
3840	dry	dry	0.54	0.32	0.29	0.12	0.59	0.525	0.34	-0.01	dry	0.505	dry	0.65
4920	dry	dry	0.559	0.34	dry	0.144	0.615	0.544	0.36	0.005	dry	0.532	dry	0.675
5400	dry	dry	0.565	0.35	dry	0.15	0.59	0.55	0.37	-0.52	dry	0.525	dry	0.675
6405	dry	dry	0.58	0.39	dry		0.63	0.56		-0.38	dry	0.54	dry	0.685
6735	dry	dry	0.58	0.37	dry	0.17	0.65	0.56	0.385	-0.34	dry	0.545	dry	0.69
7770	dry	dry	0.59	0.38	dry	0.185	0.66	0.57		-0.24	dry	0.55	dry	0.695
8085	dry	dry	0.59	0.38	dry	0.185	0.66	0.57	0.4	-0.22	dry	0.553	dry	0.695
9360	dry	dry	0.595	0.385	dry	dry	0.655	0.575	dry	-0.185	dry	0.555	dry	0.695
9720	dry	dry	0.595	0.39	dry	dry	0.65	0.58	dry	-0.17	dry	0.555	dry	0.7
10560	dry	dry	0.6	0.39	dry	dry	0.65	0.58	dry	-0.15	dry	0.56	dry	0.705
Recovery														
165	0.3	0.27	0.24	0.23	0.245	dry	0.28	0.235	0.235	-0.145	dry	0.23	0.24	0.315
1425	0.135	0.13	0.125	0.12	0.13	0.12	0.13	0.12	0.12	-0.125	dry	0.115	0.115	0.21
4430	0.075	0.07	0.07	0.07	0.075	0.08	0.08	0.07	0.065	-0.09	0.07	0.065	0.07	0.155
8750	0.065	0.065	0.091	0.069	0.072	0.08	0.081	0.069	0.07	-0.065	0.063	0.065	0.064	0.16

Appendix C

Neutron Moisture Content Data – Test 1, Aug. 2000

Moisture content logging was performed by counting returning thermal neutrons over a 4-second counting window. Results are automatically standardized to a 16-second window.

Calculating moisture content from number of neutron counts:

Data for a single access hole was plotted on one figure. In the residually saturated zone, all temporal data clustered near a single value for neutron counts. The same was true of the fully saturated zone. For each hole, the average number of counts for both residual and full saturation was estimated from the figures. From previous research, it is known that residual saturation has a moisture content of 0.07 and that full saturation has a moisture content of 0.37 (Nwankwor et al. (1984, 1992). The moisture content for each data sampling point was calculated using the number of counts and a linear relation between residual to full saturation.

The standard deviation of the number of counts results in a maximum potential error in the calculated moisture content at full saturation of 0.011.

Please see the following file on the accompanying CD-ROM:

M.Bevan Thesis\Aug 2000 Test\Water Content\Test1 Neutron Data for CD.xls

Please see the following file on the accompanying CD-ROM:

M.Bevan Thesis\Aug 2000 Test\Water Content\Test1 Neutron Data for CD.xls

Appendix D

Neutron Moisture Content Data – Test 2, Aug. 2001

Moisture content logging was performed by counting returning thermal neutrons over a 4-second counting window. Results are automatically standardized to a 16-second window.

Calculating moisture content from number of neutron counts:

Data for a single access hole was plotted on one figure. In the residually saturated zone, all temporal data clustered near a single value for neutron counts. The same was true of the fully saturated zone. For each hole, the average number of counts for both residual and full saturation was estimated from the figures. From previous research, it is known that residual saturation has a moisture content of 0.07 and that full saturation has a moisture content of 0.37 (Nwankwor et al. (1984, 1992). The moisture content for each data sampling point was calculated using the number of counts and a linear relation between residual to full saturation.

The standard deviation of the number of counts results in a maximum potential error in the calculated moisture content at full saturation of 0.011.

Please see the following file on the accompanying CD-ROM:

M.Bevan Thesis\Aug 2001 Test\Water Content\Test2 Neutron Data1 for CD.xls

Please see the following file on the accompanying CD-ROM:

M.Bevan Thesis\Aug 2001 Test\Water Content\Test2 Neutron Data1 for CD.xls

Please see the following file on the accompanying CD-ROM:

M.Bevan Thesis\Aug 2001 Test\Water Content\Test2 Neutron Data1 for CD.xls

Please see the following file on the accompanying CD-ROM:

M.Bevan Thesis\Aug 2001 Test\Water Content\Test2 Neutron Data1 for CD.xls

Please see the following file on the accompanying CD-ROM:

M.Bevan Thesis\Aug 2001 Test\Water Content\Test2 Neutron Data1 for CD.xls

Please see the following file on the accompanying CD-ROM:

M.Bevan Thesis\Aug 2001 Test\Water Content\Test2 Neutron Data1 for CD.xls

Please see the following file on the accompanying CD-ROM:

M.Bevan Thesis\Aug 2001 Test\Water Content\Test2 Neutron Data1 for CD.xls

Please see the following file on the accompanying CD-ROM:

M.Bevan Thesis\Aug 2001 Test\Water Content\Test2 Neutron Data1 for CD.xls

Please see the following file on the accompanying CD-ROM:

M.Bevan Thesis\Aug 2001 Test\Water Content\Test2 Neutron Data1 for CD.xls

Please see the following file on the accompanying CD-ROM:

M.Bevan Thesis\Aug 2001 Test\Water Content\Test2 Neutron Data1 for CD.xls

Please see the following file on the accompanying CD-ROM:

M.Bevan Thesis\Aug 2001 Test\Water Content\Test2 Neutron Data1 for CD.xls

Please see the following file on the accompanying CD-ROM:

M.Bevan Thesis\Aug 2001 Test\Water Content\Test2 Neutron Data1 for CD.xls

Appendix E

Hydraulic Parameters from the Pumping Tests

Parameter	Test 1 (Aug, 2000)	Test 2 (Aug, 2001)		Nwankwor et al. (1984)
		Water Table Wells	Deep Observation Wells	
Transmissivity (m^2/sec)	$5x10^{-4}$	$5.65x10^{-4}$	$3.59x10^{-4}$	1.32 to $1.47x10^{-3}$
Storativity	0.0001	0.002	0.006	0.002-0.005
Specific yield	0.01	0.097	0.33	0.05
Kz/Kr		0.84	0.45	0.58

Values in the above table were obtained using Neuman (1974) type-curve methods in the AQTESOLV software package.

Appendix F

Summary of GPR Data Files – Test 1, Aug. 2000

File types are as follows:

TIME = stationary GPR reflection (antennae in fixed position, recording through time)

Reflection = standard GPR profiling

CMP = common midpoint survey

"Line 0" refers to the stationary GPR position where "TIME" data files were acquired.

Some filenames are of the form "CFB*999*.dt1". These files are a composite of two or more profile line segments that were obtained in the field.

Summary of GPR acquisition parameters:

Profiles

Transmitter voltage:	400V
Antennae frequency:	200 MHz
Antennae separation:	0.5 m
Antennae step size:	0.2 m (Lines 1, 2, 4, 6, 7, 8)
	0.1 m (Lines 3, 5)

CMP's

Transmitter voltage:	400V
Antennae frequency:	200 MHz
Initial antennae separation:	0.1 m
Antennae step size:	0.1 m

GPR File Summary - Test 1 - Aug.

***Line Number** 0 (Stationary Position)*

Pump/Recover	*Date*	*ElapsedT(hrs)*	*File Type*	*FileName*	*PickFileName*
B	02-Aug-00	0.0	TIME	CFBA0012	
P	02-Aug-00		TIME	CFBA0015	
P	02-Aug-00	1.4	TIME	CFBA0013	
P	03-Aug-00		TIME	CFBB0001	
P	03-Aug-00	19.5	TIME	CFBB0003	
P	03-Aug-00	23.2	TIME	CFBB0012	
P	04-Aug-00	42.2	TIME	CFBC0001	
P	04-Aug-00	48.5	TIME	CFBC0016	
P	05-Aug-00	67.0	TIME	CFBD0001	
P	05-Aug-00	76.3	TIME	CFBD0017	
P	06-Aug-00	89.2	TIME	CFBE0001	
P	06-Aug-00	100.6	TIME	CFBE0018	
P	07-Aug-00	115.2	TIME	CFBF0001	
P	08-Aug-00	140.3	TIME	CFBG0001	
R	09-Aug-00	0.0	TIME	CFBH0013	
R	09-Aug-00	0.5	TIME	CFBH0014	
R	10-Aug-00		TIME	CFBI0015	
R	10-Aug-00		TIME	CFBI0014	
R	11-Aug-00	46.1	TIME	CFBJ0001	
R	11-Aug-00	46.2	TIME	CFBJ0002	

***Line Number** 1*

Pump/Recover	*Date*	*ElapsedT(hrs)*	*File Type*	*FileName*	*PickFileName*
B	02-Aug-00	0.0	Reflection	CFBA0001	PICKA1
P	03-Aug-00	19.8	Reflection	CFBB0004	PICKB4
P	04-Aug-00	43.9	Reflection	CFBC0003	PICKC3
P	05-Aug-00	69.5	Reflection	CFBD0004	PICKD4
P	06-Aug-00	92.2	Reflection	CFBE0004	PICKE4
P	07-Aug-00	115.5	Reflection	CFBF0002	PICKF2
P	08-Aug-00	140.9	Reflection	CFBG0002	PICKG2
P	09-Aug-00	162.5	Reflection	CFBH0001	PICKH1
R	10-Aug-00	23.5	Reflection	CFBI0001	PICKI1
R	11-Aug-00	46.6	Reflection	CFBJ0003	PICKJ3
R	14-Aug-00	118.8	Reflection	CFBK0001	PICKK1
R	23-Aug-00	333.9	Reflection	CFBL0001	PICKL1

***Line Number** 2*

Pump/Recover	*Date*	*ElapsedT(hrs)*	*File Type*	*FileName*	*PickFileName*
B	02-Aug-00	0.0	Reflection	CFBA0002	PICKA2
P	03-Aug-00	20.1	Reflection	CFBB0005	PICKB5
P	04-Aug-00	44.1	Reflection	CFBC0004	PICKC4

P	05-Aug-00	69.8	Reflection	CFBD0005	PICKD5
P	06-Aug-00	92.5	Reflection	CFBE0005	PICKE5
P	07-Aug-00	115.7	Reflection	CFBF0003	PICKF3
P	08-Aug-00	141.1	Reflection	CFBG0003	PICKG3
P	09-Aug-00	162.7	Reflection	CFBH0002	PICKH2
R	10-Aug-00	23.7	Reflection	CFBI0002	PICKI2
R	11-Aug-00	46.7	Reflection	CFBJ0004	PICKJ4
R	14-Aug-00	119.0	Reflection	CFBK0002	PICKK2
R	23-Aug-00	334.1	Reflection	CFBL0002	PICKL2

Line Number 3

Pump/Recover	*Date*	*ElapsedT(hrs)*	*File Type*	*FileName*	*PickFileName*
B	02-Aug-00		Reflection	CFBA9993	PICKA3FT
B	02-Aug-00	0.0	Reflection	CFBA0003	
B	02-Aug-00	0.0	CMP	CFBA0010	
P	03-Aug-00	20.4	Reflection	CFBB9996	PICKB6
P	03-Aug-00	20.4	Reflection	CFBB0006	
P	03-Aug-00	24.6	CMP	CFBB0015	
P	04-Aug-00	44.4	Reflection	CFBC9995	PICKC5
P	04-Aug-00	44.4	Reflection	CFBC0005	
P	04-Aug-00	47.9	CMP	CFBC0013	
P	05-Aug-00	68.0	Reflection	CFBD0003	PICKD3
P	05-Aug-00	70.0	Reflection	CFBD9996	PICKD6
P	05-Aug-00	70.0	Reflection	CFBD0006	
P	05-Aug-00	72.4	CMP	CFBD0013	
P	05-Aug-00	76.2	Reflection	CFBD0016	PICKD16
P	06-Aug-00	90.3	Reflection	CFBE0003	PICKE3
P	06-Aug-00	92.4	CMP	CFBE0014	
P	06-Aug-00	92.7	Reflection	CFBE9996	PICKE6
P	06-Aug-00	92.7	Reflection	CFBE0006	
P	06-Aug-00	100.2	Reflection	CFBE0017	PICKE17
P	07-Aug-00	115.9	Reflection	CFBF0004	PICKF4
P	07-Aug-00	117.5	CMP	CFBF0011	
P	08-Aug-00	141.4	Reflection	CFBG0004	PICKG4
P	08-Aug-00	143.9	CMP	CFBG0011	
P	09-Aug-00	163.0	Reflection	CFBH0003	PICKH3
P	09-Aug-00	164.3	CMP	CFBH0011	
R	09-Aug-00	4.3	Reflection	CFBH0015	PICKH15
R	10-Aug-00	24.0	Reflection	CFBI0003	PICKI3
R	10-Aug-00	25.6	CMP	CFBI0012	
R	11-Aug-00	47.2	Reflection	CFBJ0005	PICKJ5
R	11-Aug-00	48.7	CMP	CFBJ0012	
R	14-Aug-00	119.3	Reflection	CFBK0003	PICKK3
R	14-Aug-00	120.9	CMP	CFBK0010	
R	23-Aug-00	334.3	Reflection	CFBL0003	PICKL3
R	23-Aug-00	336.0	CMP	CFBL0010	

Line Number 4

Pump/Recover	*Date*	*ElapsedT(hrs)*	*File Type*	*FileName*	*PickFileName*
B	02-Aug-00	0.0	Reflection	CFBA0004	PICKA4
P	03-Aug-00	20.6	Reflection	CFBB0007	PICKB7
P	04-Aug-00	44.6	Reflection	CFBC0006	PICKC6
P	05-Aug-00	70.3	Reflection	CFBD0007	PICKD7
P	06-Aug-00	92.9	Reflection	CFBE0007	
P	06-Aug-00	92.9	Reflection	CFBE9997	PICKE7
P	06-Aug-00	92.9	Reflection	CFBE0008	
P	07-Aug-00	116.2	Reflection	CFBF0005	PICKF5
P	08-Aug-00	141.7	Reflection	CFBG0005	PICKG5
P	09-Aug-00	163.3	Reflection	CFBH0004	PICKH4
R	10-Aug-00	24.4	Reflection	CFBI0004	PICKI4
R	11-Aug-00	47.5	Reflection	CFBJ0006	PICKJ6
R	14-Aug-00	119.6	Reflection	CFBK0004	PICKK4
R	23-Aug-00	334.7	Reflection	CFBL0004	PICKL4

Line Number 5

Pump/Recover	*Date*	*ElapsedT(hrs)*	*File Type*	*FileName*	*PickFileName*
B	02-Aug-00	0.0	Reflection	CFBA0005	PICKA5
B	02-Aug-00	0.0	CMP	CFBA0011	
P	02-Aug-00	1.8	Reflection	CFBA0014	PICKA14
P	03-Aug-00	18.4	Reflection	CFBB0002	PICKB2
P	03-Aug-00	20.7	Reflection	CFBB0008	PICKB8
P	03-Aug-00	24.1	Reflection	CFBB0013	PICKB13
P	03-Aug-00	24.5	CMP	CFBB0014	
P	04-Aug-00	42.7	Reflection	CFBC0002	PICKC2
P	04-Aug-00	44.8	Reflection	CFBC0007	PICKC7
P	04-Aug-00	48.0	CMP	CFBC0014	
P	04-Aug-00	48.1	Reflection	CFBC0015	PICKC15
P	05-Aug-00	67.4	Reflection	CFBD0002	PICKD2
P	05-Aug-00	70.8	Reflection	CFBD0008	PICKD8
P	05-Aug-00	72.6	CMP	CFBD0014	
P	05-Aug-00	75.9	Reflection	CFBD0015	PICKD15
P	06-Aug-00	90.0	Reflection	CFBE0002	PICKE2
P	06-Aug-00	92.6	CMP	CFBE0015	
P	06-Aug-00	93.1	Reflection	CFBE0009	PICKE9
P	06-Aug-00	99.9	Reflection	CFBE0016	PICKE16
P	07-Aug-00	116.4	Reflection	CFBF0006	PICKF6
P	07-Aug-00	117.6	CMP	CFBF0012	
P	08-Aug-00	142.6	Reflection	CFBG0006	PICKG6
P	08-Aug-00	144.0	CMP	CFBG0012	
P	09-Aug-00	163.5	Reflection	CFBH0005	PICKH5
P	09-Aug-00	164.4	CMP	CFBH0012	
R	09-Aug-00	4.6	Reflection	CFBH0016	PICKH16
R	10-Aug-00	24.6	Reflection	CFBI0005	PICKI5
R	10-Aug-00	25.7	CMP	CFBI0013	
R	11-Aug-00	47.7	Reflection	CFBJ0007	PICKJ7
R	11-Aug-00	48.8	CMP	CFBJ0013	

R	14-Aug-00	119.8	Reflection	CFBK0005	PICKK5
R	14-Aug-00	121.0	CMP	CFBK0011	
R	23-Aug-00	334.9	Reflection	CFBL0005	PICKL5
R	23-Aug-00	336.0	CMP	CFBL0011	

***Line Number** 6*

Pump/Recover	*Date*	*ElapsedT(hrs)*	*File Type*	*FileName*	*PickFileName*
B	02-Aug-00	0.0	Reflection	CFBA0006	PICKA6
P	03-Aug-00	21.1	Reflection	CFBB0009	PICKB9
P	04-Aug-00	45.3	Reflection	CFBC0008	PICKC8
P	05-Aug-00	71.7	Reflection	CFBD0009	PICKD9
P	06-Aug-00	93.5	Reflection	CFBE0010	PICKE10
P	07-Aug-00	116.7	Reflection	CFBF0007	PICKF7
P	08-Aug-00	143.0	Reflection	CFBG0007	PICKG7
P	09-Aug-00	163.8	Reflection	CFBH9996	PICKH6
P	09-Aug-00	163.8	Reflection	CFBH0006	
P	09-Aug-00	163.9	Reflection	CFBH0007	
R	10-Aug-00	24.9	Reflection	CFBI9996	PICKI6
R	10-Aug-00	24.9	Reflection	CFBI0006	
R	10-Aug-00	25.0	Reflection	CFBI0009	
R	11-Aug-00	48.0	Reflection	CFBJ0008	PICKJ8
R	14-Aug-00	120.1	Reflection	CFBK0006	PICKK6
R	23-Aug-00	335.2	Reflection	CFBL0006	PICKL6

***Line Number** 7*

Pump/Recover	*Date*	*ElapsedT(hrs)*	*File Type*	*FileName*	*PickFileName*
B	02-Aug-00	0.0	Reflection	CFBA0007	PICKA7
P	03-Aug-00	21.4	Reflection	CFBB0010	PICKB10
P	04-Aug-00	45.5	Reflection	CFBC0009	PICKC9
P	05-Aug-00	72.0	Reflection	CFBD0010	PICKD10
P	06-Aug-00	93.7	Reflection	CFBE0011	PICKE11
P	07-Aug-00	117.0	Reflection	CFBF0008	PICKF8
P	08-Aug-00	143.3	Reflection	CFBG0008	PICKG8
P	09-Aug-00	164.0	Reflection	CFBH0008	PICKH8
R	10-Aug-00	25.3	Reflection	CFBI0008	PICKI8
R	11-Aug-00	48.2	Reflection	CFBJ0009	PICKJ9
R	14-Aug-00	120.4	Reflection	CFBK0007	PICKK7
R	23-Aug-00	335.5	Reflection	CFBL0007	PICKL7

***Line Number** 8*

Pump/Recover	*Date*	*ElapsedT(hrs)*	*File Type*	*FileName*	*PickFileName*
B	02-Aug-00	0.0	CMP	CFBA0009	
B	02-Aug-00	0.0	Reflection	CFBA0008	PICKA8
P	03-Aug-00	21.6	Reflection	CFBB0011	PICKB11
P	03-Aug-00	24.7	CMP	CFBB0016	
P	04-Aug-00	45.7	Reflection	CFBC9910	PICKC10

P	04-Aug-00	45.7	Reflection	CFBC0010	
P	04-Aug-00	45.9	Reflection	CFBC0011	
P	04-Aug-00	46.0	CMP	CFBC0012	
P	05-Aug-00	72.2	Reflection	CFBD0011	PICKD11
P	05-Aug-00	72.3	CMP	CFBD0012	
P	06-Aug-00	92.2	Reflection	CFBE0012	PICKE12
P	06-Aug-00	92.3	CMP	CFBE0013	
P	07-Aug-00	117.2	Reflection	CFBF0009	PICKF9
P	07-Aug-00	117.4	CMP	CFBF0010	
P	08-Aug-00	143.4	Reflection	CFBG0009	PICKG9
P	08-Aug-00	143.7	CMP	CFBG0010	
P	09-Aug-00	164.2	Reflection	CFBH0009	PICKH9
P	09-Aug-00	164.3	CMP	CFBH0010	
R	10-Aug-00	25.3	Reflection	CFBI0010	PICKI10
R	10-Aug-00	25.5	CMP	CFBI0011	
R	11-Aug-00	48.5	Reflection	CFBJ0010	PICKJ10
R	11-Aug-00	48.6	CMP	CFBJ0011	
R	14-Aug-00	120.6	Reflection	CFBK0008	PICKK8
R	14-Aug-00	120.8	CMP	CFBK0009	
R	23-Aug-00	335.8	Reflection	CFBL0008	PICKL8
R	23-Aug-00	336.0	CMP	CFBL0009	

Appendix G

Summary of GPR Data Files – Test 2, Aug. 2001

File types are as follows:

TIME = stationary GPR reflection (antennae in fixed position, recording through time)

Reflection = standard GPR profiling

CMP = common midpoint survey

Some filenames are of the form "CFB*999*.dt1". These files are a composite of two or more profile line segments that were obtained in the field.

Summary of GPR acquisition parameters:

Profiles

Transmitter voltage:	400V
Antennae frequency:	200 MHz
Antennae separation:	0.5 m
Antennae step size:	0.2 m (Lines 1, 2, 4, 6, 7)
	0.1 m (Lines 3, 5, 8)

CMP's

Transmitter voltage:	400V
Antennae frequency:	200 MHz
Initial antennae separation:	0.1 m
Antennae step size:	0.1 m

GPR File Summary - Test 2 - Aug.

Line Number 1

Pump/Recover	*Date*	*ElapsedT(hrs)*	*File Type*	*FileName*	*PickFileName*
B	08-Aug-01		Reflection	CFBA01	2picka1
B	13-Aug-01		Reflection	CFBB01	2pickb1
B	16-Aug-01		Reflection	CFBC01	2pickc1
P	19-Aug-01	63.5	Reflection	CFBF08	2pickf8
P	21-Aug-01	106.2	Reflection	CFBH01	2pickh1
P	24-Aug-01	178.0	Reflection	CFBK07	2pickk7
R	25-Aug-01	24.8	Reflection	CFBL01	2pickl1
R	30-Aug-01	143.7	Reflection	CFBN01	2pickn1

Line Number 2

Pump/Recover	*Date*	*ElapsedT(hrs)*	*File Type*	*FileName*	*PickFileName*
B	08-Aug-01		Reflection	CFBA02	
B	13-Aug-01		Reflection	CFBB02	
B	16-Aug-01		Reflection	CFBC02	2pickc2
P	19-Aug-01	63.7	Reflection	CFBF09	2pickf9
P	21-Aug-01	106.4	Reflection	CFBH02	
P	21-Aug-01	106.5	Reflection	CFBH02B	
P	21-Aug-01	106.5	Reflection	CFBH92	2pickh2
P	24-Aug-01	178.3	Reflection	CFBK08	2pickk8
R	25-Aug-01	25.0	Reflection	CFBL02	2pickl2
R	30-Aug-01	144.0	Reflection	CFBN02	2pickn2

Line Number 3

Pump/Recover	*Date*	*ElapsedT(hrs)*	*File Type*	*FileName*	*PickFileName*
B	08-Aug-01		CMP	CFBA010	
B	08-Aug-01		Reflection	CFBA03	
B	13-Aug-01		Reflection	CFBB03	
B	13-Aug-01		CMP	CFBB010	
B	16-Aug-01		Reflection	CFBC03	2pickc3
B	16-Aug-01		CMP	CFBC010	
P	17-Aug-01	10.0	Reflection	CFBD02	2pickd2
P	17-Aug-01	15.5	Reflection	CFBD05	2pickd5
P	17-Aug-01	16.1	CMP	CFBD08	
P	18-Aug-01	33.7	Reflection	CFBE02	2picke2
P	18-Aug-01	42.8	Reflection	CFBE06	2picke6
P	19-Aug-01	61.8	Reflection	CFBF02	2pickf2
P	19-Aug-01	63.9	CMP	CFBF010	
P	20-Aug-01	87.0	Reflection	CFBG03	2pickg3
P	20-Aug-01	88.8	CMP	CFBG07	
P	21-Aug-01	106.8	Reflection	CFBH03	2pickh3
P	21-Aug-01	110.9	CMP	CFBH010	

P	21-Aug-01	112.0	Reflection	CFBH014	2pickh14
P	22-Aug-01	131.4	Reflection	CFBI03	
P	22-Aug-01	131.6	Reflection	CFBI93	2picki3
P	22-Aug-01	131.6	Reflection	CFBI03B	
P	22-Aug-01	131.9	CMP	CFBI04	
P	22-Aug-01	136.3	Reflection	CFBI09	2picki9
P	23-Aug-01	157.5	Reflection	CFBJ03	2pickj3
P	23-Aug-01	157.7	CMP	CFBJ04	
P	23-Aug-01	163.5	Reflection	CFBJ09	2pickj9
P	24-Aug-01	176.5	Reflection	CFBK01	2pickk1
R	24-Aug-01	3.8	Reflection	CFBK012	2pickk12
R	25-Aug-01	25.3	Reflection	CFBL03	2pickl3
R	25-Aug-01	27.0	CMP	CFBL010	
R	27-Aug-01	71.6	Reflection	CFBM03	2pickm3
R	30-Aug-01	144.2	Reflection	CFBN03	2pickn3
R	30-Aug-01	146.1	CMP	CFBN010	

Line Number 4

Pump/Recover	*Date*	*ElapsedT(hrs)*	*File Type*	*FileName*	*PickFileName*
B	08-Aug-01		Reflection	CFBA04	
B	13-Aug-01		Reflection	CFBB04	
B	16-Aug-01		Reflection	CFBC04	2pickc4
P	19-Aug-01	62.1	Reflection	CFBF03	2pickf3
P	21-Aug-01	107.0	Reflection	CFBH04	2pickh4
P	24-Aug-01	176.8	Reflection	CFBK02	2pickk2
R	25-Aug-01	25.6	Reflection	CFBL04	2pickl4
R	30-Aug-01	144.5	Reflection	CFBN04	2pickn4

Lin eNumber 5

Pump/Recover	*Date*	*ElapsedT(hrs)*	*File Type*	*FileName*	*PickFileName*
B	08-Aug-01		CMP	CFBA011	
B	08-Aug-01		Reflection	CFBA05A	
B	08-Aug-01		Reflection	CFBA05	
B	08-Aug-01		Reflection	CFBA95	
B	13-Aug-01		CMP	CFBB011	
B	13-Aug-01		Reflection	CFBB05	
B	16-Aug-01		Reflection	CFBC05	2pickc5
B	16-Aug-01		CMP	CFBC011	
P	17-Aug-01	9.5	Reflection	CFBD01	2pickd1
P	17-Aug-01	15.0	Reflection	CFBD04	2pickd4
P	17-Aug-01	16.3	CMP	CFBD09	
P	17-Aug-01	19.0	Reflection	CFBD010	2pickd10
P	18-Aug-01	33.4	Reflection	CFBE01	2picke1
P	18-Aug-01	37.8	Reflection	CFBE04	2picke4
P	18-Aug-01	42.2	Reflection	CFBE05	2picke5
P	19-Aug-01	56.7	Reflection	CFBF01	2pickf1
P	19-Aug-01	62.3	Reflection	CFBF04	2pickf4

P	19-Aug-01	64.0	CMP	CFBF011	
P	20-Aug-01	83.5	Reflection	CFBG01	2pickg1
P	20-Aug-01	88.0	Reflection	CFBG04	2pickg4
P	20-Aug-01	88.5	CMP	CFBG05	
P	21-Aug-01	107.4	Reflection	CFBH05	2pickh5
P	21-Aug-01	111.0	CMP	CFBH011	
P	21-Aug-01	111.1	Reflection	CFBH012	2pickh12
P	22-Aug-01	130.6	Reflection	CFBI01	2picki1
P	22-Aug-01	132.1	CMP	CFBI06	
P	22-Aug-01	135.5	Reflection	CFBI07	2picki7
P	23-Aug-01	156.8	Reflection	CFBJ01	2pickj1
P	23-Aug-01	158.0	CMP	CFBJ06	
P	23-Aug-01	162.8	Reflection	CFBJ07	2pickj7
P	24-Aug-01	176.9	Reflection	CFBK03	2pickk3
R	24-Aug-01	0.0	TIME	CFBK09	
R	24-Aug-01	3.3	Reflection	CFBK010	2pickk10
R	25-Aug-01	25.8	Reflection	CFBL05	2pickl5
R	25-Aug-01	27.1	CMP	CFBL011	
R	27-Aug-01	70.7	Reflection	CFBM01	2pickm1
R	27-Aug-01	72.0	TIME	CFBM04	
R	30-Aug-01	144.8	Reflection	CFBN05	2pickn5
R	30-Aug-01	146.2	CMP	CFBN011	

***Line Number** 6*

Pump/Recover	*Date*	*ElapsedT(hrs)*	*File Type*	*FileName*	*PickFileName*
B	08-Aug-01		Reflection	CFBA06	
B	13-Aug-01		Reflection	CFBB06	
B	16-Aug-01		Reflection	CFBC06	2pickc6
P	19-Aug-01	62.6	Reflection	CFBF05	2pickf5
P	21-Aug-01	107.8	Reflection	CFBH06	2pickh6
P	24-Aug-01	177.2	Reflection	CFBK04	
P	24-Aug-01	177.4	Reflection	CFBK94	2pickk4
P	24-Aug-01	177.4	Reflection	CFBK04B	
R	25-Aug-01	26.2	Reflection	CFBL06	2pickl6
R	30-Aug-01	145.1	Reflection	CFBN06	2pickn6

***Line Number** 7*

Pump/Recover	*Date*	*ElapsedT(hrs)*	*File Type*	*FileName*	*PickFileName*
B	08-Aug-01		Reflection	CFBA07	
B	13-Aug-01		Reflection	CFBB07	
B	16-Aug-01		Reflection	CFBC07	2pickc7
P	19-Aug-01	62.9	Reflection	CFBF06	2pickf6
P	21-Aug-01	108.0	Reflection	CFBH07	2pickh7
P	24-Aug-01	177.5	Reflection	CFBK05	2pickk5
R	25-Aug-01	26.4	Reflection	CFBL07	2pickl7
R	30-Aug-01	145.5	Reflection	CFBN07	2pickn7

***Line Number** 8*

Pump/Recover	*Date*	*ElapsedT(hrs)*	*File Type*	*FileName*	*PickFileName*
B	08-Aug-01		Reflection	CFBA08	
B	08-Aug-01		CMP	CFBA09	
B	13-Aug-01		CMP	CFBB09	
B	13-Aug-01		Reflection	CFBB08	
B	16-Aug-01		Reflection	CFBC08	2pickc8
B	16-Aug-01		CMP	CFBC09	
P	17-Aug-01	10.5	Reflection	CFBD03	2pickd3
P	17-Aug-01	15.8	Reflection	CFBD06	2pickd6
P	17-Aug-01	16.0	CMP	CFBD07	
P	18-Aug-01	34.0	Reflection	CFBE03	2picke3
P	19-Aug-01	63.2	Reflection	CFBF07	2pickf7
P	19-Aug-01	64.1	CMP	CFBF012	
P	20-Aug-01	86.7	Reflection	CFBG02	2pickg2
P	20-Aug-01	88.6	CMP	CFBG06	
P	21-Aug-01	108.2	Reflection	CFBH08	2pickh8
P	21-Aug-01	110.7	CMP	CFBH09	
P	21-Aug-01	111.7	Reflection	CFBH013	2pickh13
P	22-Aug-01	131.0	Reflection	CFBI02	2picki2
P	22-Aug-01	132.0	CMP	CFBI05	
P	22-Aug-01	136.0	Reflection	CFBI08	2picki8
P	23-Aug-01	157.1	Reflection	CFBJ02	2pickj2
P	23-Aug-01	157.8	CMP	CFBJ05	
P	23-Aug-01	163.2	Reflection	CFBJ08	2pickj8
P	24-Aug-01	177.7	Reflection	CFBK06	2pickk6
R	24-Aug-01	3.5	Reflection	CFBK011	2pickk11
R	25-Aug-01	26.6	Reflection	CFBL08	2pickl8
R	25-Aug-01	26.9	CMP	CFBL09	
R	27-Aug-01	71.1	Reflection	CFBM02	
R	27-Aug-01	71.2	Reflection	CFBM92	2pickm2
R	27-Aug-01	71.2	Reflection	CFBM02B	
R	30-Aug-01	145.7	Reflection	CFBN08	2pickn8
R	30-Aug-01	146.0	CMP	CFBN09	

Appendix H
CD ROM Contents

\M.Bevan Thesis\Contents.txt – summary of the contents on the Thesis CD-ROM

\M.Bevan Thesis\M Bevan Thesis.pdf – copy of UW M.Sc. Thesis

\M.Bevan Thesis\Site Information\Site Co-ordinates.xls - Spatial coordinates of observation wells, neutron access tubes, GPR data points.

\M.Bevan Thesis\Site Information\GPR elevations.xls - Elevation survey data for GPR profile lines.

\M.Bevan Thesis\Aug 2000 Test\GPR\Raw Data.hd* and **.dt1*- Raw GPR files.

\M.Bevan Thesis\Aug 2000 Test\GPR\CMP & Velocity.hd* and **.dt1* – CMP data files; *CMP's.doc & CMP's.xls* – summary of CMP analyses.

\M.Bevan Thesis\Aug 2000 Test\GPR\Time Picking.hd* and **.dt1* – GPR data files used for time picking; **.pik* – picking data files; *L*RawPicks.xls* – summary of time picking data

\M.Bevan Thesis\Aug 2000 Test\Potentiometric Data\Test1 Water Data for CD.XLS – raw water level data for all wells monitored.

\M.Bevan Thesis\Aug 2000 Test\Water Content\Test1 Neutron Data for CD.xls – raw neutron counts data, calculated water content data, calculations of drawdown.

\M.Bevan Thesis\Aug 2000 Test\Analyses\Volumes\Volume Calc for CD.xls – calculations of pumped water volumes; *VolumeExplanation.cdr* – schematic explanation of annular ring method.

\M.Bevan Thesis\Aug 2001 Test\GPR\Raw Data.hd* and **.dt1*- Raw GPR files.

\M.Bevan Thesis\Aug 2001 Test\GPR\CMP's.hd* and **.dt1* – CMP data files; *CMP velocities.doc* & *CMP's.xls* – summary of CMP analyses.

\M.Bevan Thesis\Aug 2001 Test\GPR\Time Picking.hd* and **.dt1*– GPR data files used for time picking; **.pik* – picking data files; *L*RawPicks.xls* – summary of time picking data

\M.Bevan Thesis\Aug 2001 Test\Potentiometric Data\Test2 Water Data for CD.XLS – raw water level data for all wells monitored through pressure transducers and acoustic sounders.

\M.Bevan Thesis\Aug 2001 Test\Water Content\Test2 Neutron Data1 for CD.xls – raw neutron counts data; *Test2 Neutron Data2 for CD.xls* – sorted raw neutron counts data, calculated water content data, depth and elevation information for neutron data, transition zone drawdown calcuations.